Innovations and Applications of Tomosynthesis

Andrew D. A. Maidment, Ph.D.
University of Pennsylvania
Department of Radiology

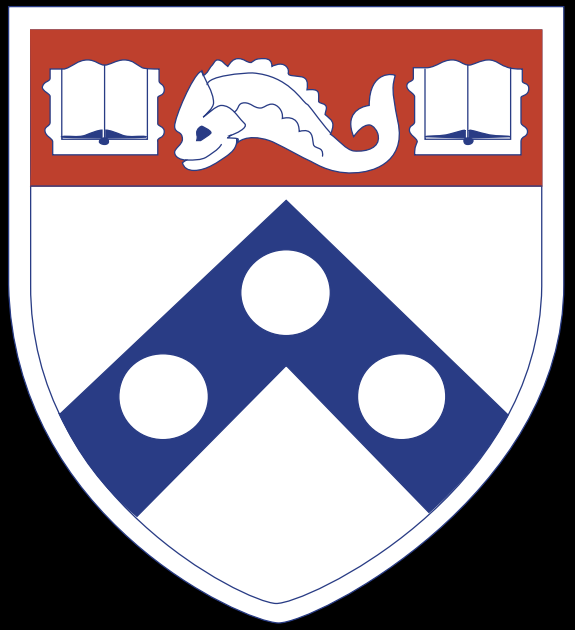

Acknowledgements of Support

- Grant support from the Komen Foundation, DOD, NIH, and Hologic.
- Dr. Maidment is a scientific advisor to and shareholder of Real Time Tomography, LLC.
- Dr. Maidment is a member of the Scientific Advisory Board of Gamma Medica, Inc.

FDA Statement

- This presentation will include off-label uses and applications and devices not yet approved for human use in the United States.

Tomosynthesis Pedigree

Linear Tomography

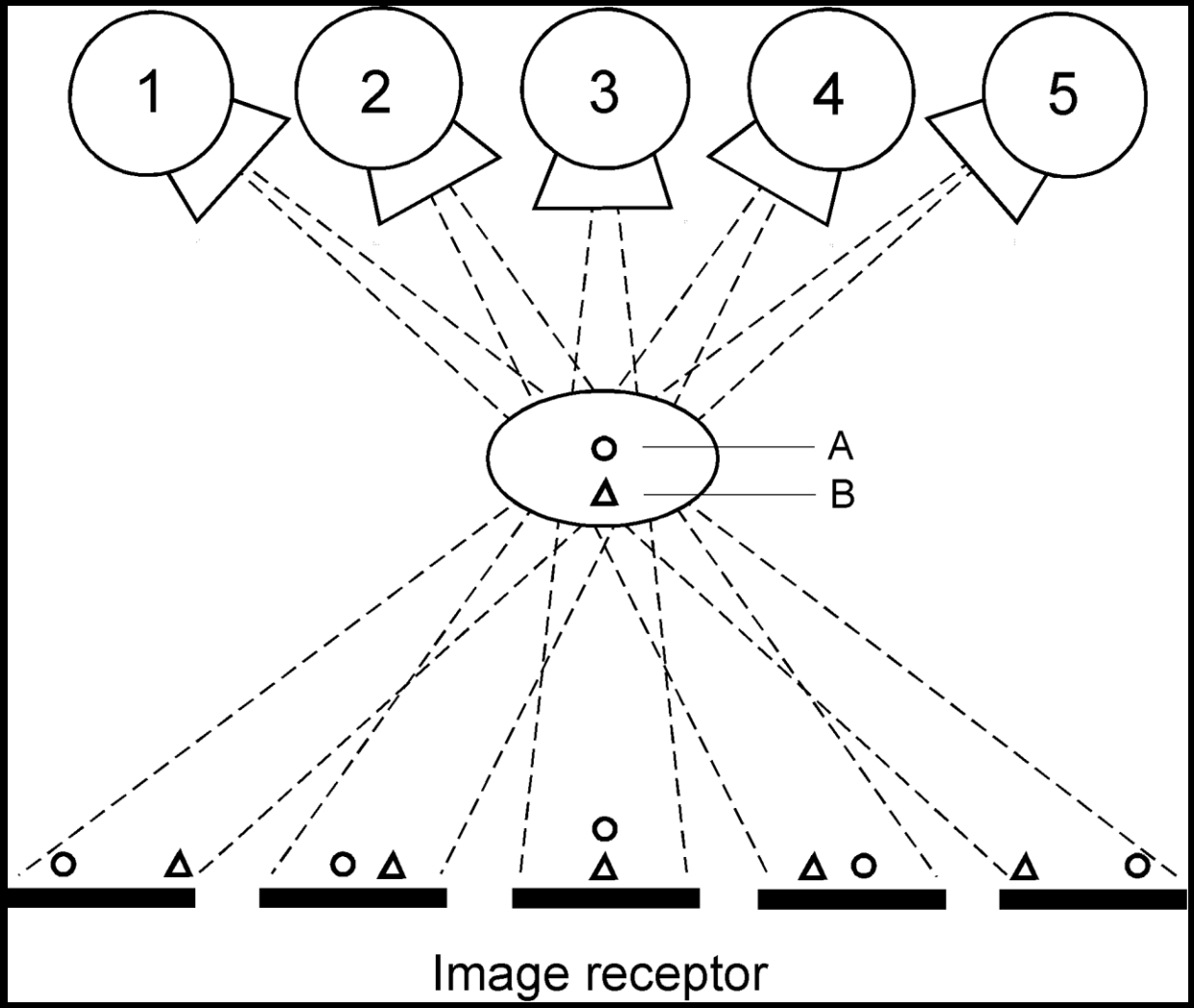

Simple Tomosynthesis

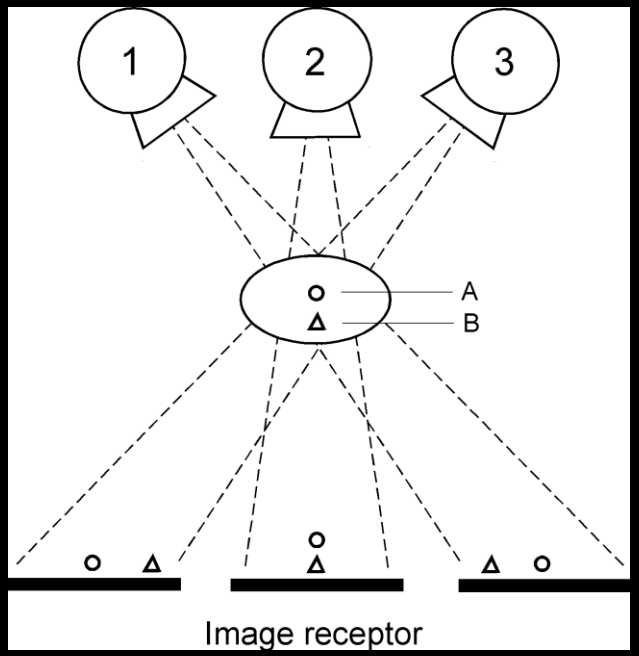

Acquisition geometry

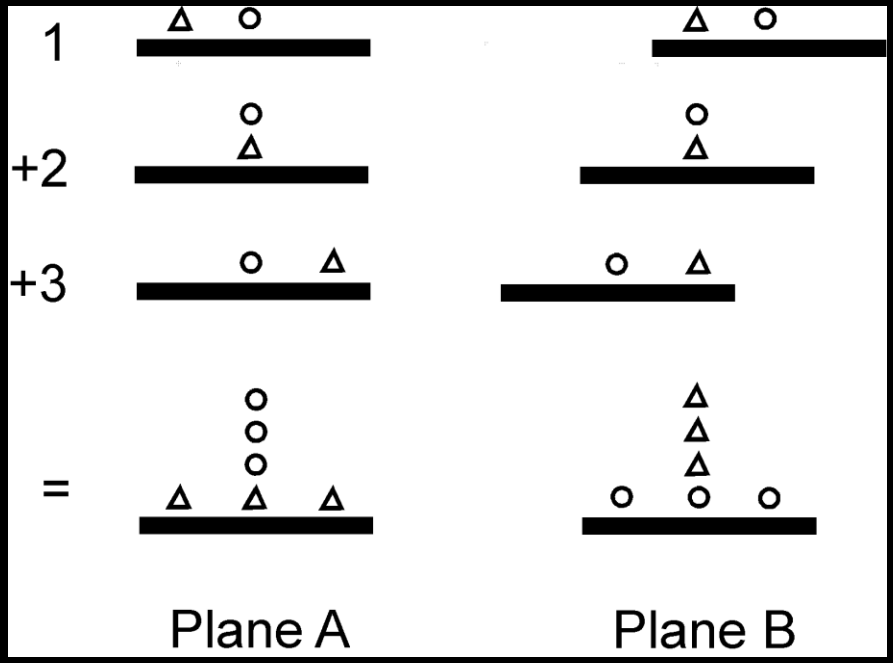

Backprojection image formation

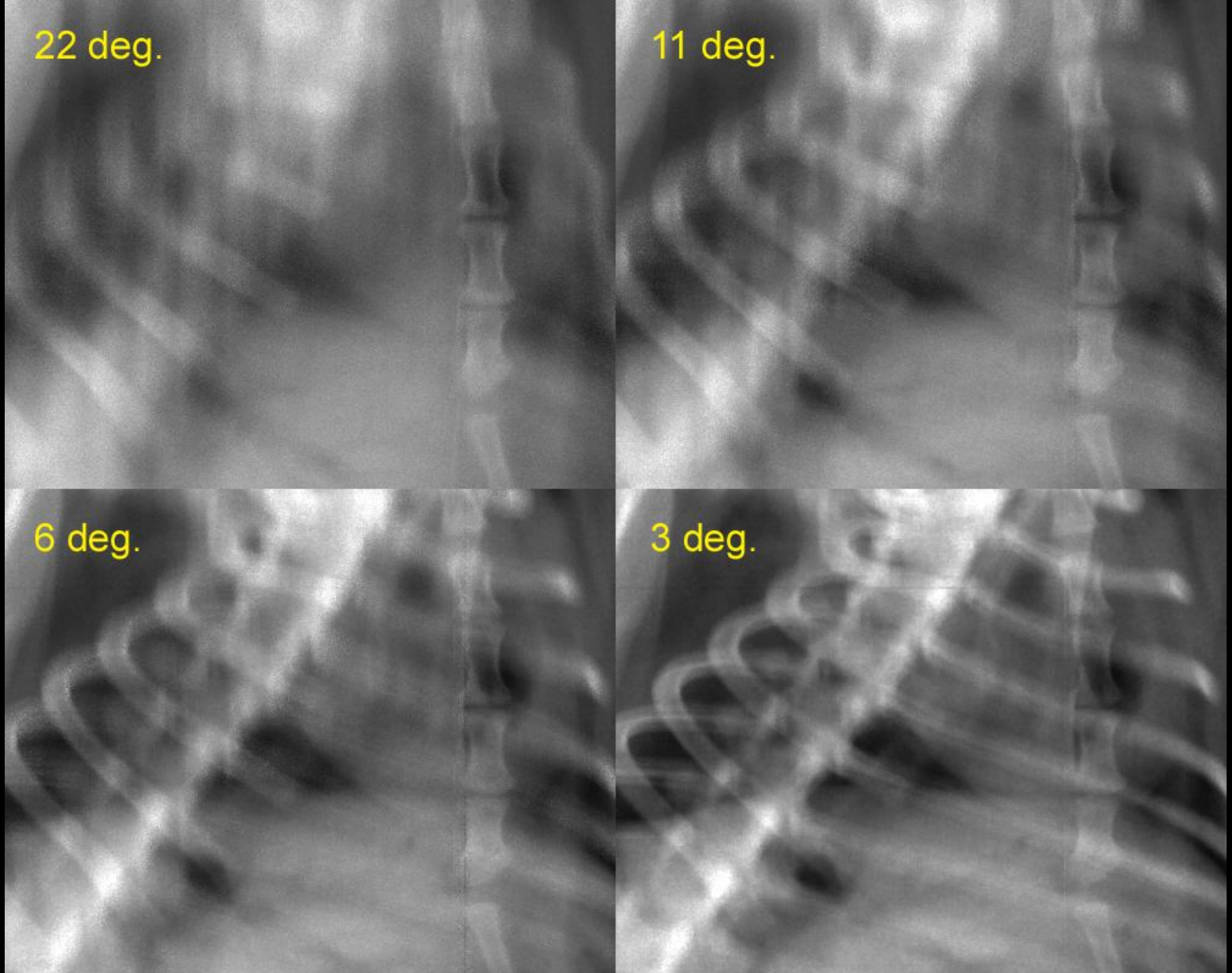
22 deg.
11 deg.
6 deg.
3 deg.

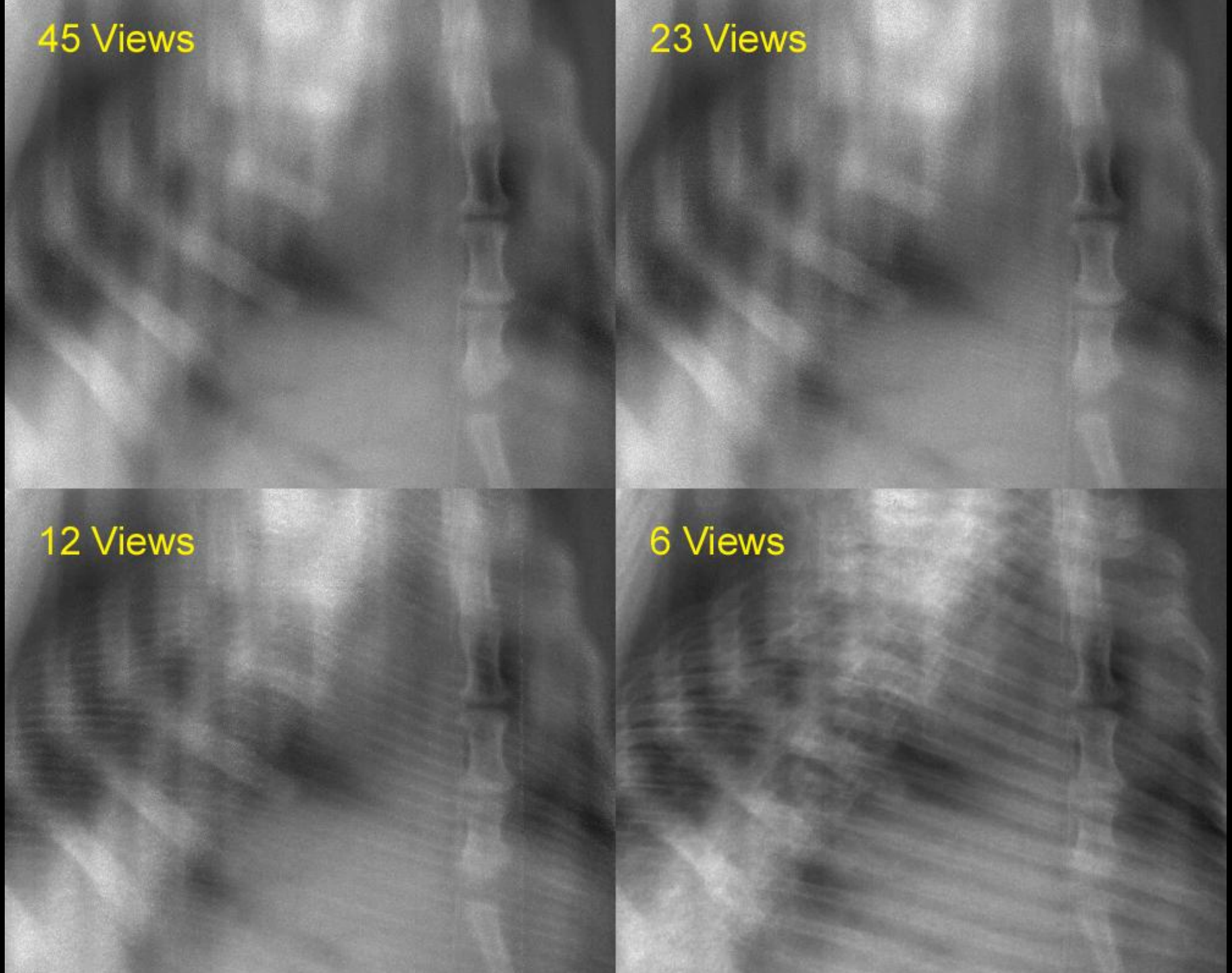
45 Views
23 Views
12 Views
6 Views

Computed Tomography

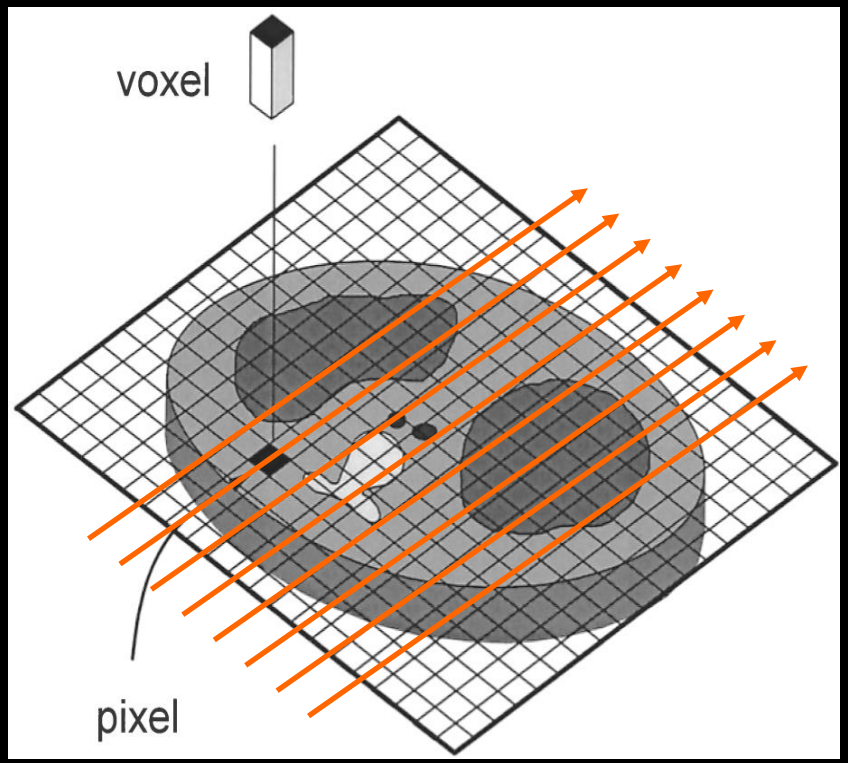

Breast CT

Breast Tomosynthesis

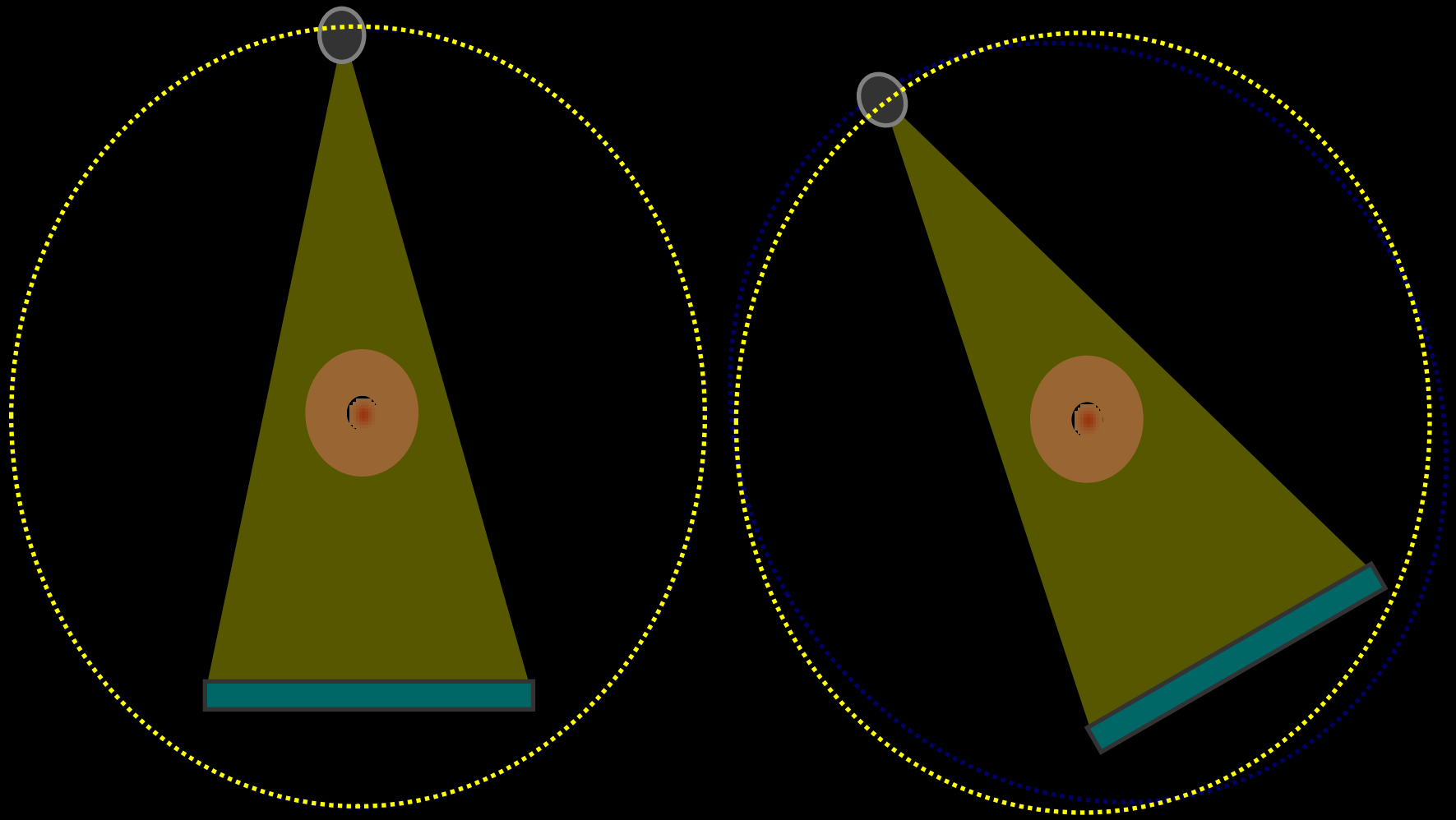

Courtesy J. Boone

Tomosynthesis Reconstruction

Sampling geometry

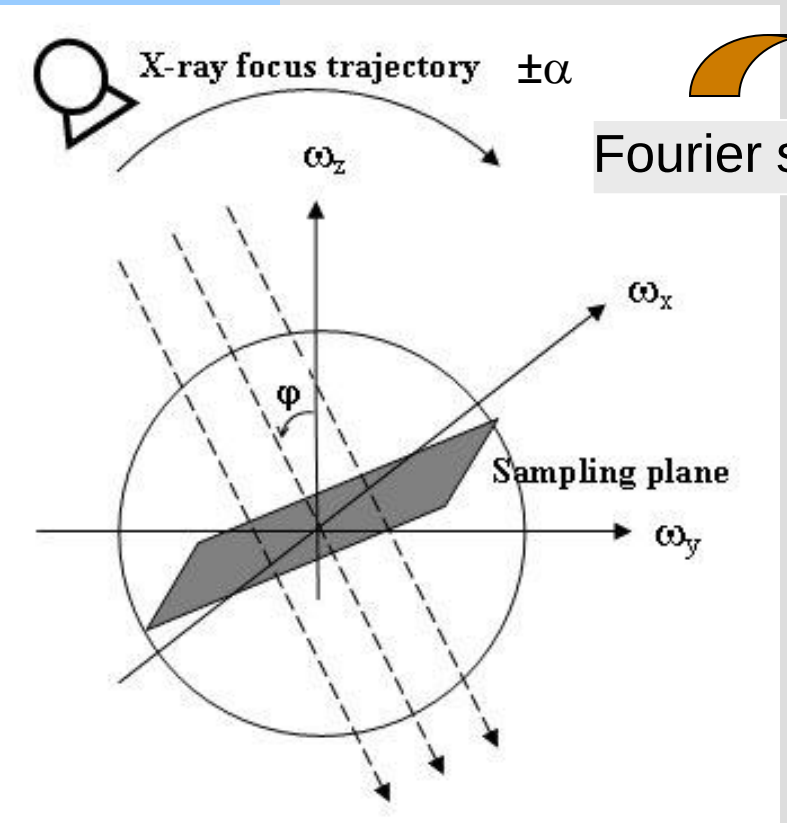

Fourier slice theorem

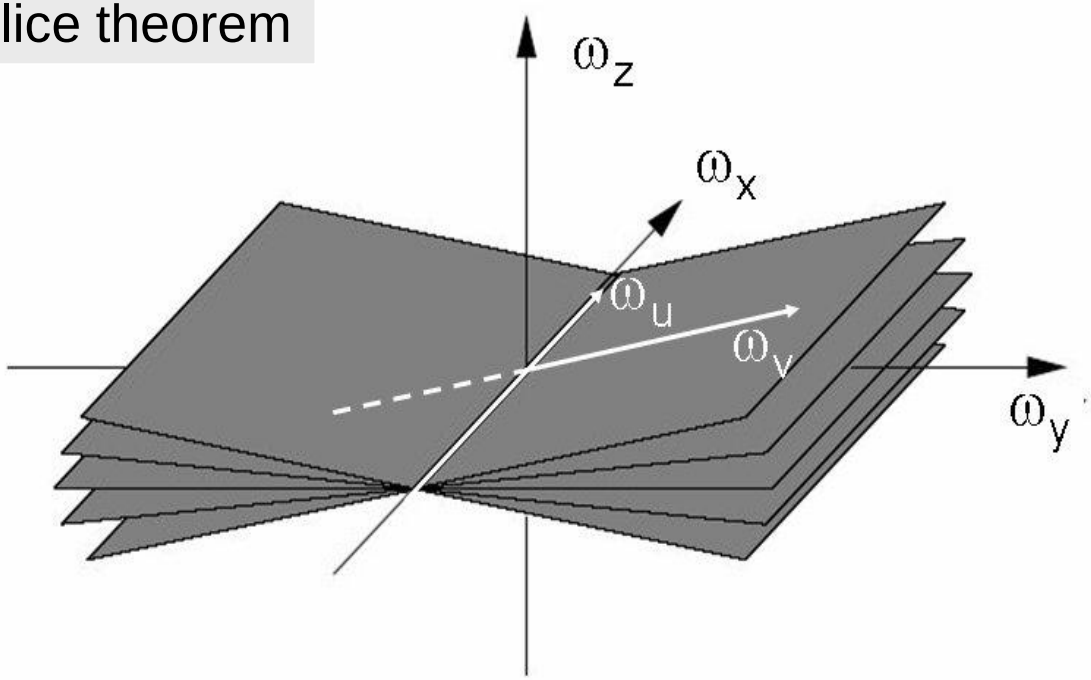

- sampling is incomplete (in Fourier space)
- approximative inversion only
- artifacts

B.3 - 3D spatial frequency domain

CT

Modern Multi-slice VCT scanners have nearly isotropic response with maximum spatial frequencies of .8 to 1.0 cycles/mm

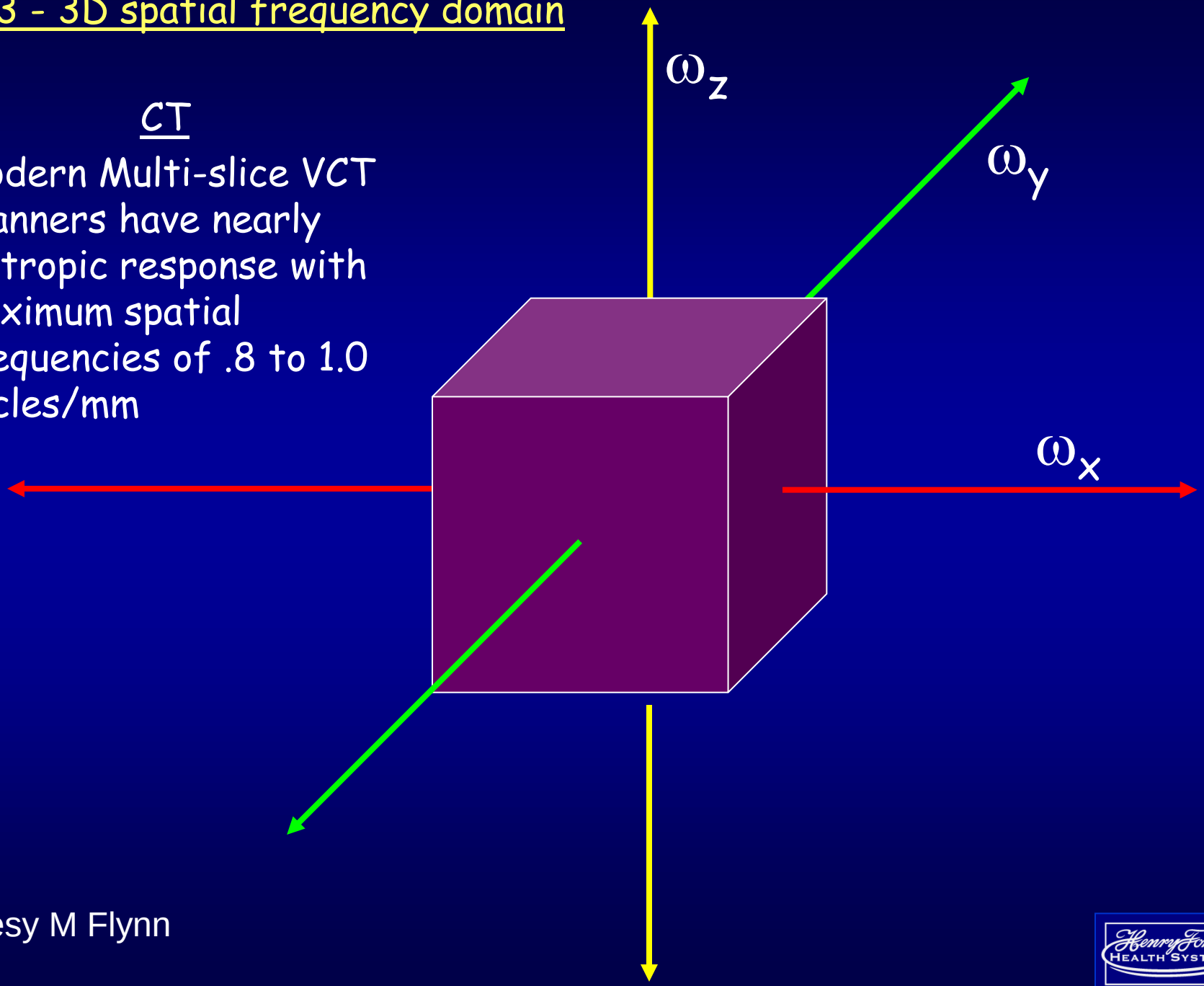

Courtesy M Flynn

B.3 - 3D spatial frequency domain

TS vs CT

Unsampled frequencies along the ω_y axis make TS and CT complimentary.

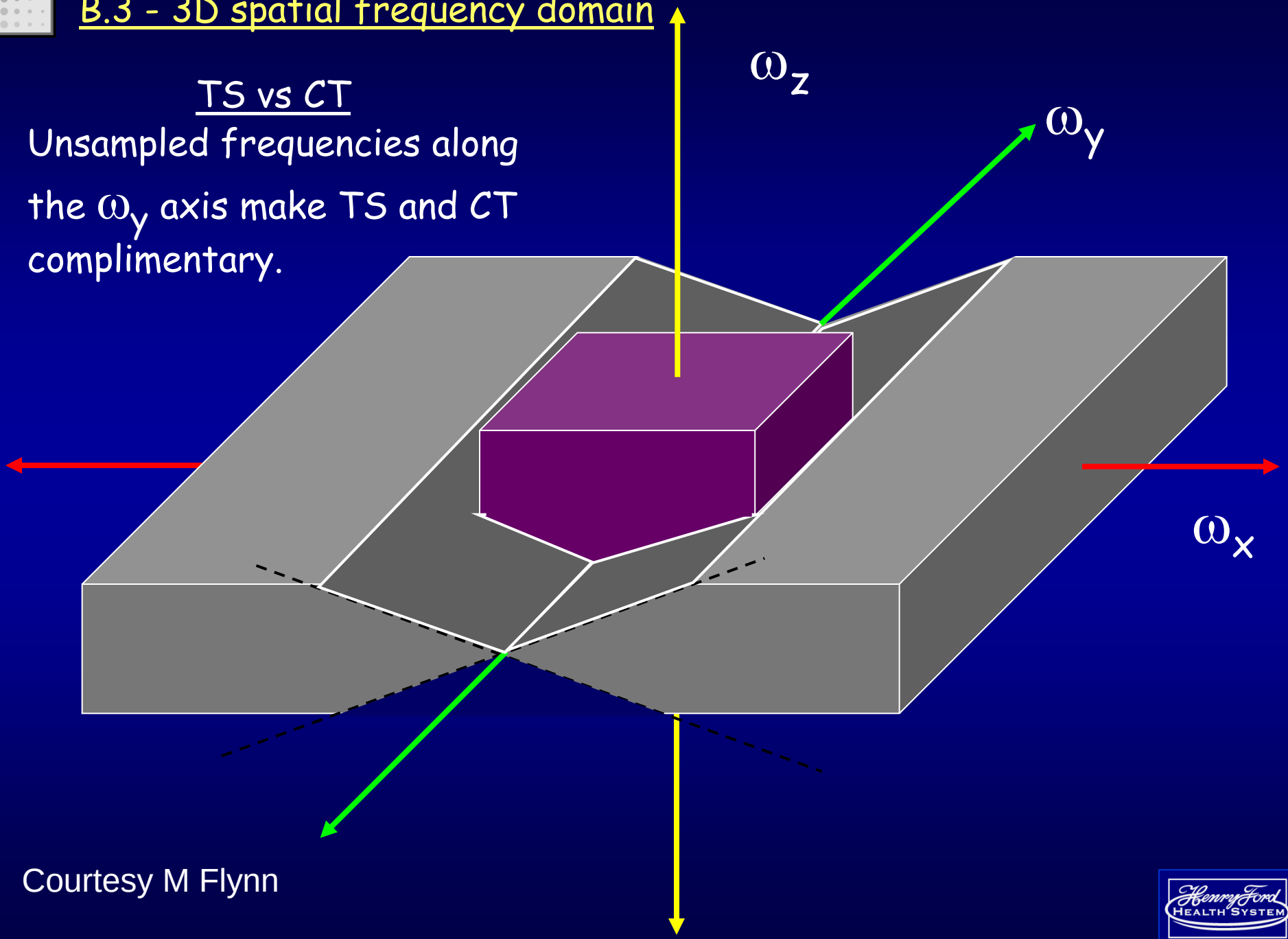

Courtesy M Flynn

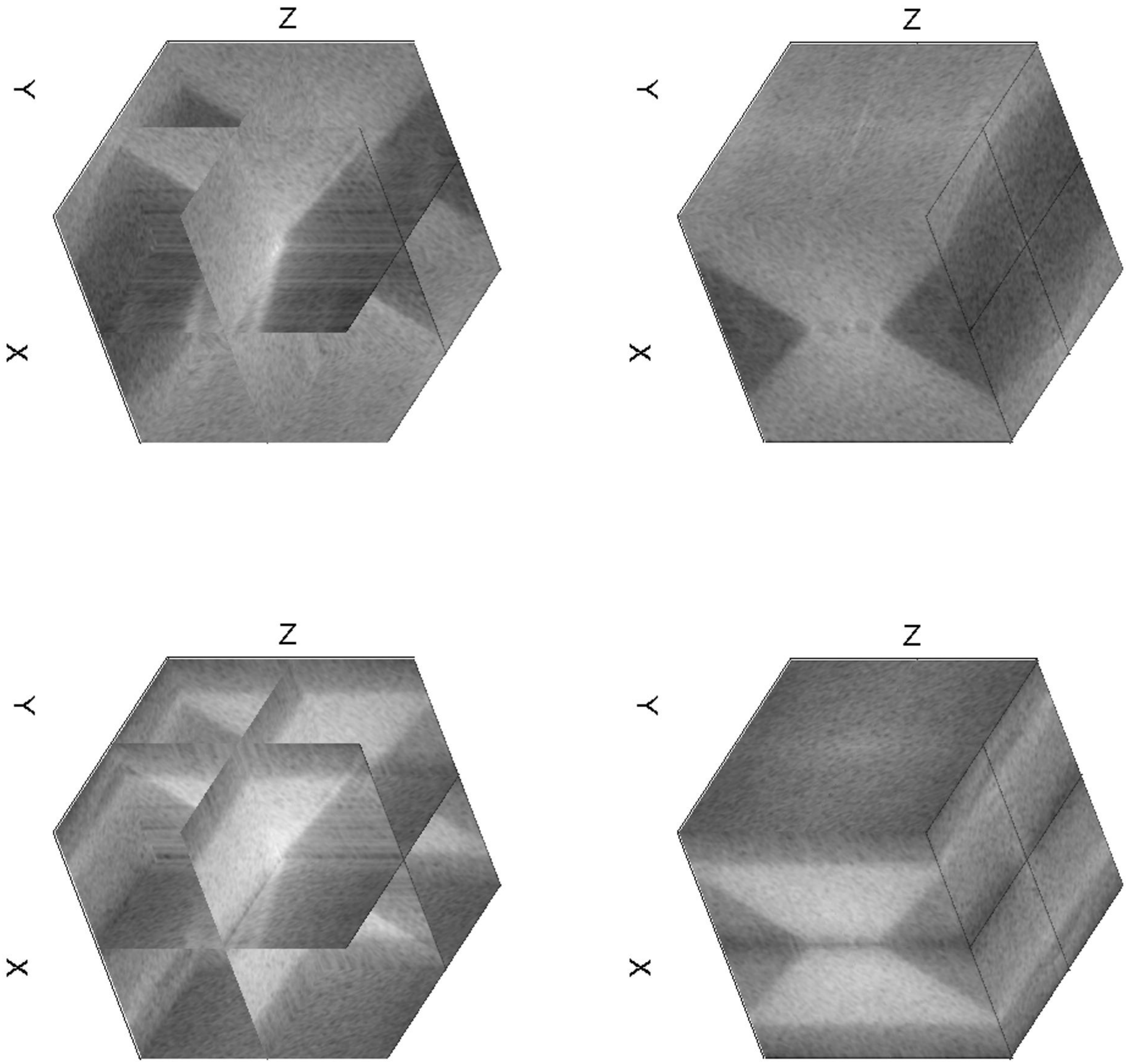

Maidment et al. SPIE 6142 Physics of Medical Imaging 2006

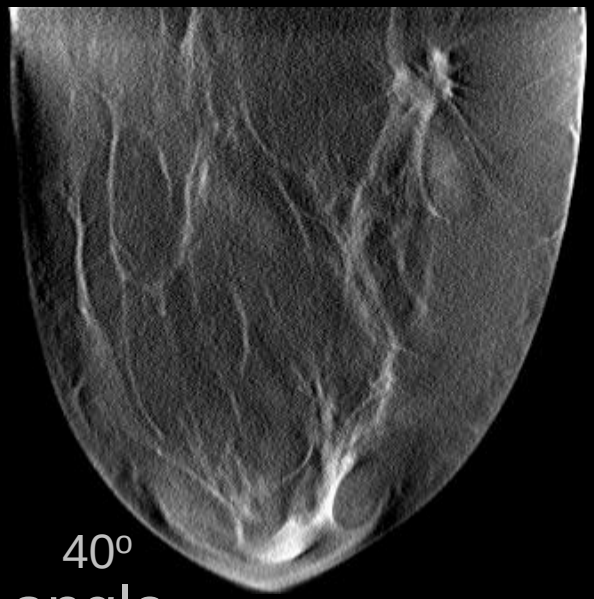

40° angle

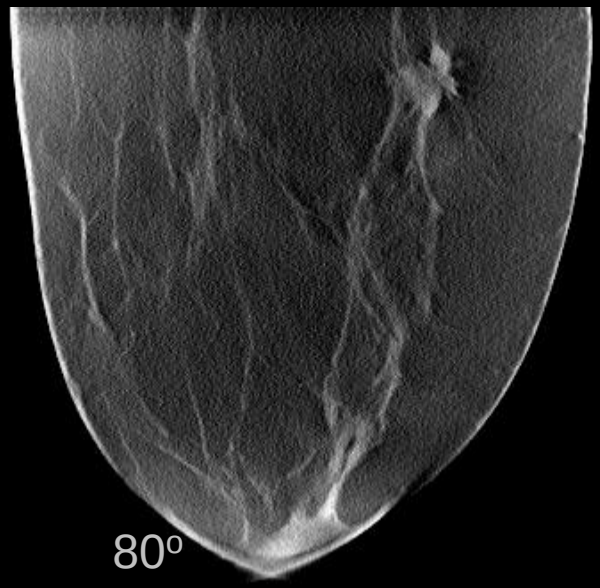

80°

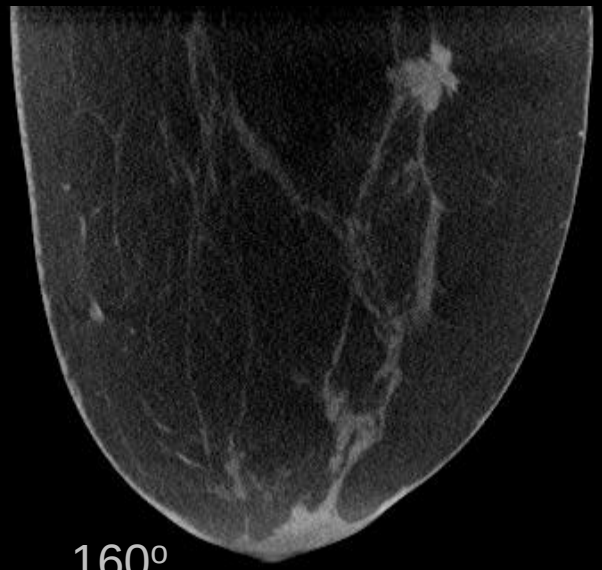

160°

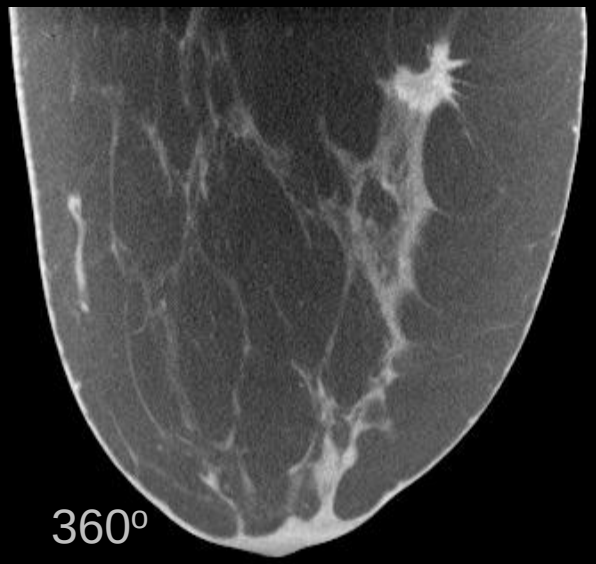

360°

Images Courtesy J. Boone

Tissue Imaging

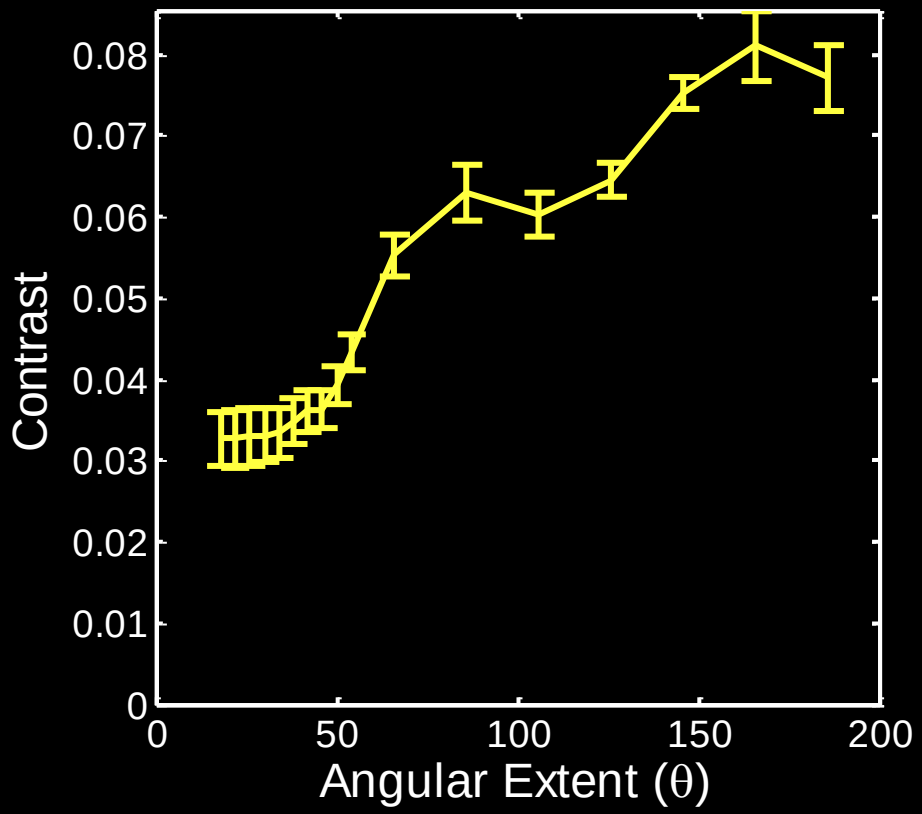

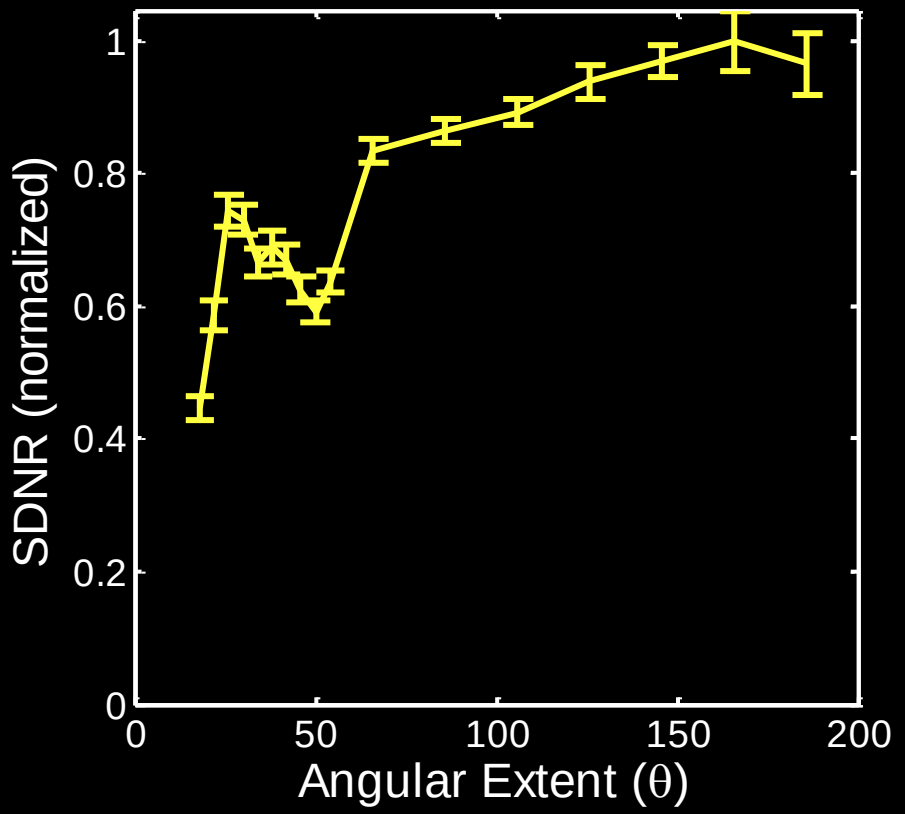

Angular Spacing, $\Delta\theta$=2°

Courtesy M.J. Yaffe

Dose Determines Lesion Detectability

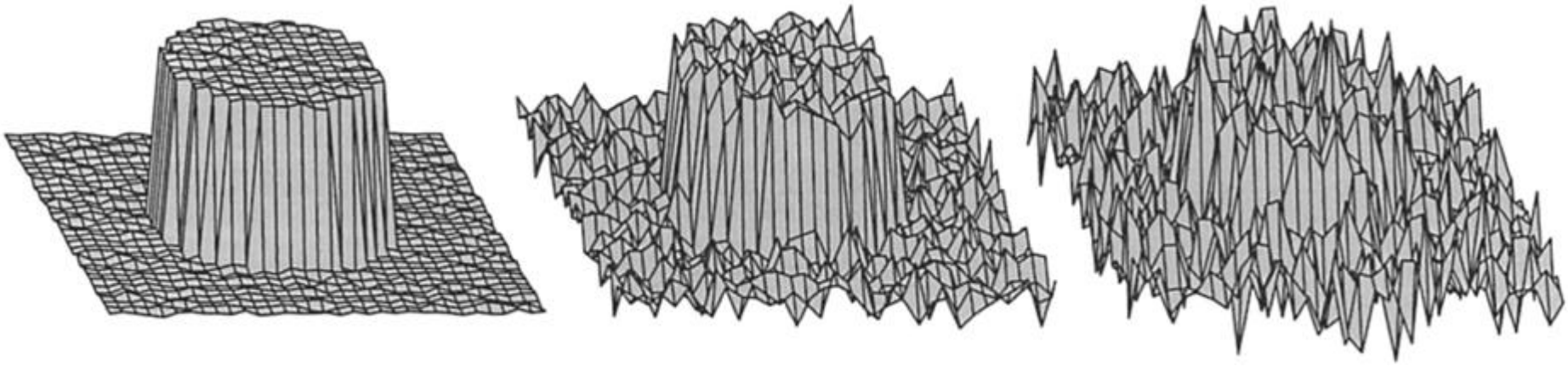

High Dose Medium Dose Low Dose

For an ideal detector, the dose for tomosynthesis should be equal to or less than the dose for digital mammography

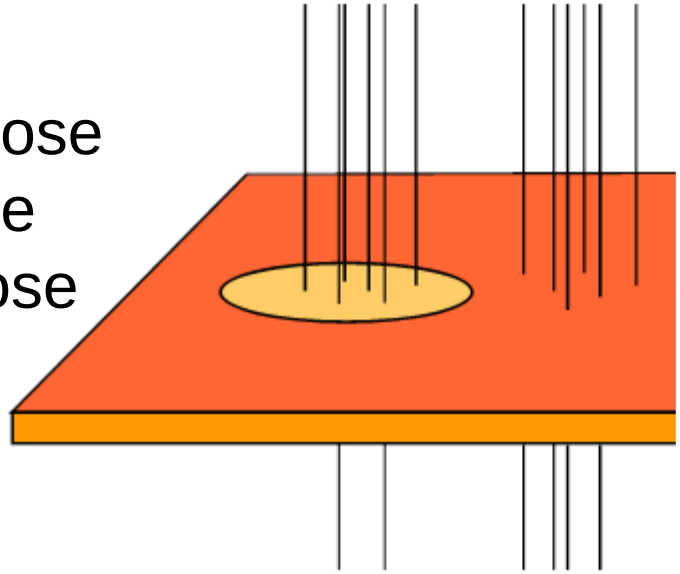

Determinants of Dose

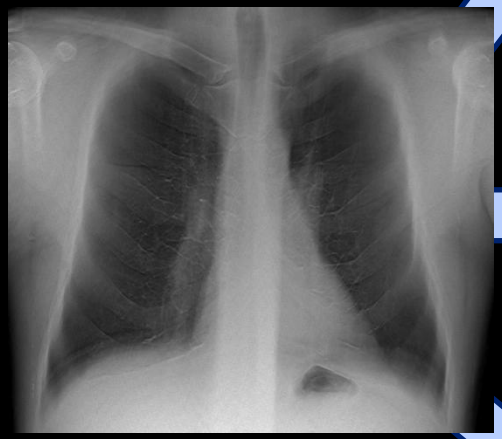

X-ray Beam Quality

- kVp
- Filtration
- Total mAs

Angular Exposure

- Change in SID
- Collimation
- Dose Depth Dependence

Projection Factors

- Number of projections
- mAs per projection
- Technical Limitations (det./gen.)

Tomosynthesis

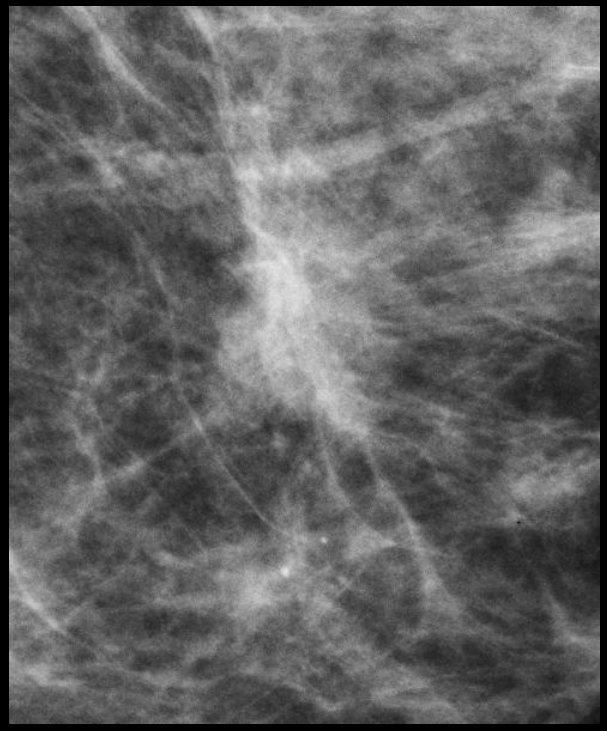

Mammogram

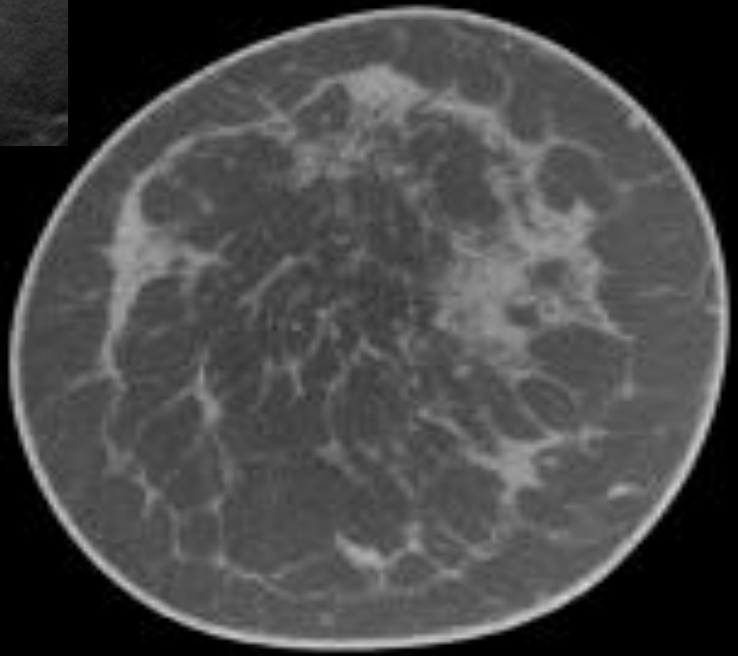

Breast CT

Clinical applications

- Breast
- Chest
- Muskuloskeletal
- Head and Neck
- Angiography
- Dental imaging
- Radiation therapy

Breast Imaging

Hologic Selenia Dimensions Tomosynthesis

- 2D and 3D Imaging under same compression
- W Tube with Rh, Ag and Al Filtration
- 15 degree continuous sweep, 15 images, 3.7 s acquisition
- 200 mA generator, 0.1/0.3 mm focal spot
- 70 cm source-to-detector distance
- Retractable High Transmission Cellular grid
- 24 x 29 cm Selenium Direct Detector, 70 µm pixels

GE Senoclaire Tomosynthesis

- 2D or 3D Imaging under one compression
- Mo/Rh Tube with Mo and Rh Filtration
- 15 degree step and shoot sweep, 9 images, 9 s acquisition
- Grid to reduce scatter
- 24 x 30 cm CsI Indirect Detector, 100 µm pixels
- Iterative Reconstruction

Siemens Mammomat Inspiration With True-Breast Tomosynthesis

- Mo/W Tube with Mo and Rh Filtration
- 50 degree continuous sweep, 25 images, 25 s acquisition
- Retractable grid, with optional digital scatter removal software (mammo)
- 24 x 30 cm Selenium Direct Detector, 85 µm pixels

Case 1:
Potential to reduce false-negative diagnoses

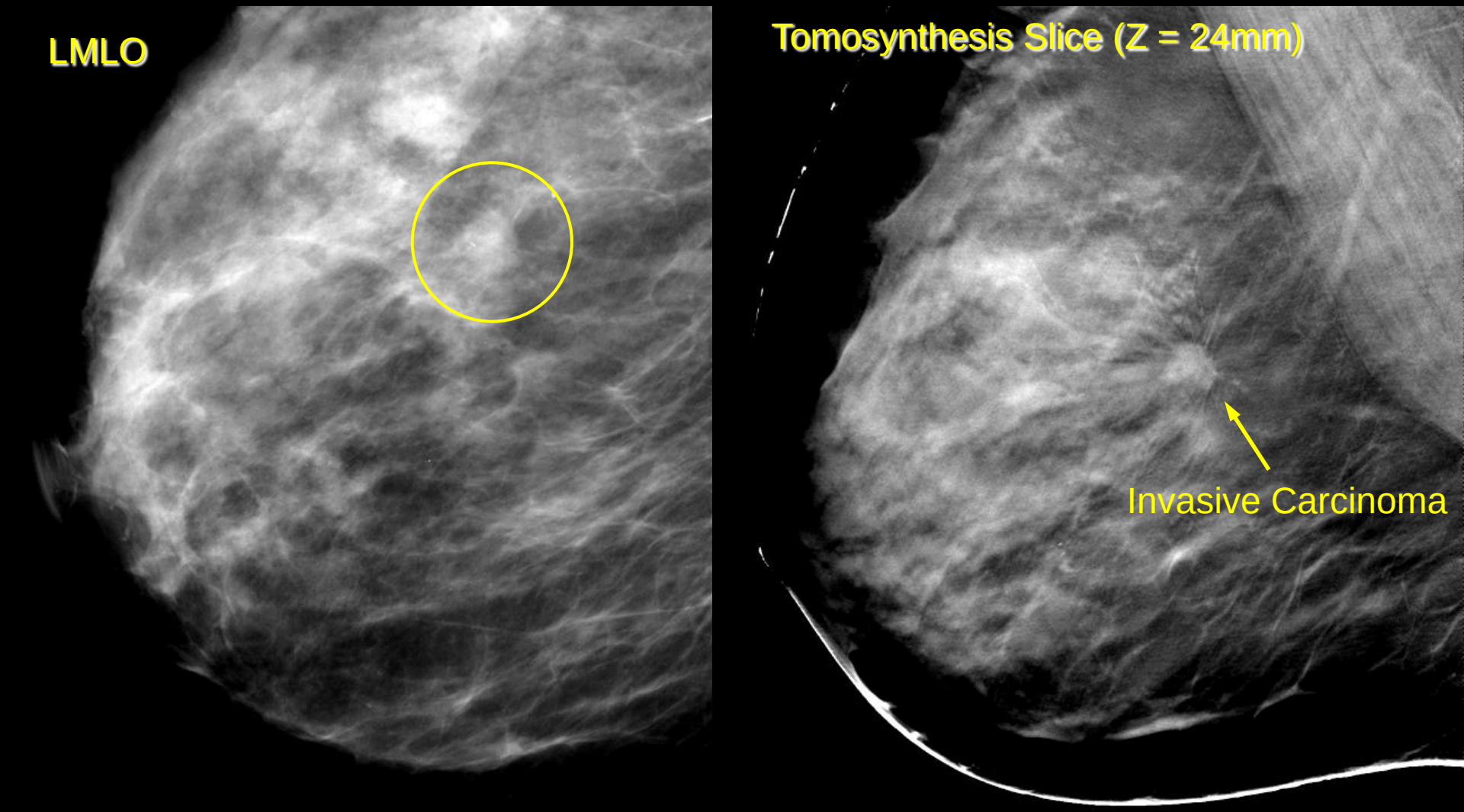

Courtesy of Tao Wu, Ph.D.

Tomosynthesis Mammography Reconstruction Using a Maximum Likelihood Method

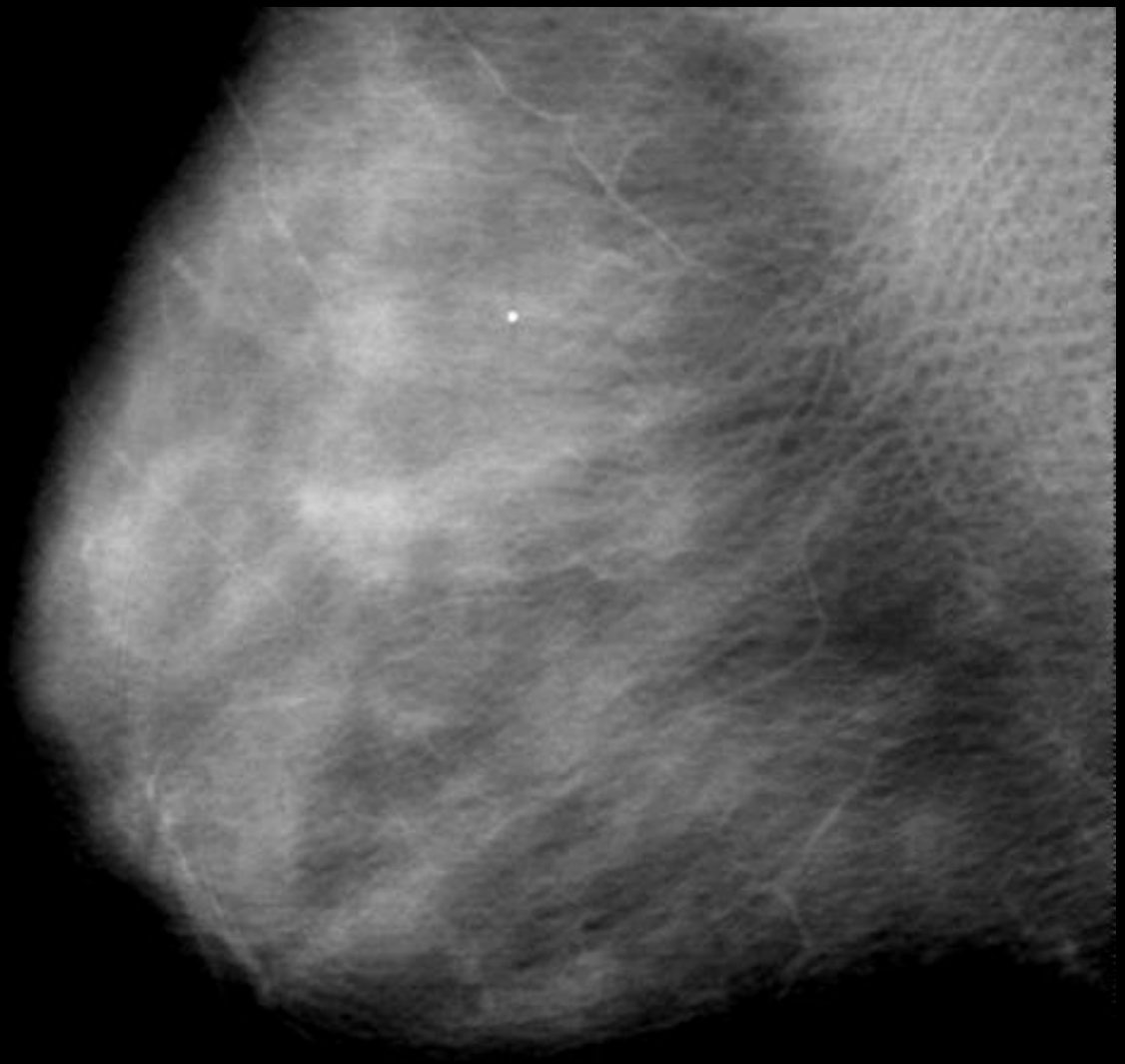

Invasive Ductal Carcinoma

Images courtesy of Dr. Jelle Teertstra
NKI-AVL, The Netherlands

Case 2:
Potential to reduce false-positive diagnoses

LMLO

Courtesy of Tao Wu, Ph.D.

Case 2:
Potential to reduce false-positive diagnoses

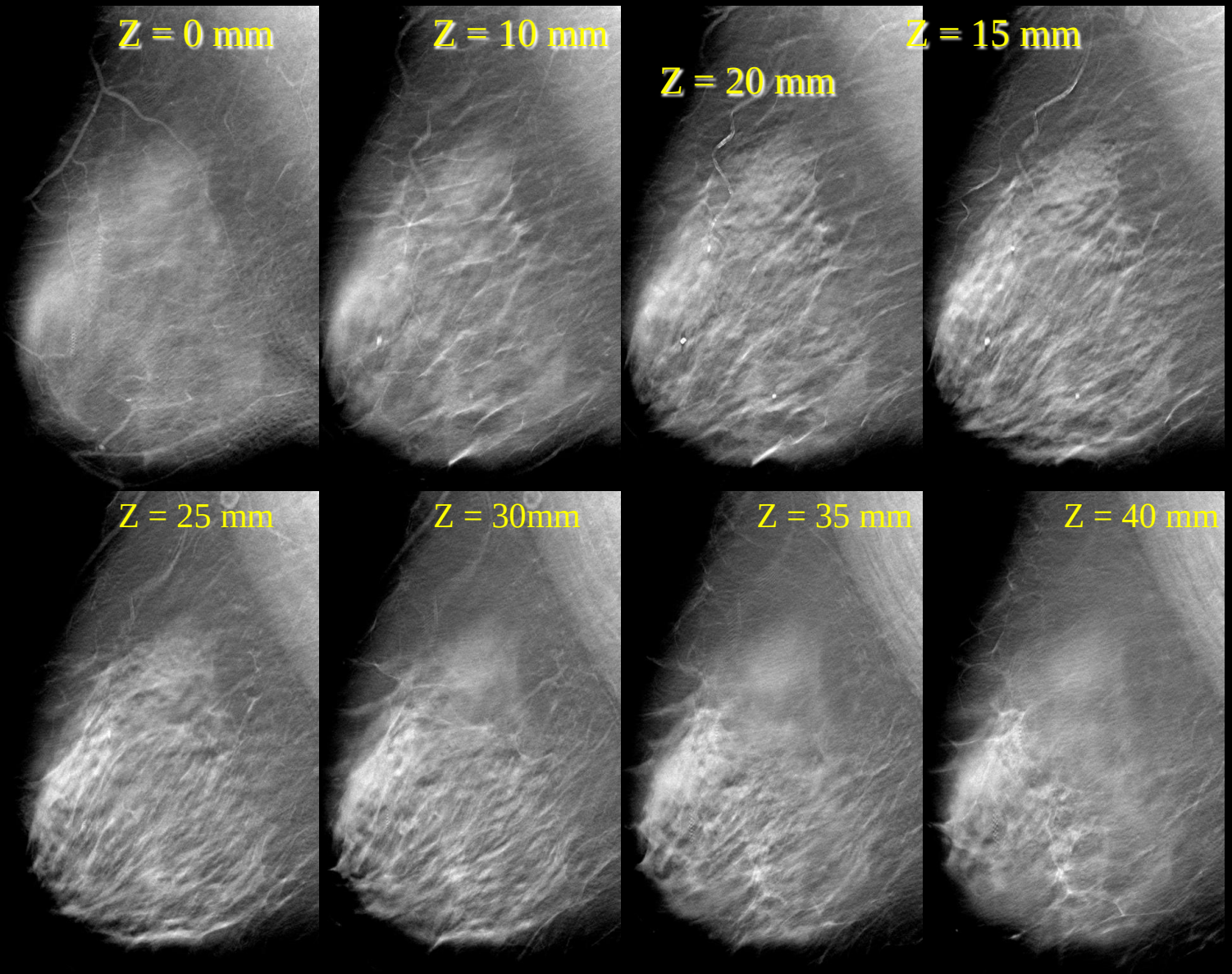

Courtesy of Tao Wu, Ph.D.

Pooled ROC curves for 2 reader studies

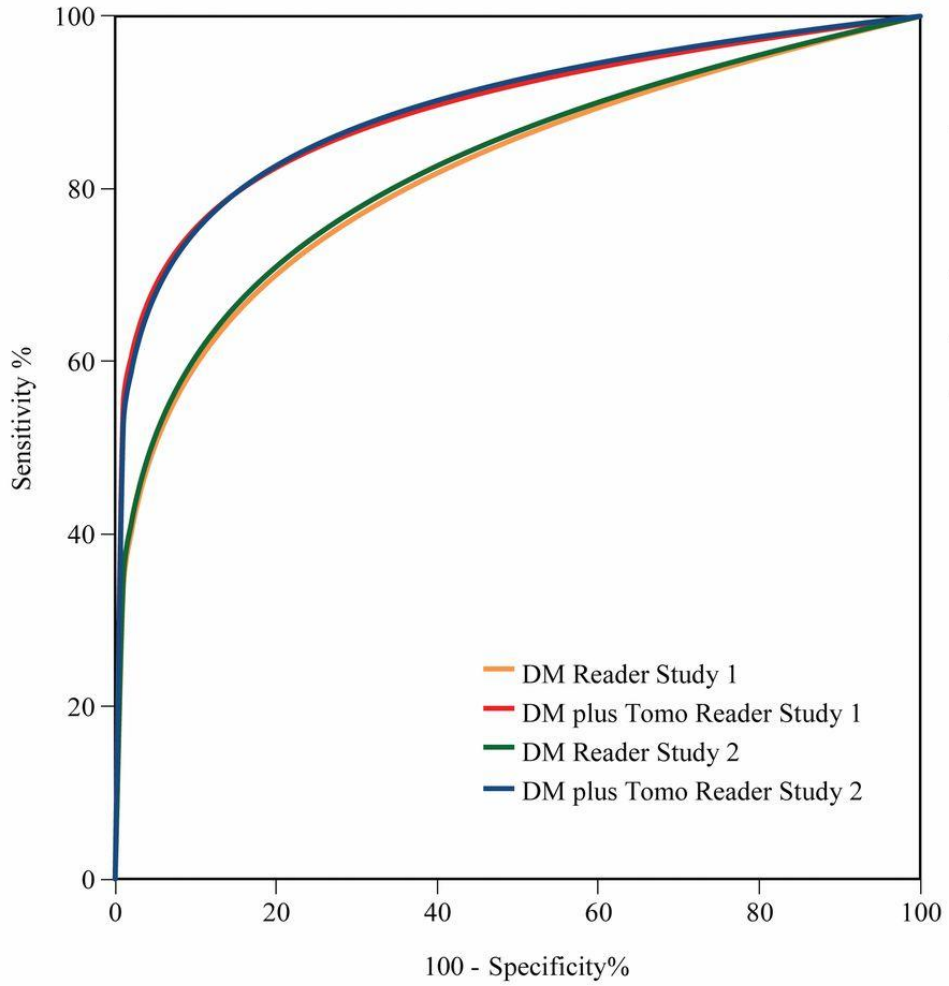

Area under the ROC curve

	DM	DM † plus Tomo	Difference	p-value	95% CI
Reader Study 1	82.1	89.4	7.2	<0.001	3.7 , 10.8
Reader Study 2	82.8	89.5	6.8	<0.001	4.1 , 9.5

Using probability of malignancy scores; curves represent average ROC performance for 12 readers in study 1 and 15 in study 2.

Rafferty E A et al. Radiology doi:10.1148/radiol.12120674

Radiology

Recall rates for individual readers

Non-Cancers

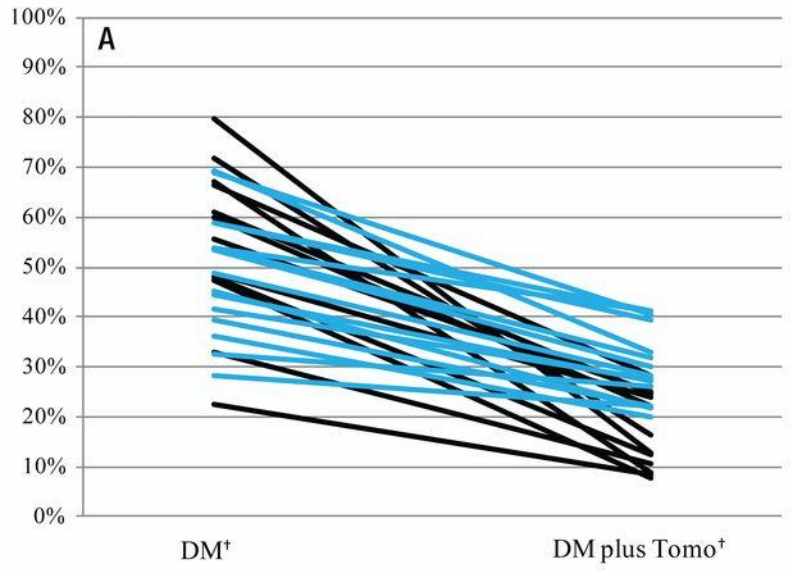

Cancers

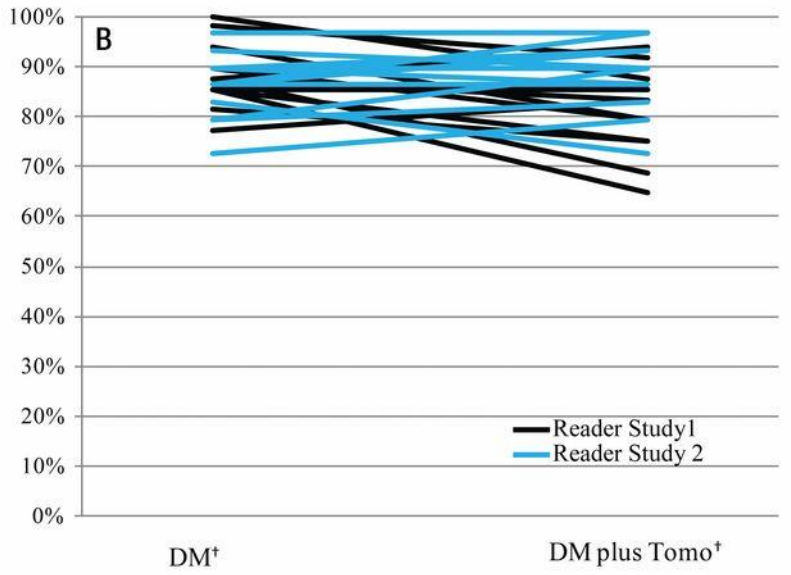

		Recall Rates (Average of Readers)					
		DM			DM plus Tomo		
Case Type	Reader Study	Mean	Range	SD	Mean	Range	SD
Non-Cancer	1	55.1%	22.3% - 79.8%	16.3%	16.7%	7.6% - 28.4%	7.6%
	2	48.8%	28.2% - 69.1%	12.3%	30.1%	19.8% - 41.3%	7.6%
Cancer	1	87.2%	77.0% - 100%	6.5%	80.4%	64.6% - 93.8%	8.8%
	2	84.8%	76.0% - 92.2%	6.1%	85.7%	78.0% - 92.2%	6.4%

Rafferty E A et al. Radiology doi:10.1148/radiol.12120674

Radiology

University of Pennsylvania

2010: 2D Mammo

Sept 2010-Sept 2011:
10814 patients

Call- Back Rate:
10.33%

Cancer Detection Rate:
4.25/1000

2011: Combo-Tomo

Sept 2011-Sept 2012
11115 patients

Call- Back Rate:
8.77%

Cancer Detection Rate:
5.58/1000

Courtesy Emily Conant,

Group Call-Back Rates (CBR) by Month

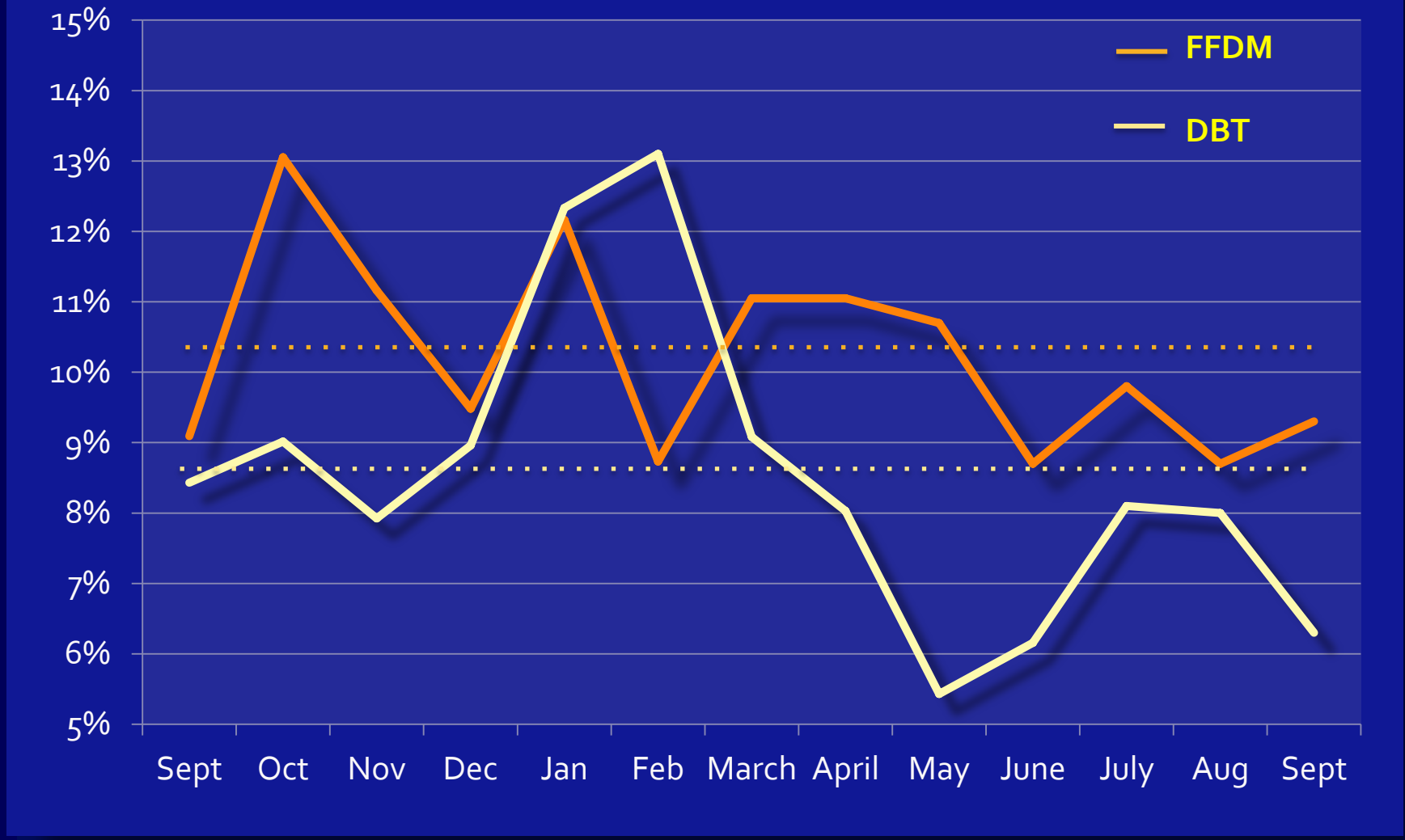

Courtesy Emily Conant,

Cancer Detection Rate (cancers/1000)

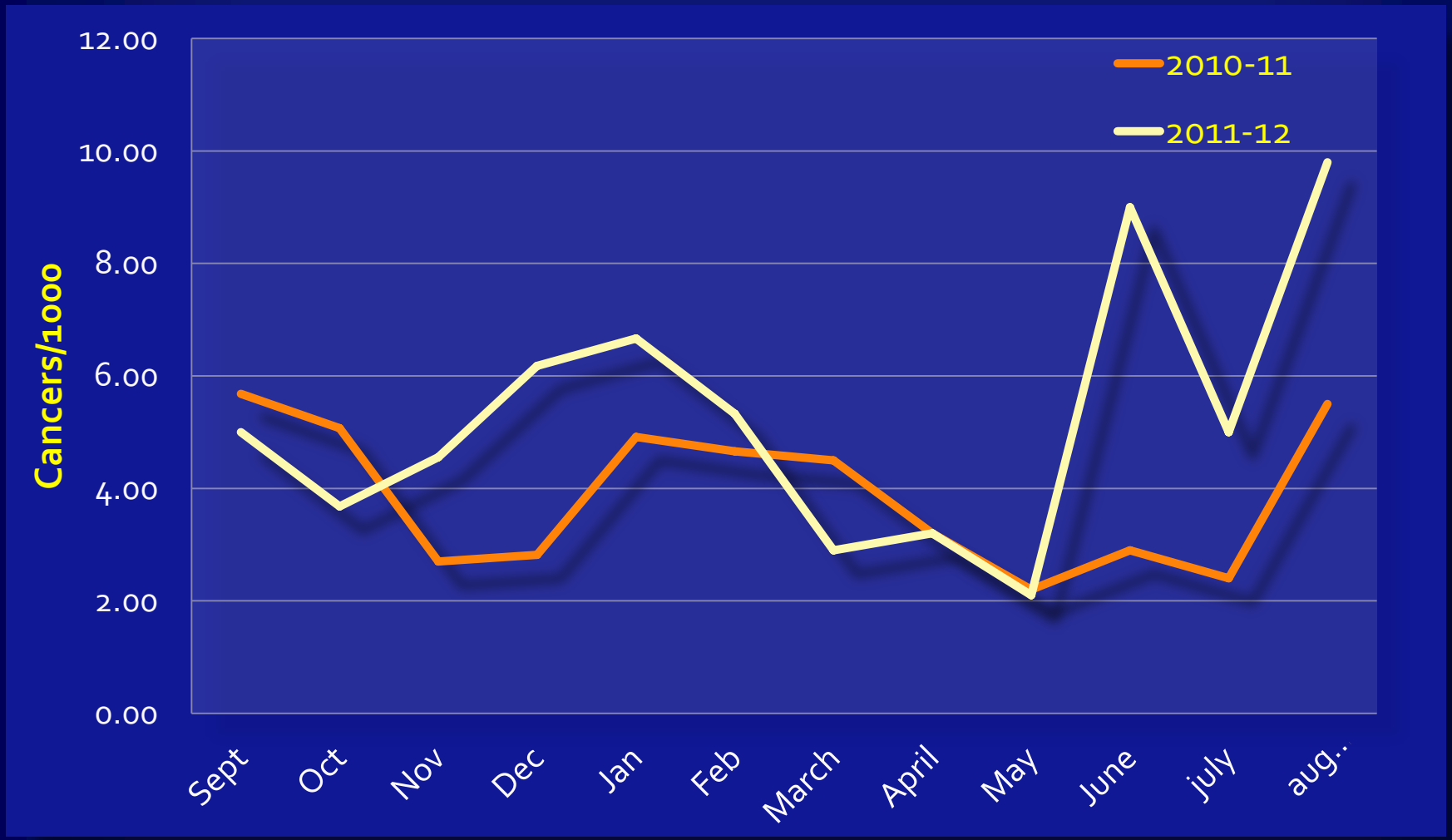

Courtesy Emily Conant,

CBRs pre and post Tomo implementation

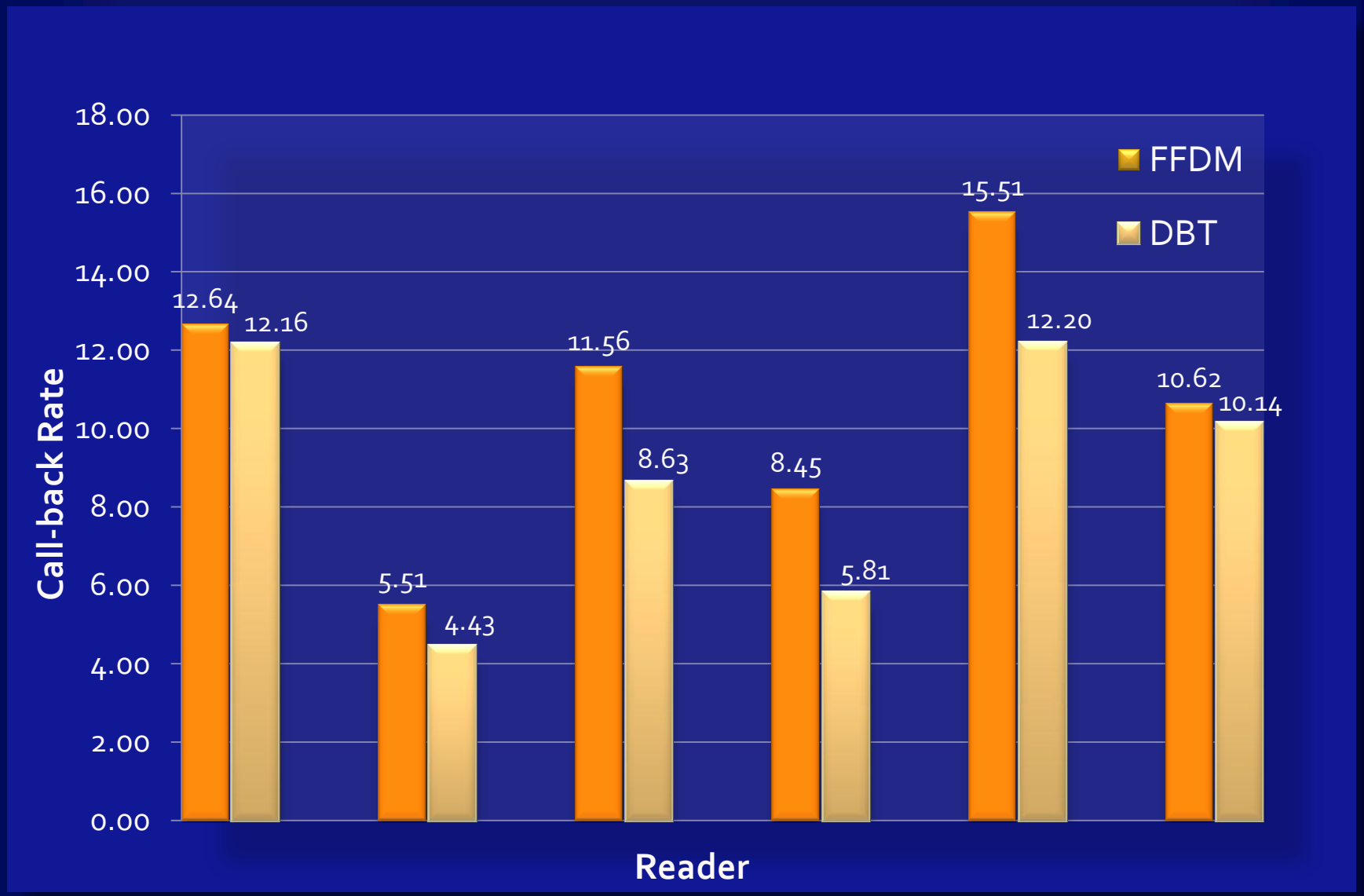

Courtesy Emily Conant,

Tomosynthesis Screening Outcomes

- Individual CBR varied significantly
  - 2010-11 (pre-tomo): from 5.5 to 15.5%
  - 2011-12 (post-tomo) : from 4.4 to 12.2%
- All Readers reduced their CBR
  - Reduction was not based on initial CBR or years in experience
- Group CBR went from 10.33 to 8.7%
  - Largest reduction was from 8.5% to 5.8% (=31.2%)
  - Smallest reduction was from 12.6% to 12.2% (=3.8%)

When controlled for variable reader volumes, OR = 1.24 (p=0.004)
Therefore, the call-back rate decreased by 24% with DBT

Courtesy Emily Conant,

		Mammography Alone				
Radiologist	Years of Experience*	False-Positive Rate†	Cancer Detection Rate†	No. of Known Cancers‡	Detected Cancers (%)§	No. of Patients
1	8	110.7 (80)	6.9 (5)	6	83.3	723
2	21	62.2 (175)	4.6 (13)	24	54.2	2812
3	2	83.3 (131)	4.5 (7)	12	58.3	1573
4	31	39.5 (64)	11.1 (18)	24	75.0	1622
5	29	45.2 (106)	4.7 (11)	19	57.9	2346
6	10	53.8 (78)	6.2 (9)	15	60.0	1451
7	20	71.8 (67)	4.3 (4)	5	80.0	933
8	6	60.3 (70)	8.6 (10)	16	62.5	1161
All		61.1 (771)	6.1 (77)	121	63.6	12621

		Mammography Plus Tomosynthesis				
Radiologist	Years of Experience*	False-Positive Rate†	Cancer Detection Rate†	No. of Known Cancers‡	Detected Cancers (%)§	No. of Patients
1	8	73.6 (46)	11.2 (7)	8	87.5	625
2	21	68.3 (119)	7.5 (13)	15	86.7	1743
3	2	55.3 (82)	4.7 (7)	9	77.8	1483
4	31	44.4 (78)	5.1 (9)	10	90.0	1758
5	29	52.7 (147)	13.3 (37)	43	86.0	2790
6	10	50.6 (71)	5.7 (8)	14	57.1	1402
7	20	52.4 (71)	8.9 (12)	14	85.7	1355
8	6	38.2 (56)	5.5 (8)	8	100.0	1465
All		53.1 (670)	8.0 (101)	121	83.5	12621

Pooled ROC by Lesion Type

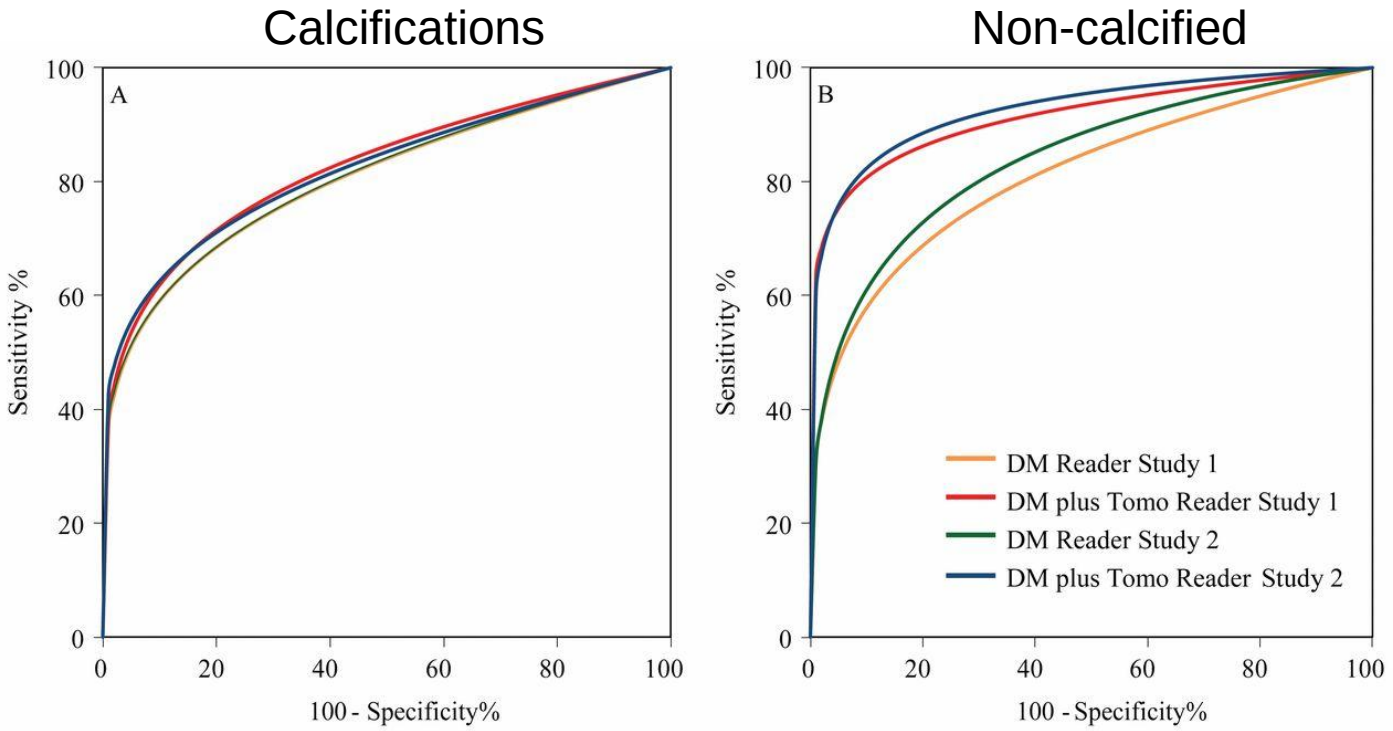

Area under the ROC curve

Case Type	Reader Study	DM†	DM plus† Tomo	Difference	p-value	95% CI
Calcification	1	80.4	84.0	3.5	0.073	-0.4 , 7.4
	2	81.7	83.1	1.4	0.082	-0.2 , 2.9
Non -Calcification	1	80.7	91.2	10.4	<0.001	4.7 , 16.1
	2	84.2	93.0	8.8	<0.001	5.1 , 12.5

Rafferty E A et al. Radiology doi:10.1148/radiol.12120674

ROC curves for average probability of malignancy

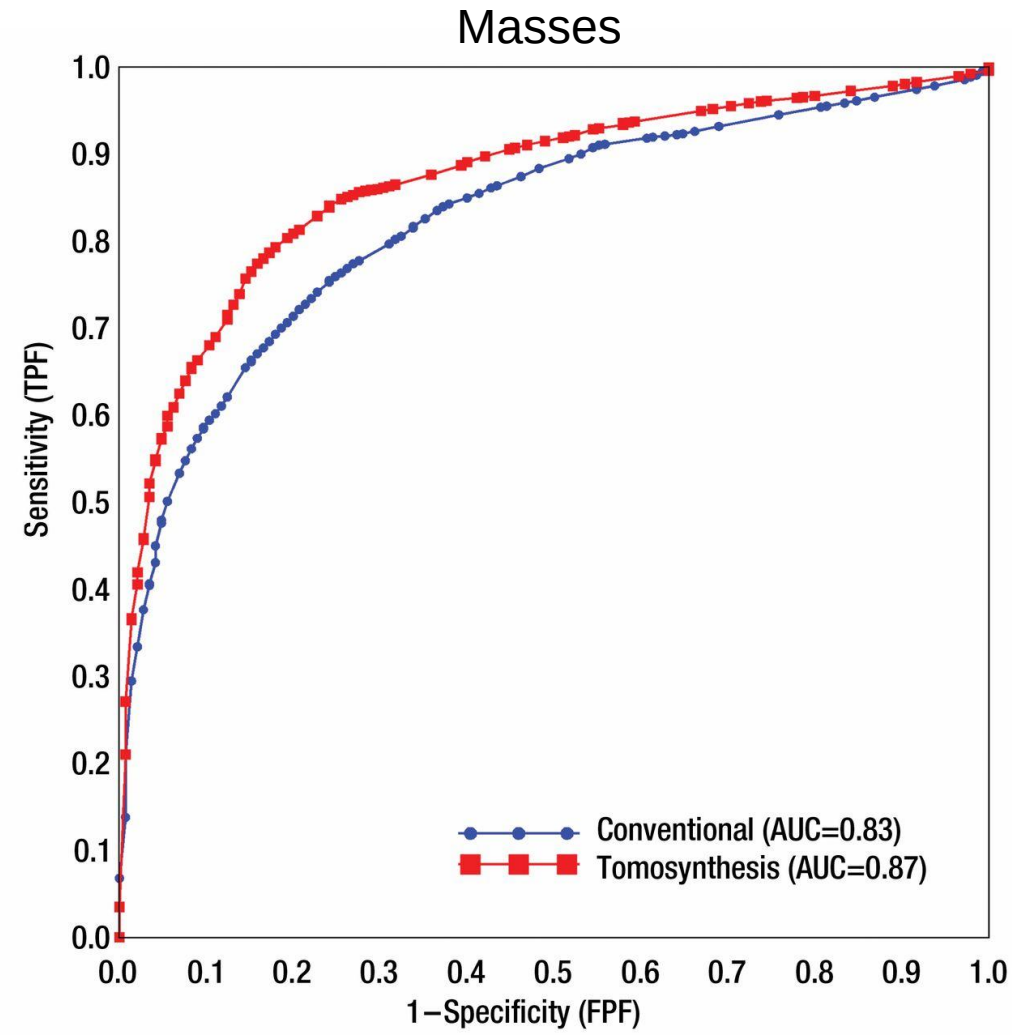

Zuley M L et al. Radiology doi:10.1148/radiol.12120552

Radiology

Digital mammography image of an invasive ductal carcinoma.

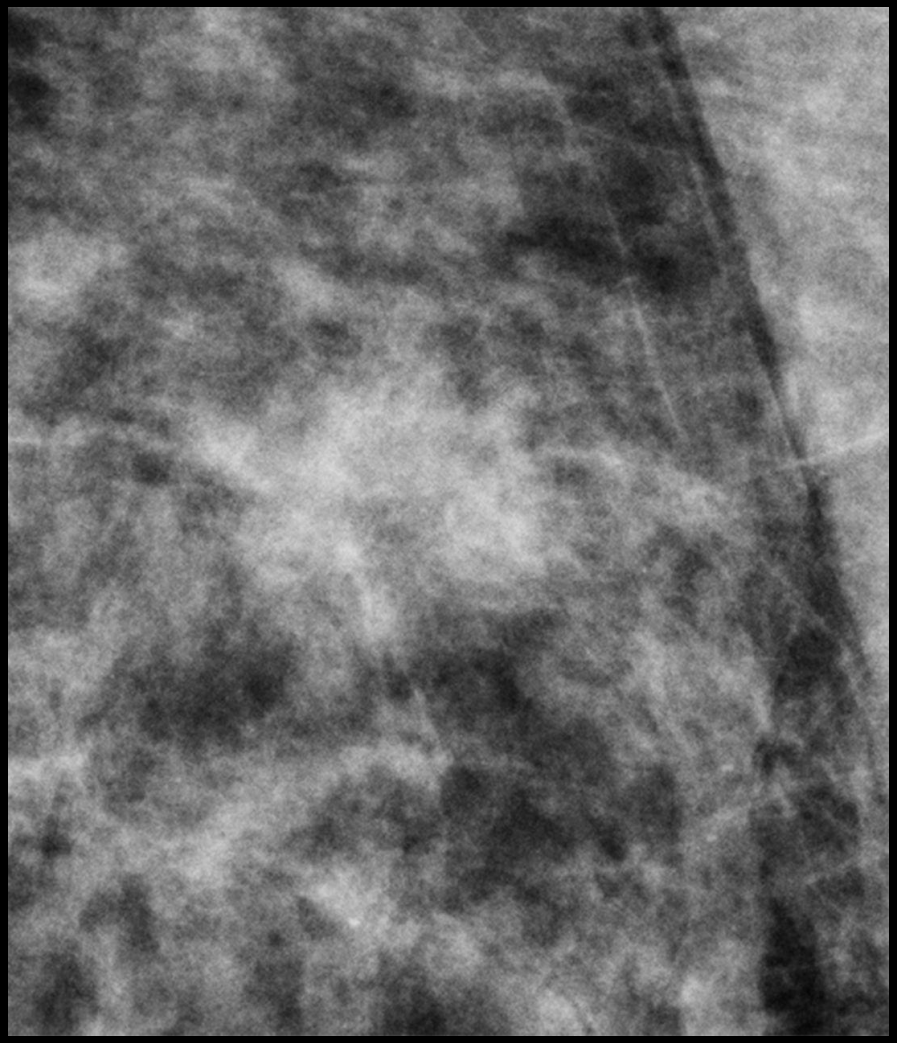

Rafferty E A et al. Radiology doi:10.1148/radiol.12120674

Tomosynthesis image of an invasive ductal carcinoma.

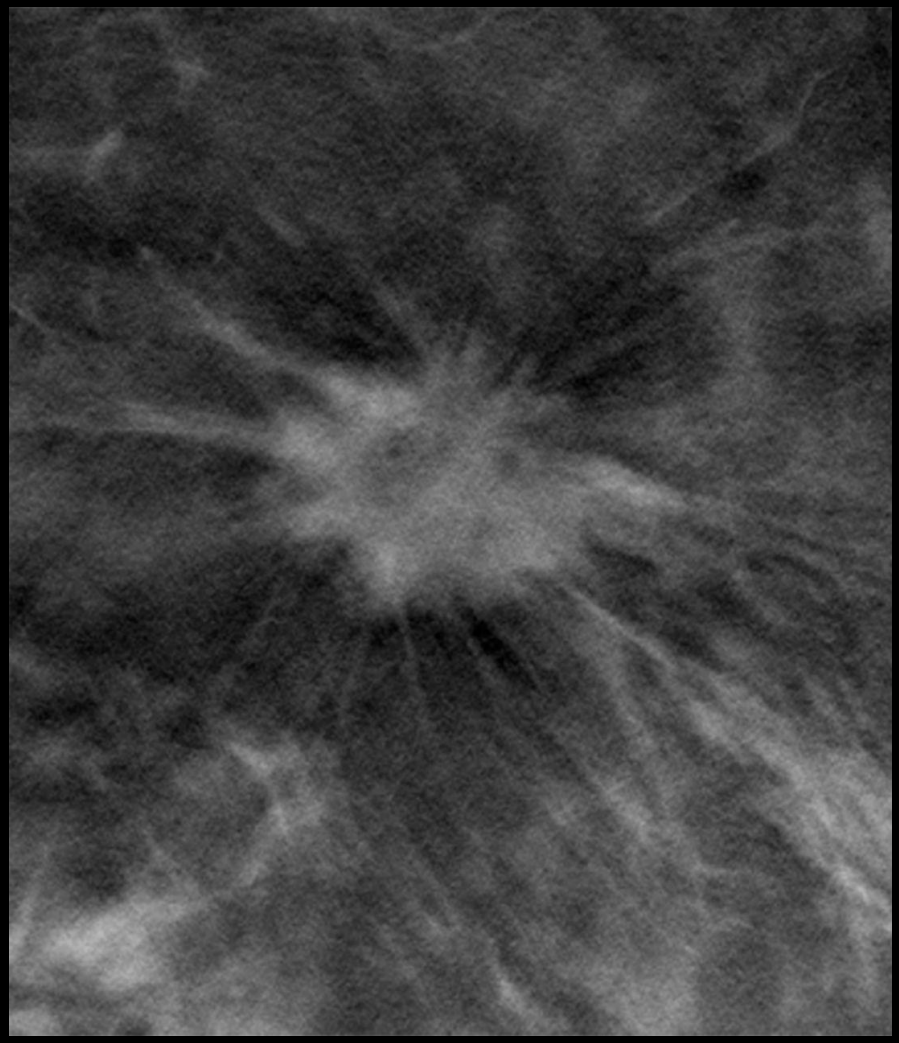

Rafferty E A et al. Radiology doi:10.1148/radiol.12120674

Pooled ROC by Lesion Type

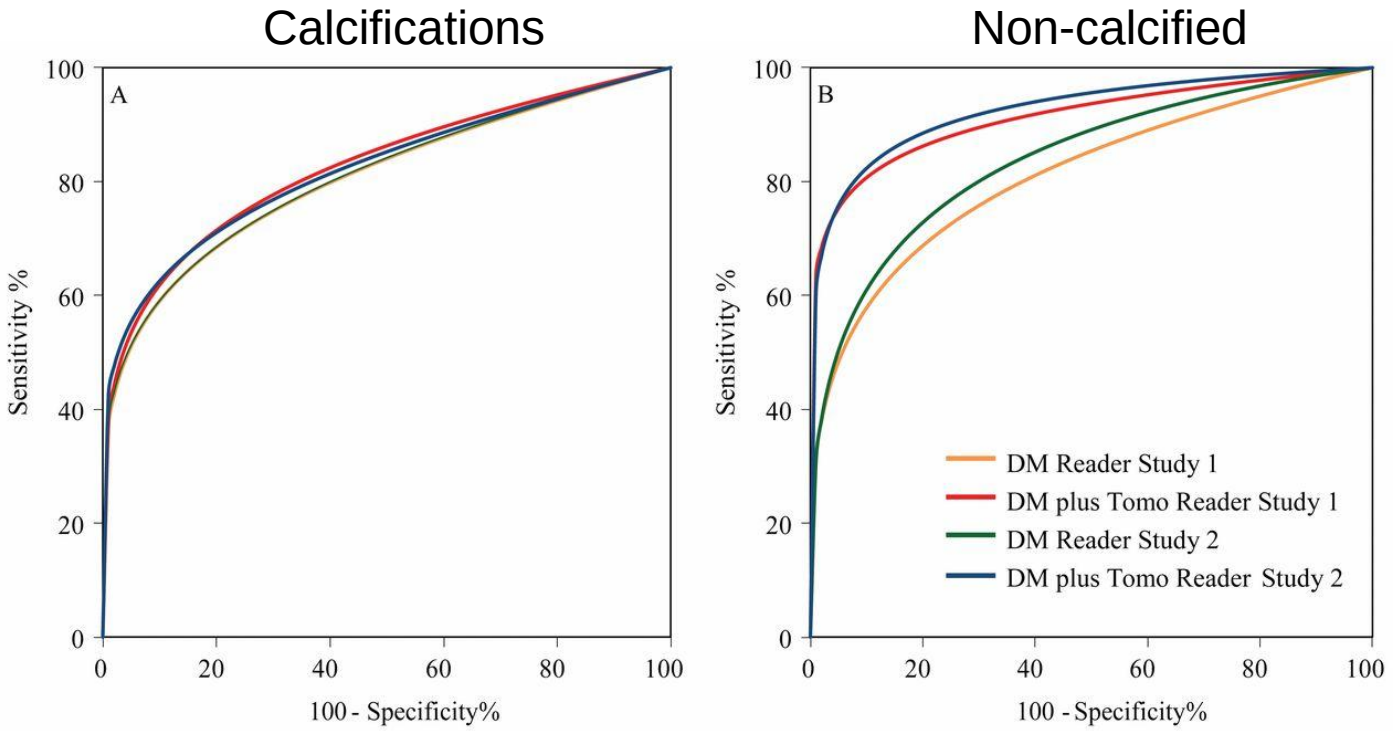

Area under the ROC curve

Case Type	Reader Study	DM†	DM plus† Tomo	Difference	p-value	95% CI
Calcification	1	80.4	84.0	3.5	0.073	-0.4 , 7.4
	2	81.7	83.1	1.4	0.082	-0.2 , 2.9
Non -Calcification	1	80.7	91.2	10.4	<0.001	4.7 , 16.1
	2	84.2	93.0	8.8	<0.001	5.1 , 12.5

Rafferty E A et al. Radiology doi:10.1148/radiol.12120674

Visualization of micro-calcifications

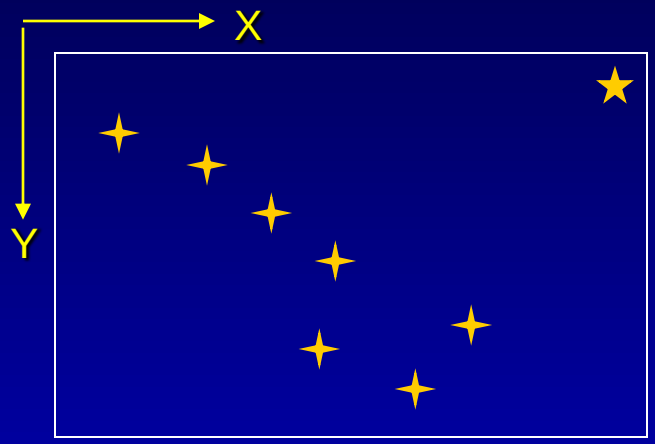

Simulated pattern of clustered μCas
(Pattern: Big Dipper and Pole Star)

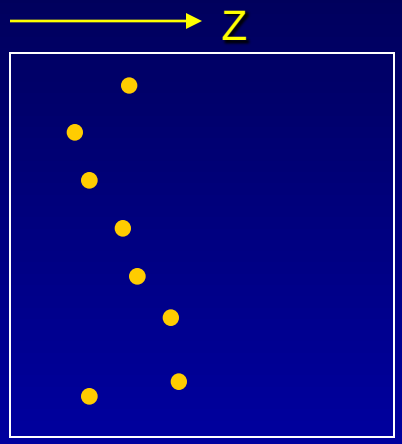

Distribution along z-direction

Conventional mammography:

- Clustered μCa are projected onto a 2-D plane.
- The pattern of μCa distribution is obvious.
- The pattern of μCa distribution contains important diagnostic information.

Visualization of micro-calcifications

DBT reconstruction

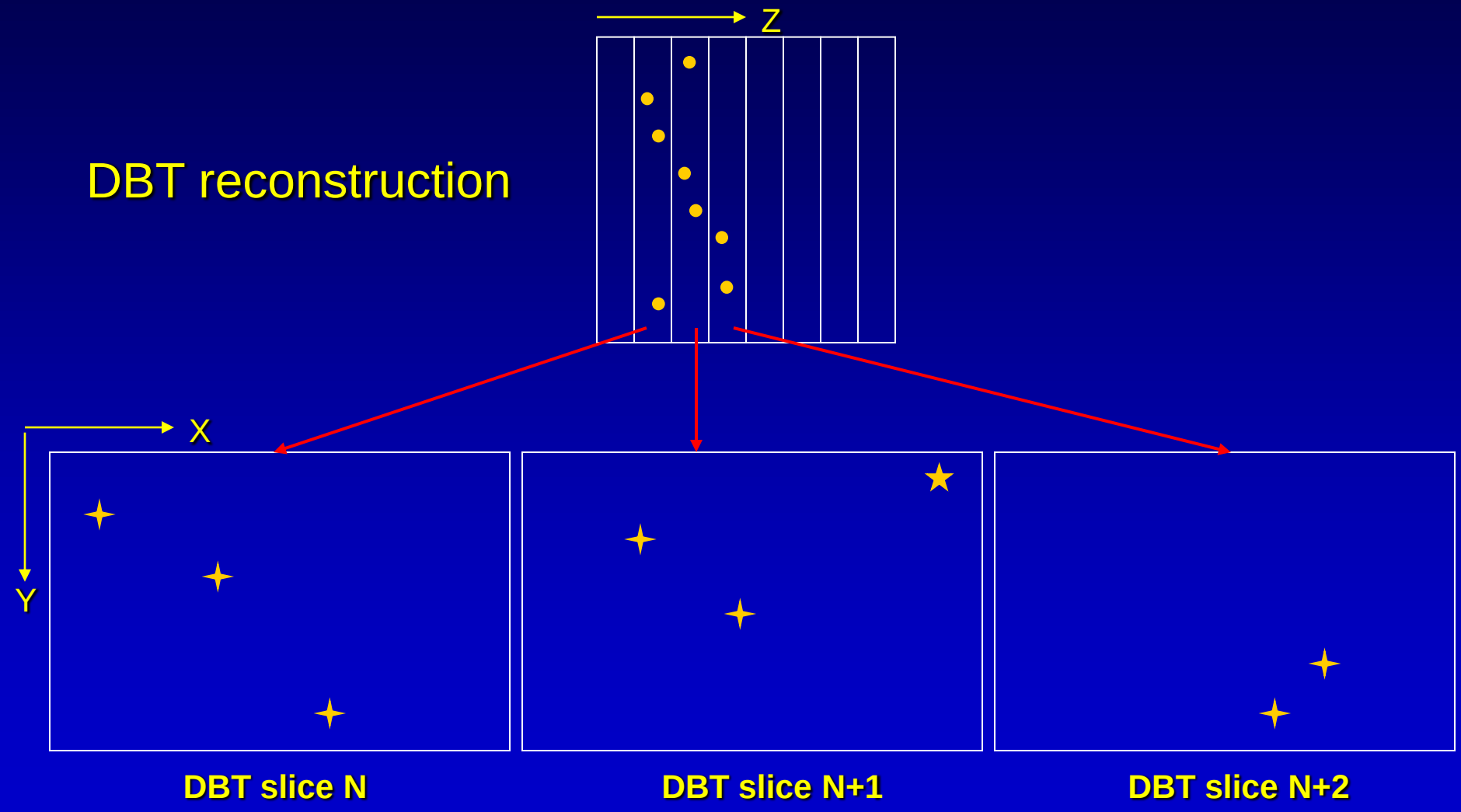

The pattern of μCa cluster is lost.

Visualization of micro-calcifications

"Slab View" for showing clustered μCa:
- Combine multiple slices into a "slab"
- Maximum intensity projection (MIP) within the slab
- Slide the "slab window" through the reconstruction

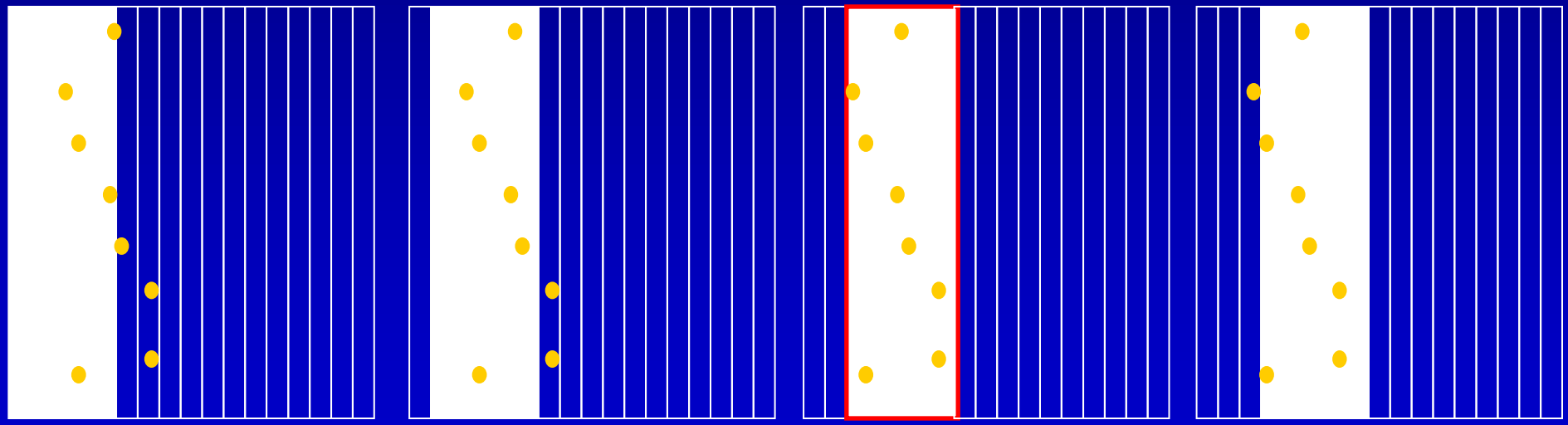

Visualization of micro-calcifications

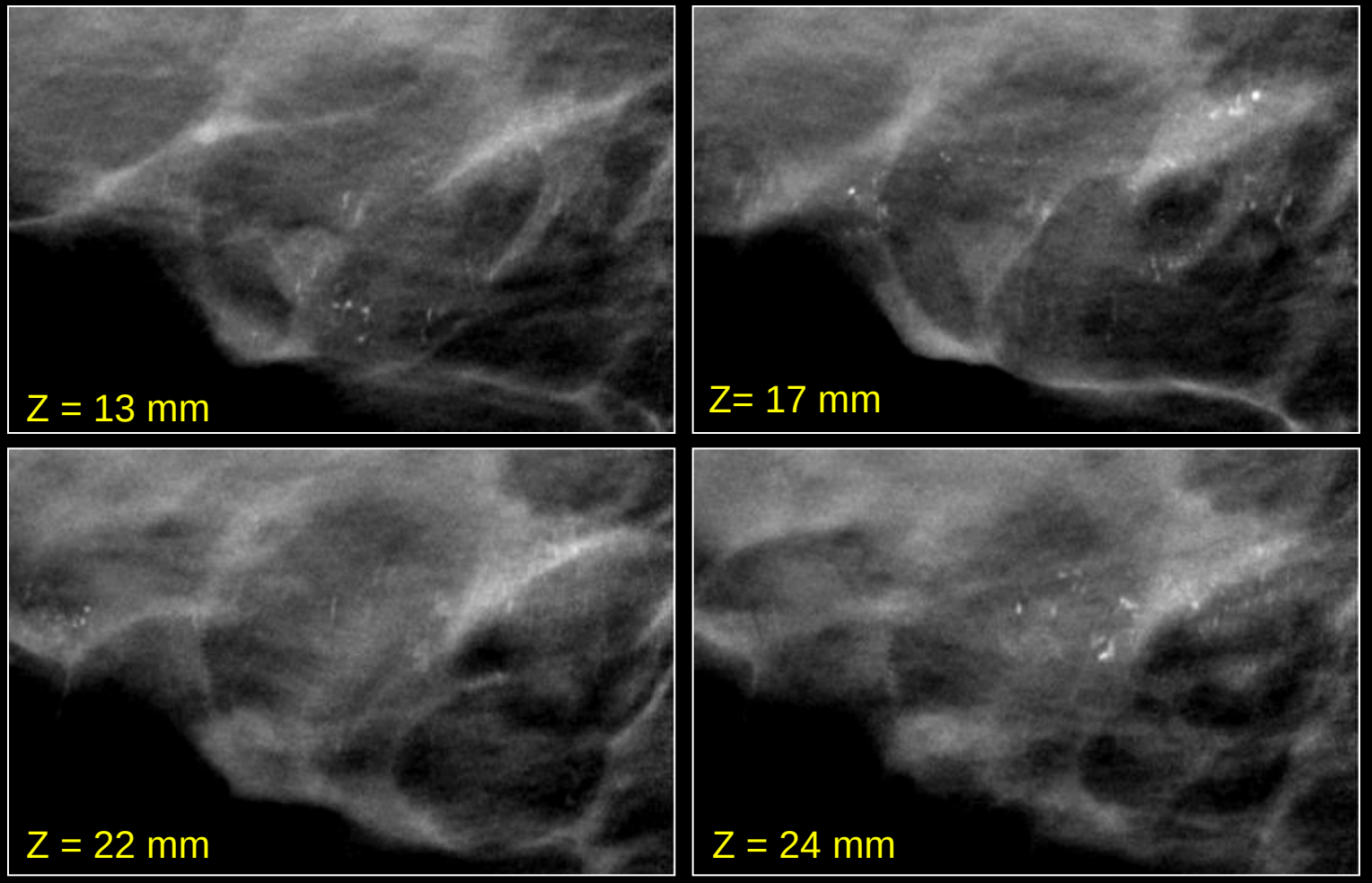

DBT reconstruction (1 mm slice)

Visualization of micro-calcifications

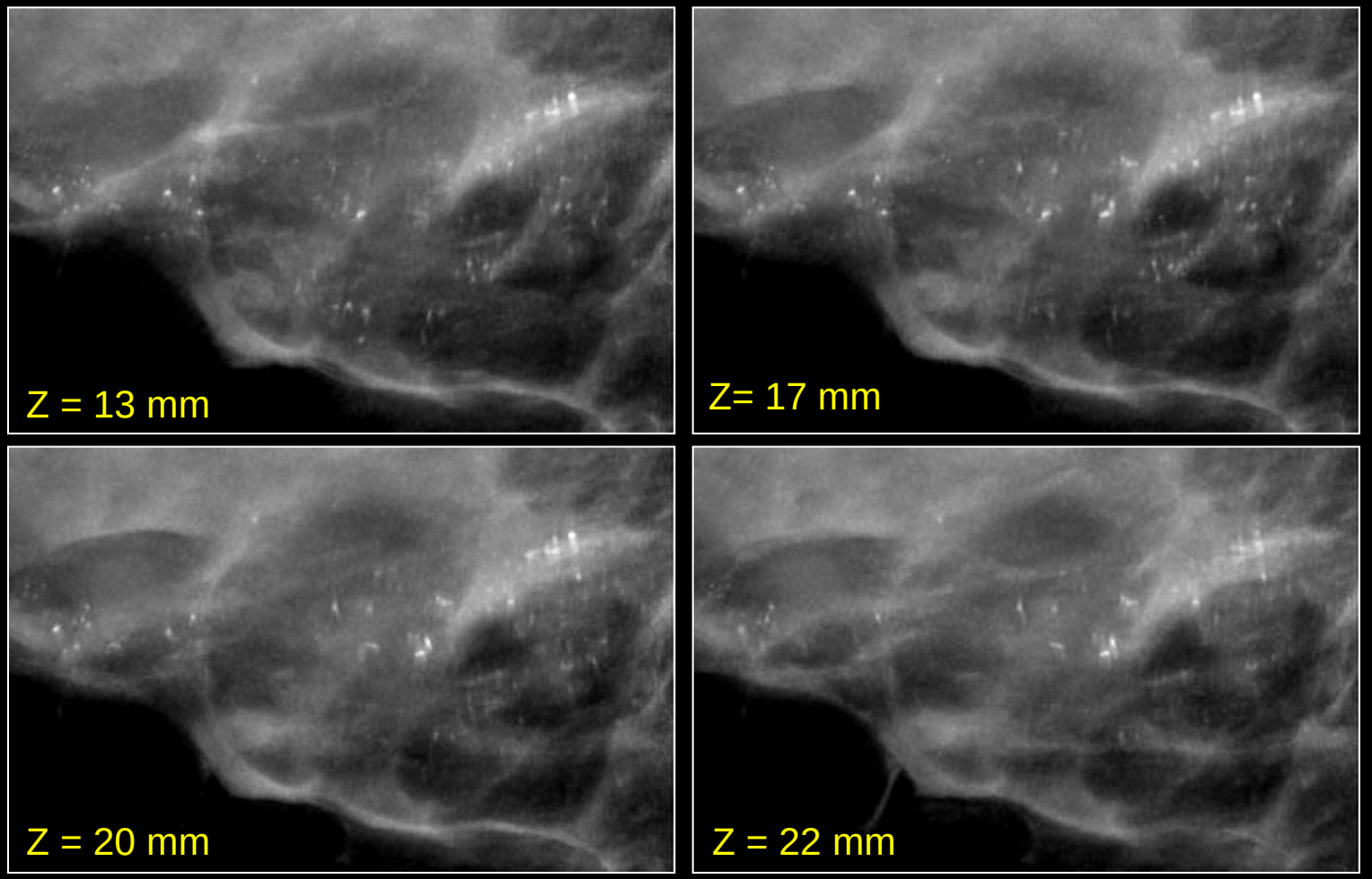

Slab View: 10 mm slab

Average Glandular Dose in Digital Mammography and Breast Tomosynthesis

Mittlere Parenchymdosis bei der digitalen Mammografie und der Brusttomosynthese

Authors T. Olgar[1,2], T. Kahn[2], D. Gosch[2]

Affiliations
[1] Faculty of Engineering, Department of Engineering Physics, Ankara University
[2] Klinik und Poliklinik für Diagnostische und Interventionelle Radiologie, Universitätsklinikum Leipzig AöR

2D: AGD 1.61 mGy

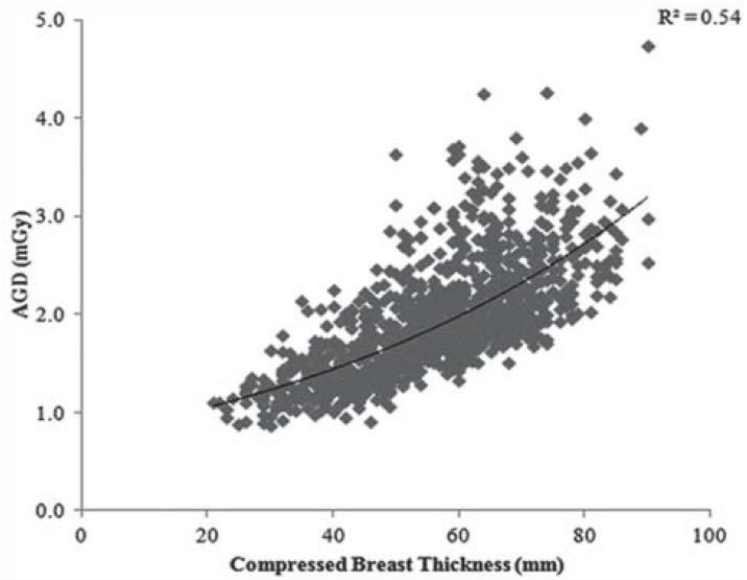

3D: AGD 2.22 mGy

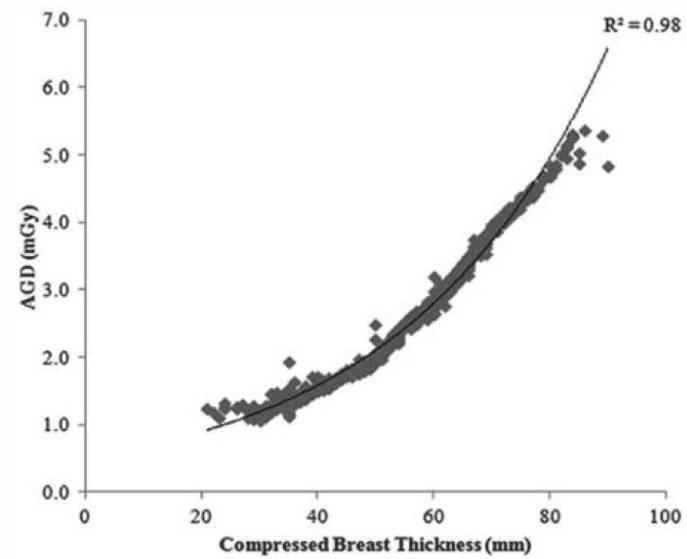

Average Breast Thickness – 55 mm

Results – MGD and Thickness & Glandularity

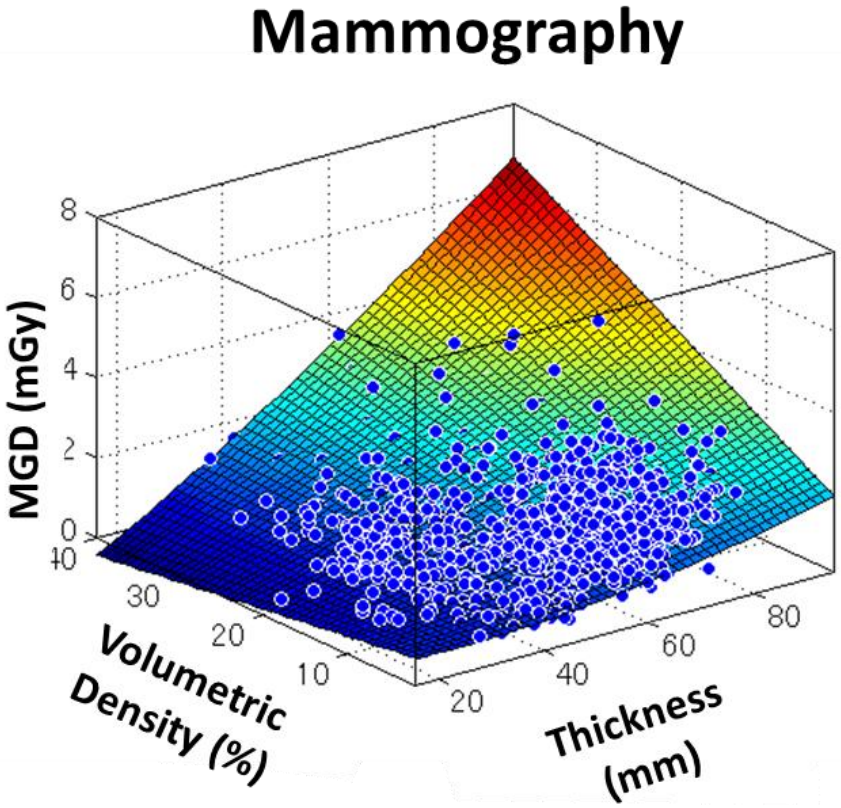

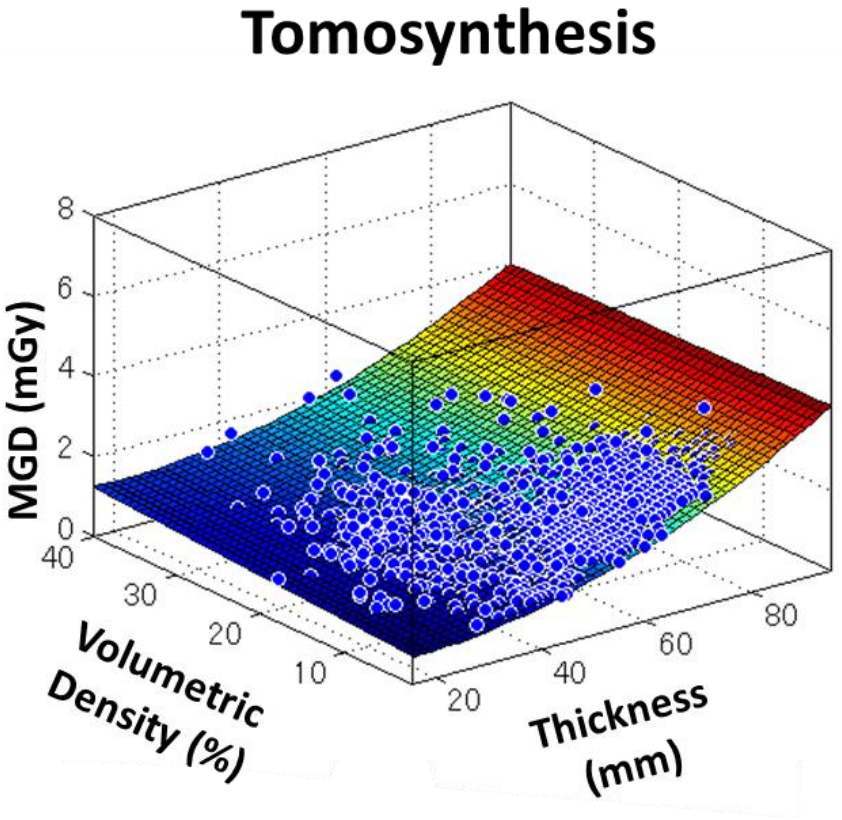

Digital Mammography:

- MGD is dependent on *both* **thickness** and **glandularity** (**p<0.001**)

Tomosynthesis:

- MGD is dependent on **thickness** (**p<0.001**) but **not glandularity** (**p=0.11**)

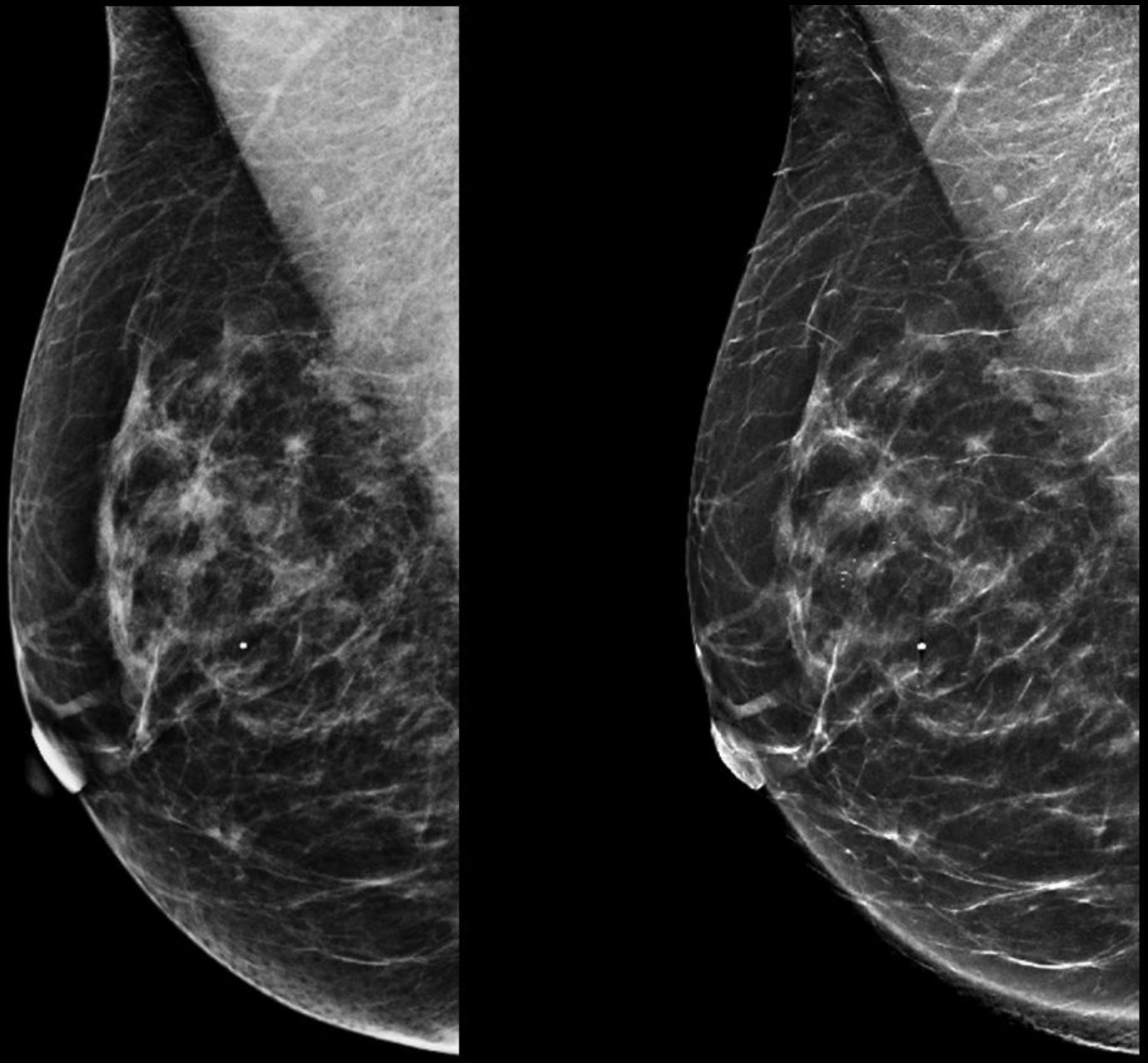
True 2D
Synthesized 2D

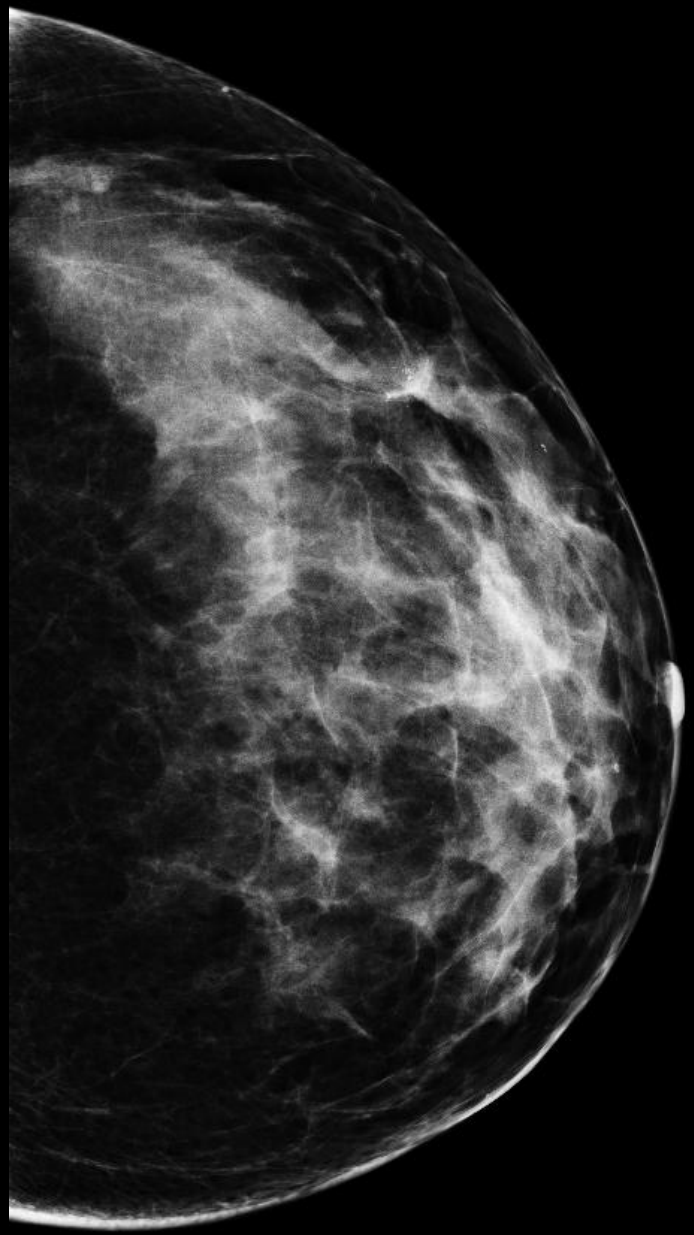

True 2D

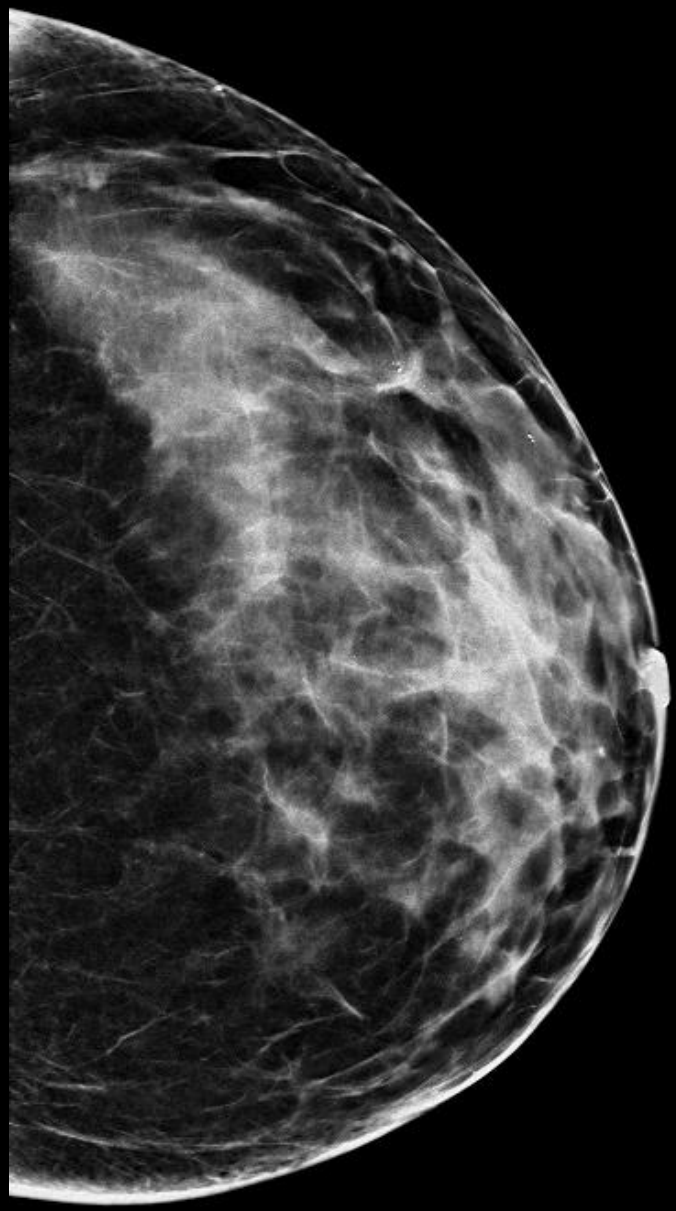

Synthesized 2D

2D vs 3Ds

Hologic FDA data:

- 302 subjects
- 15 readers
- 3Ds superior to 2D alone
- ΔAUC = 0,04 (p=0.005)
- Recall Rate reduced by 30.2%

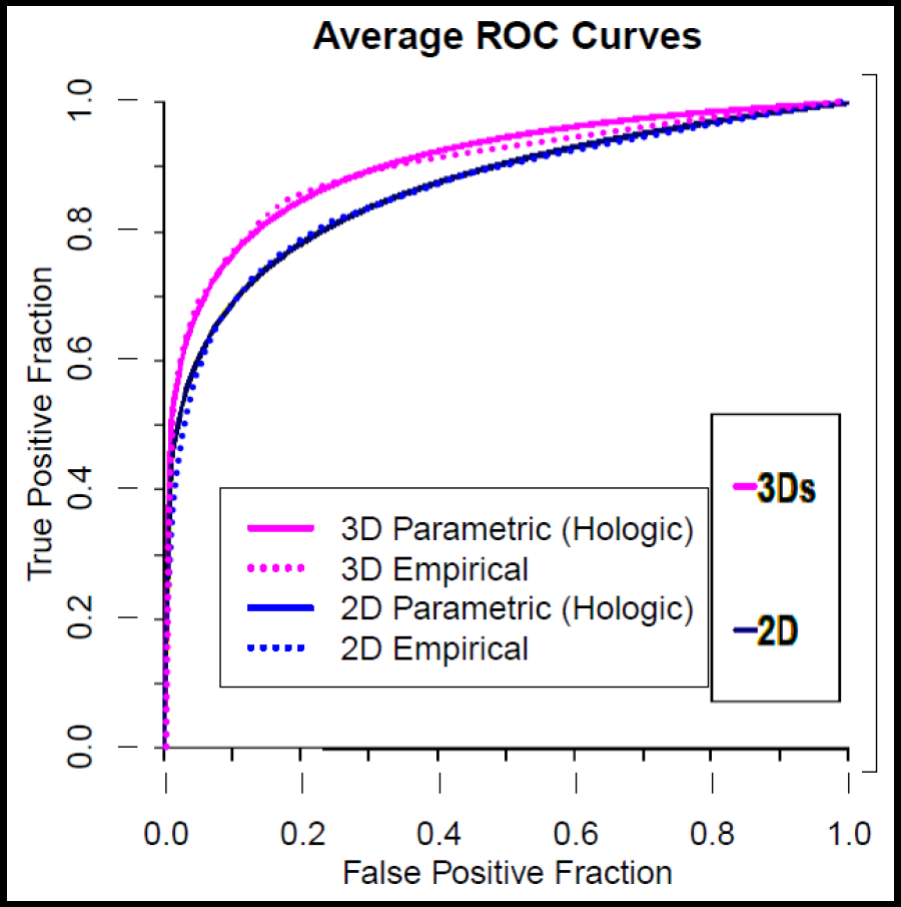

Mode	FFDM Views	DBT Views	Synthesized Views	Exam Dose per Breast
FFDM	MLO + CC	-	-	2.4 mGy
FFDM + 3D MLO	MLO + CC	MLO	-	3.85 mGy
FFDM + DBT	MLO + CC	MLO + CC	-	5.3 mGy
DBT + Synthesized 2D	-	MLO + CC	MLO + CC	2.9 mGy

Other Issues

- Reimbursement
- Computer-aided diagnosis (CAD)
- Automated density estimation (Quantra)
- Tomo-guided procedures

Thoracic Imaging

Experimental System

- Computer-controlled tube mover
- GE flat-panel detector
- Matrix inversion tomosynthesis reconstruction algorithm (Duke)

Digital Tomosynthesis

Conventional tomography

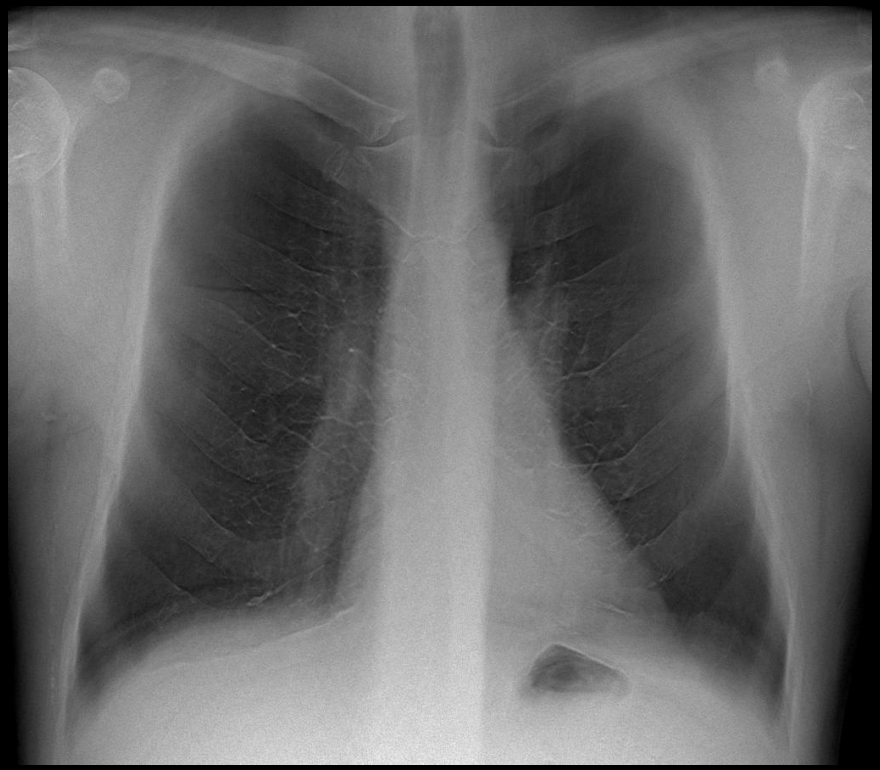

Tomosynthesis

Images Courtesy J. Dobbins

Routine follow-up; history of breast Ca with right partial mastectomy

20-degree tube angle, 61 projection images, 5 mm slice spacing
Total tomo exposure ≈ Lateral image exposure (screen film)

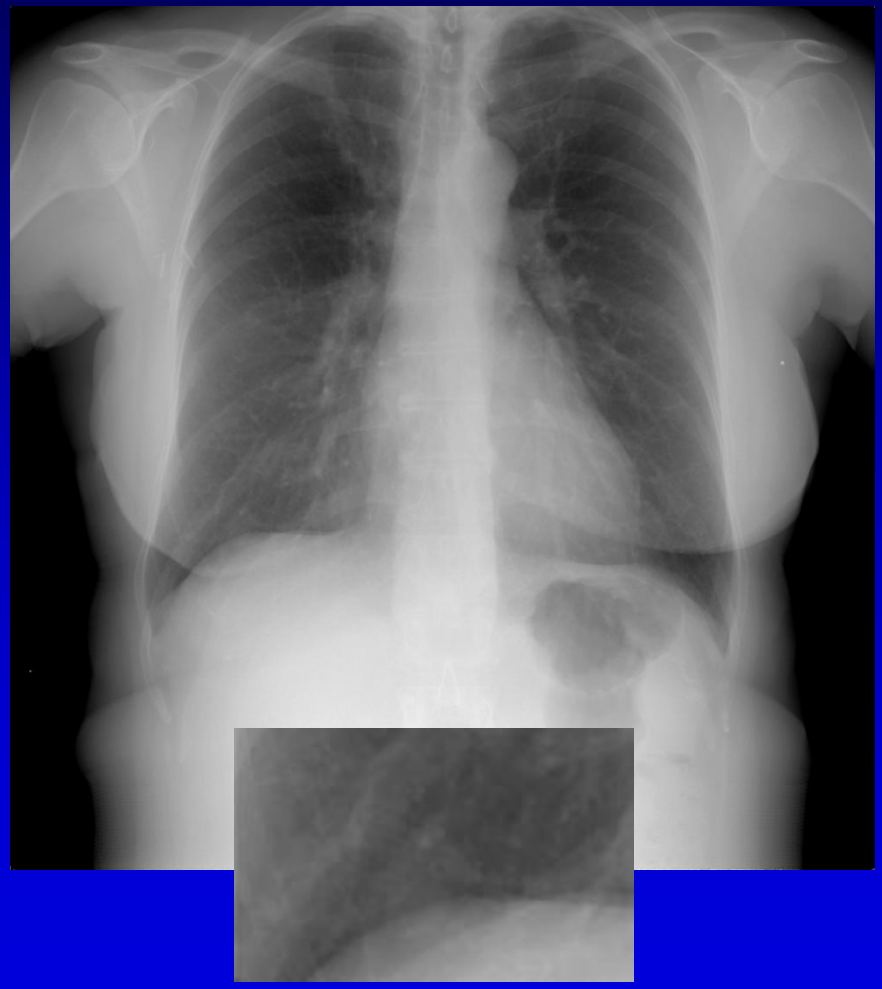

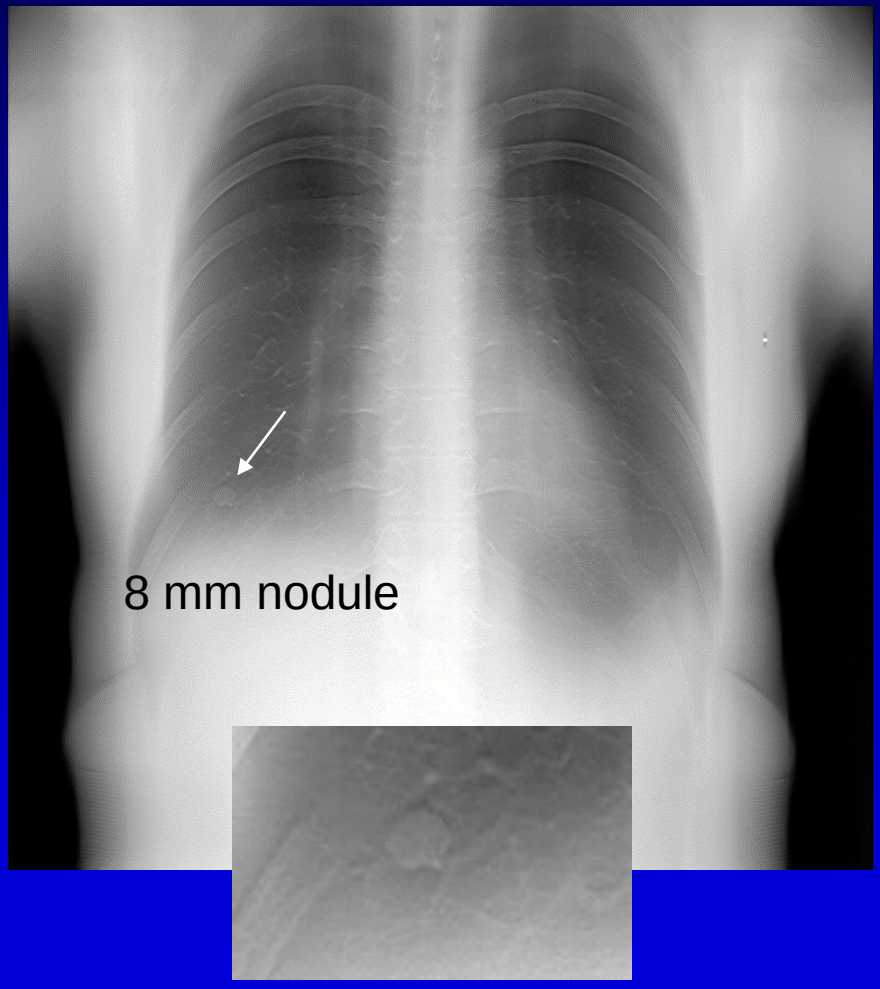

Analysis of the impact of digital tomosynthesis on the radiological investigation of patients with suspected pulmonary lesions on chest radiography

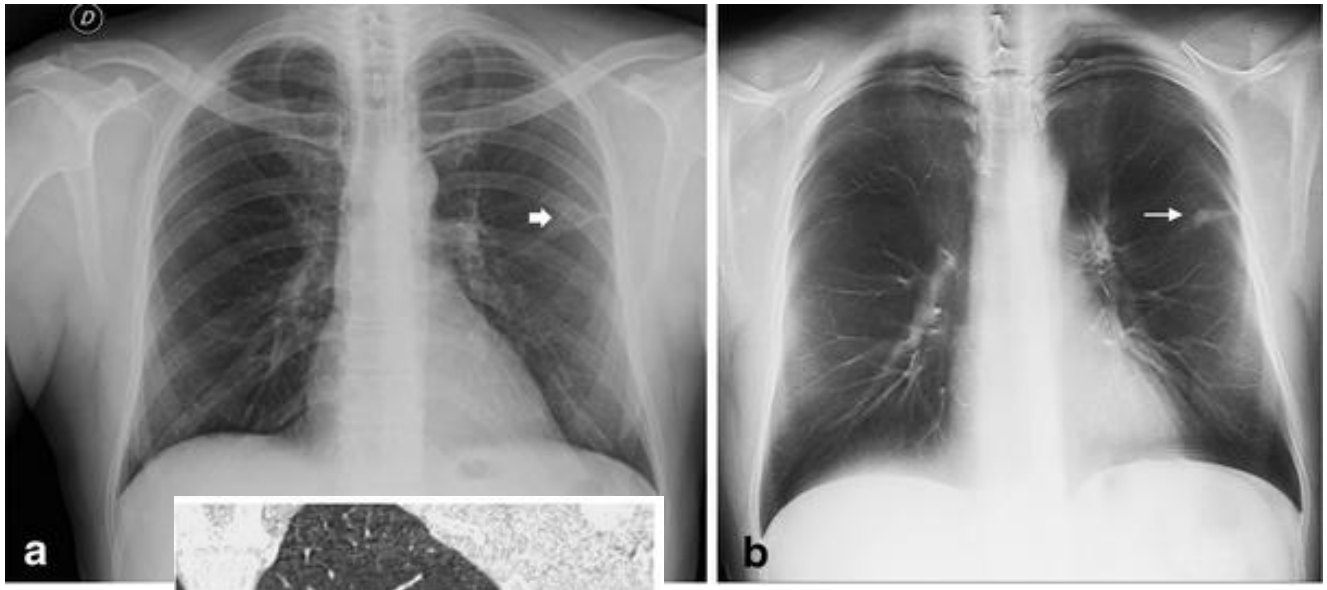

Emilio Quaia *et al.*

Eur. Radiol 2012

CXR	0.06 mSv (0.03 – 0.10 mSv)
Tomosynthesis	0.11 mSv (0.09 – 0.12 mSv
CT	3.0 mSv (2-4 mSv)

Clinical Study of 339 Patients

Tomosynthesis is almost 30 times lower dose than CT

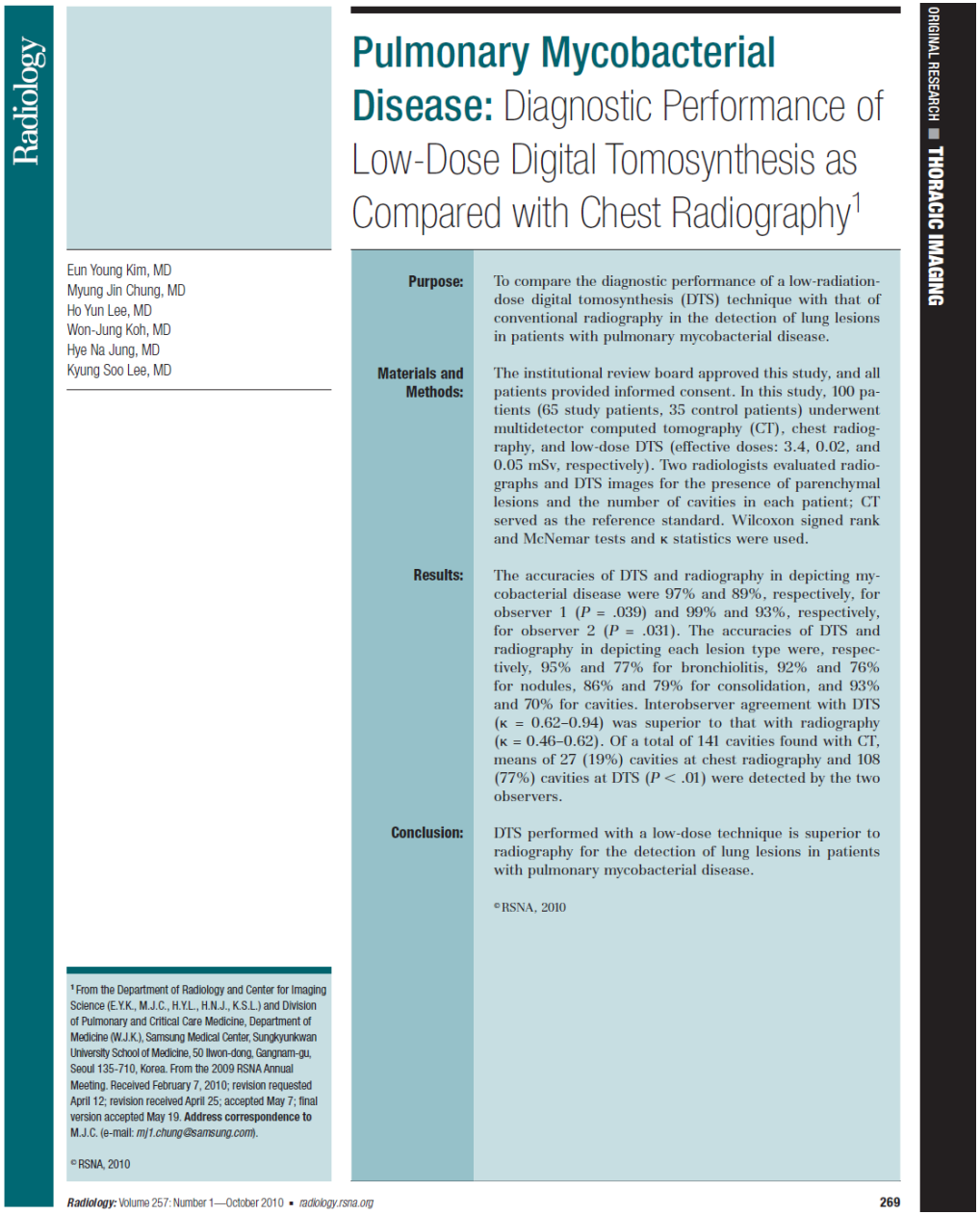

Radiology

ORIGINAL RESEARCH ■ THORACIC IMAGING

Pulmonary Mycobacterial Disease: Diagnostic Performance of Low-Dose Digital Tomosynthesis as Compared with Chest Radiography[1]

Eun Young Kim, MD
Myung Jin Chung, MD
Ho Yun Lee, MD
Won-Jung Koh, MD
Hye Na Jung, MD
Kyung Soo Lee, MD

Purpose: To compare the diagnostic performance of a low-radiation-dose digital tomosynthesis (DTS) technique with that of conventional radiography in the detection of lung lesions in patients with pulmonary mycobacterial disease.

Materials and Methods: The institutional review board approved this study, and all patients provided informed consent. In this study, 100 patients (65 study patients, 35 control patients) underwent multidetector computed tomography (CT), chest radiography, and low-dose DTS (effective doses: 3.4, 0.02, and 0.05 mSv, respectively). Two radiologists evaluated radiographs and DTS images for the presence of parenchymal lesions and the number of cavities in each patient; CT served as the reference standard. Wilcoxon signed rank and McNemar tests and κ statistics were used.

Results: The accuracies of DTS and radiography in depicting mycobacterial disease were 97% and 89%, respectively, for observer 1 (P = .039) and 99% and 93%, respectively, for observer 2 (P = .031). The accuracies of DTS and radiography in depicting each lesion type were, respectively, 95% and 77% for bronchiolitis, 92% and 76% for nodules, 86% and 79% for consolidation, and 93% and 70% for cavities. Interobserver agreement with DTS (κ = 0.62–0.94) was superior to that with radiography (κ = 0.46–0.62). Of a total of 141 cavities found with CT, means of 27 (19%) cavities at chest radiography and 108 (77%) cavities at DTS (P < .01) were detected by the two observers.

Conclusion: DTS performed with a low-dose technique is superior to radiography for the detection of lung lesions in patients with pulmonary mycobacterial disease.

[1] From the Department of Radiology and Center for Imaging Science (E.Y.K., M.J.C., H.Y.L., H.N.J., K.S.L.) and Division of Pulmonary and Critical Care Medicine, Department of Medicine (W.J.K.), Samsung Medical Center, Sungkyunkwan University School of Medicine, 50 Ilwon-dong, Gangnam-gu, Seoul 135-710, Korea. From the 2009 RSNA Annual Meeting. Received February 7, 2010; revision requested April 12; revision received April 25; accepted May 7; final version accepted May 19. **Address correspondence to** M.J.C. (e-mail: *mj1.chung@samsung.com*).

- Tuberculosis causes ~3 million deaths/yr globally
- Leading cause of death in HIV/AIDS population
- CXR is routinely used for detection but lacks both sensitivity and specificity

- Tomosynthesis showed statistically significant increase in sensitivity compared to CXR, without significant change in specificity

Radiol. 2010 **257**:269-277

More Dose Studies

- M. Bath, *et al.*,
  - RPD **139**: 144-152, 2010; RPD **139**: 153-158, 2010
  - Clinical and simulation studies
  - Ave. tomosynthesis dose: 0.13 mSv
  - 2% of average Chest CT dose

- Y. Yamada, *et al.,*
  - Inv. Radiol **46**: 471-477, 2011
  - Monte Carlo simulation based on 120 patients
  - Ave. tomosynthesis dose: 0.22 mSv

Muskuloskeletal Imaging

Muskuloskeletal Imaging

- Like radiology,
  - weight-bearing imaging is possible
  - multiple projections are necessary
  - new projections may be needed
  - Ideal for metal implants and hardware
  - Doses are relatively low
- Like CT,
  - Superposition is largely eliminated

B.1 - Sonialvision / Safire Tomosynthesis

- The Shimadzu Sonialvision / Safire system integrates the digital detector within a radiographic tilt table.
- Shown in the tilt position for a lateral knee tomosynthesis acquisition (60°), the detector translates up and the x-ray tube moves downward.
- The x-ray central beam is directed at the joint surface with an angle that varies from -20 to +20 degrees

B.3 - Frozen Cadaver – Tibial Plateau

Nearly matched coronal planes from reformatted 3D CT (GE)

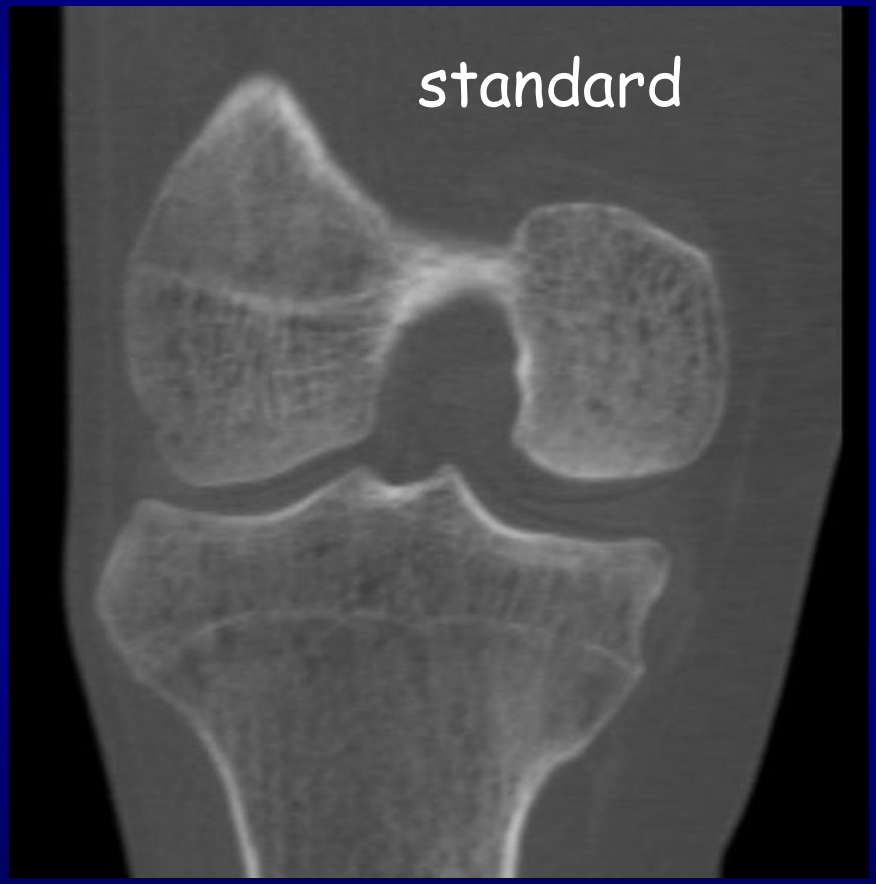

GE VCT

Shimadzu TS

B.3 - Frozen Cadaver – Tibial Plateau

Nearly matched coronal planes from reformatted 3D CT (GE)

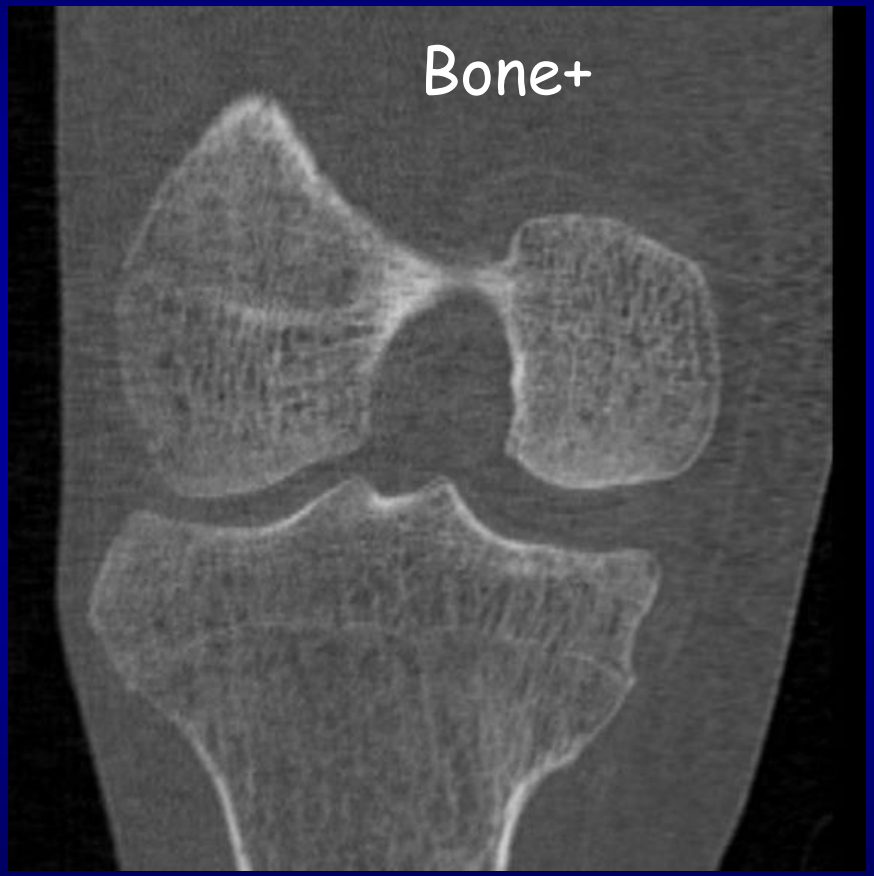

GE VCT

Shimadzu TS

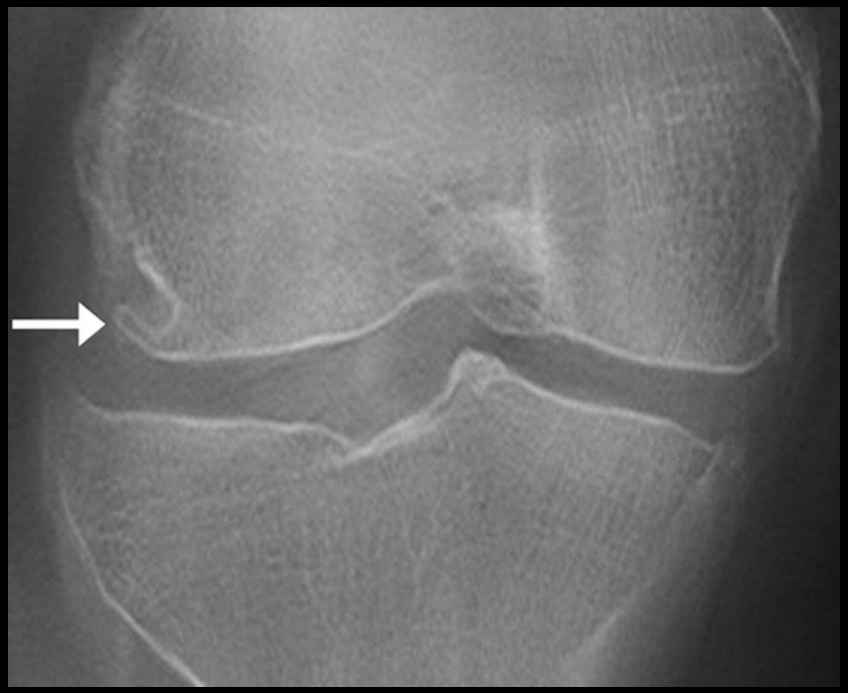

Radiograph shows no obvious osteophyte in the right lateral femur (arrow).

Tomosynthesis demonstrates osteophyte

MRI also shows focal cartilage defect

Hayashi D et al. Radiology 2012;263:206-215

Radiology

B.3 - Proximal Femur - ? Fx

reformatted coronal planes
3D CT (GE VCT, 64)

Standard

Bone

B.3 - Proximal Femur - ? Fx

Tomosynthesis
Shimadzu Sonialvision/safire II

AP View

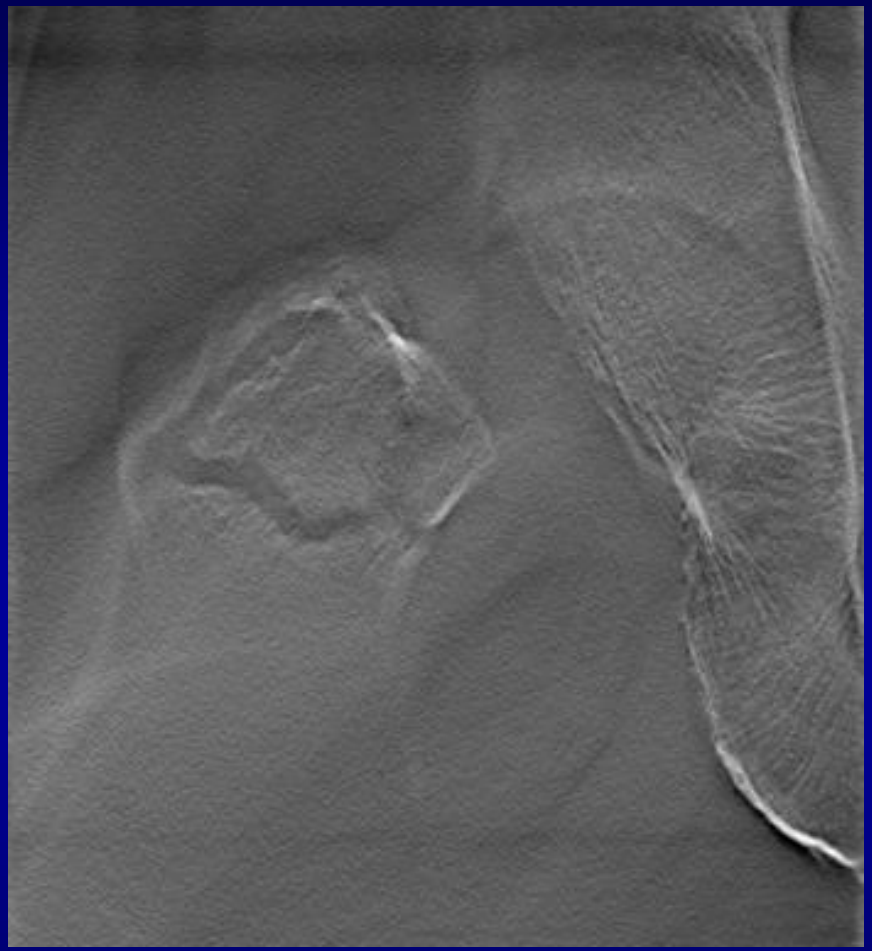

60-30 View

Multiple TS views are often used to obtain detail in planes of different orientation

B.3 – Reduced metal artifacts

Delayed Union, Femoral Fractures

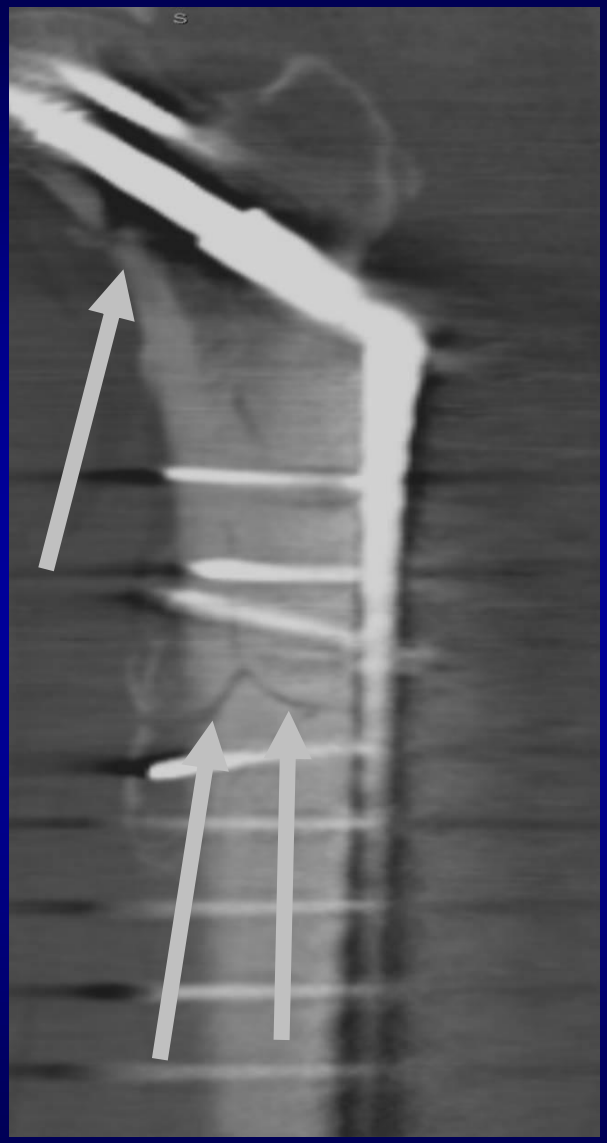

Coronal CT

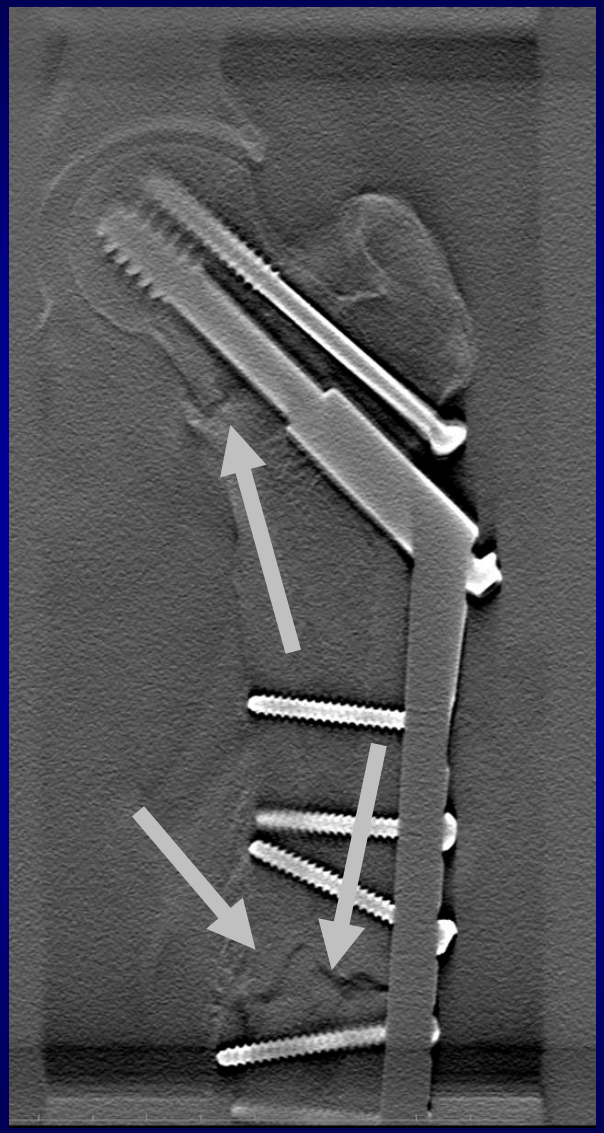

Coronal Tomosynthesis

63-year-old man with RA show three erosions (arrows) of the second metacarpophalangeal joint

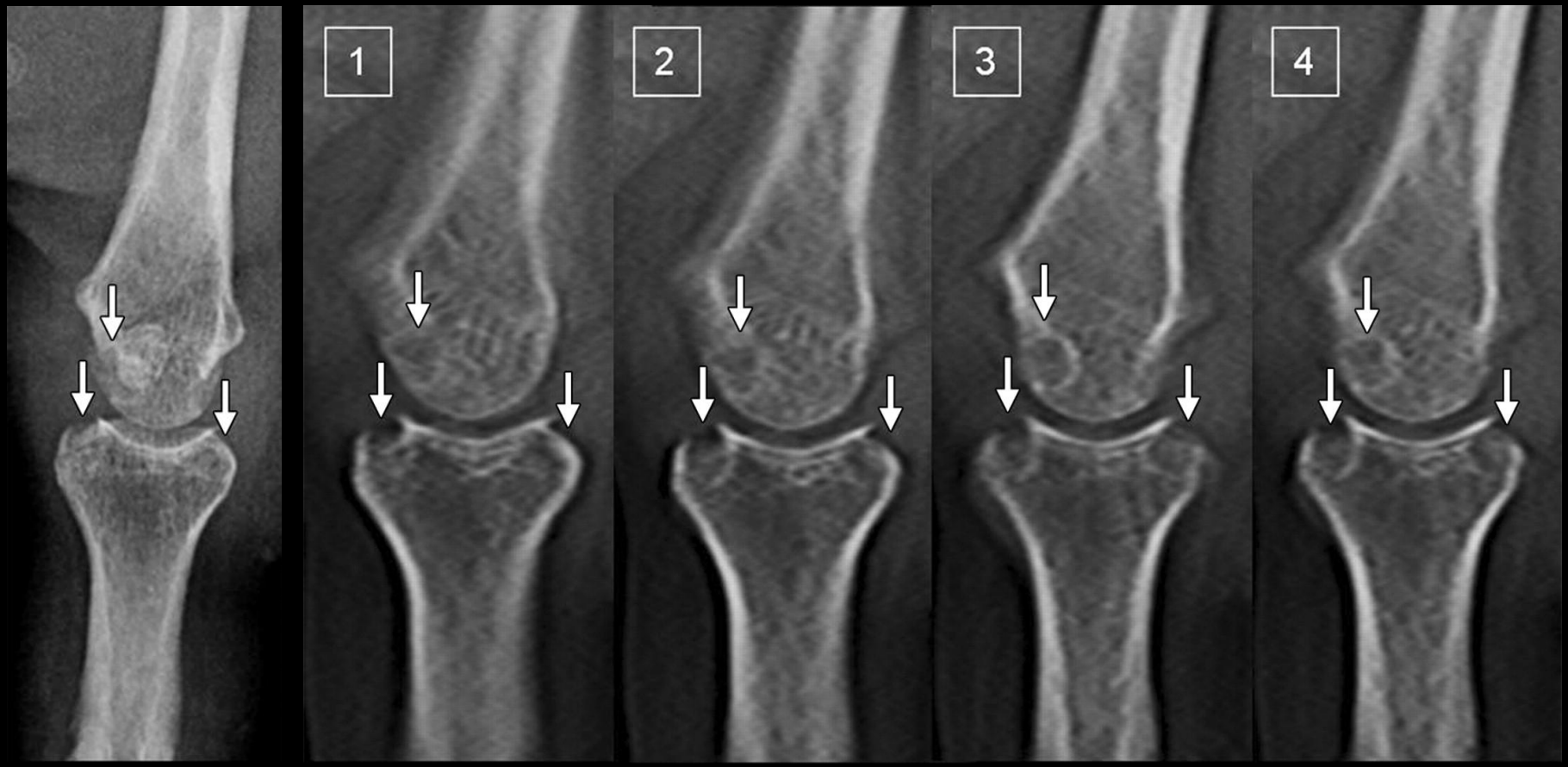

Canella C et al. Radiology 2011;258:199-205

Radiology

Other Tomosynthesis Dose Studies

Gislasson, King, Elbakri, and Reed, Winnipeg Children's Hospital:

- Tomosynthesis in pediatric spine, knee, facial, imaging
- 2-10 times dose of radiographic exam dose
- ~2-16% of CT exam dose
- Tomosynthesis dose less than total DR dose for some exams

Gislasson et al, "**Dose Assessment of Digital Tomosynthesis in Pediatric Imaging**", **Proc. of SPIE Vol. 7258**, 72585V, 2009

R.E. Gazaille, M. Flynn *et al* Henry Ford Hospital:

- Monte Carlo simulation of hip tomosynthesis
- 0.24 mSv per view, (typical exam of 3 views)
- ~3-4 times dose of radiographic exam dose
- ~10% of CT exam dose

R. E. Gazaille et al, "Technical Innovation: Digital Tomosynthesis of the Hip Following Intra-articular Administration of Contrast", **Skeletal Radiology 40**, 1467-1471, 2011

Hayashi, Guermazi *et al* Boston University:

- Clinical study of bilateral knee imaging
- 0.0072 mSv for DTS (~4X DR)

Hayashi et al, "Detection of Osteophytes and Subchondral Cysts in the Knee with Use of Tomosynthesis" Radiology **263**:206–215, 2012

Mermuys *et al* :

- Clinical study of detection of urinary stones
- 0.85 mSv for DTS (~1.7 times DR, 7-34% of CT)

K. Mermuys et al, ""Digital Tomosynthesis in the detection of urolithiasis: diagnostic performance and dosimetry compared with digital X-ray using MDCT as a reference"" AJR **195**:161–167, 2010

Canella *et al* Lille FR:

- Clinical study of rheumatoid arthritis of the wrist
- 0.1166 µSv (~2.6 times DR)

Canella et al, "Use of Tomosynthesis for Erosion Evaluation in Rheumatoid Arthritic Hands and Wrists" Radiology **258**:199–205, 2011

Head and Neck Imaging

European Journal of Radiology 81 (2012) 1140–1145

Contents lists available at ScienceDirect

European Journal of Radiology

journal homepage: www.elsevier.com/locate/ejrad

Radiation dose of digital tomosynthesis for sinonasal examination: Comparison with multi-detector CT

Haruhiko Machida[a,*], Toshiyuki Yuhara[a], Mieko Tamura[a], Tomokazu Numano[b], Shinji Abe[b], John M. Sabol[c], Shigeru Suzuki[d], Eiko Ueno[a]

[a] Department of Radiology, Tokyo Women's Medical University Medical Center East, 2-1-10 Nishiogu, Arakawa-ku, Tokyo 116-8567, Japan
[b] Department of Radiological Sciences, Tokyo Metropolitan University of Health Sciences, Tokyo 116-8551, Japan
[c] GE Healthcare, 3000 North Grandview Blvd., Waukesha, WI 53188, USA
[d] Department of Radiology, Saitama Red Cross Hospital, 8-3-33 kamiochiai, Chuo-ku, Saitama 338-0001, Japan

Acute Maxillary Sinusitis

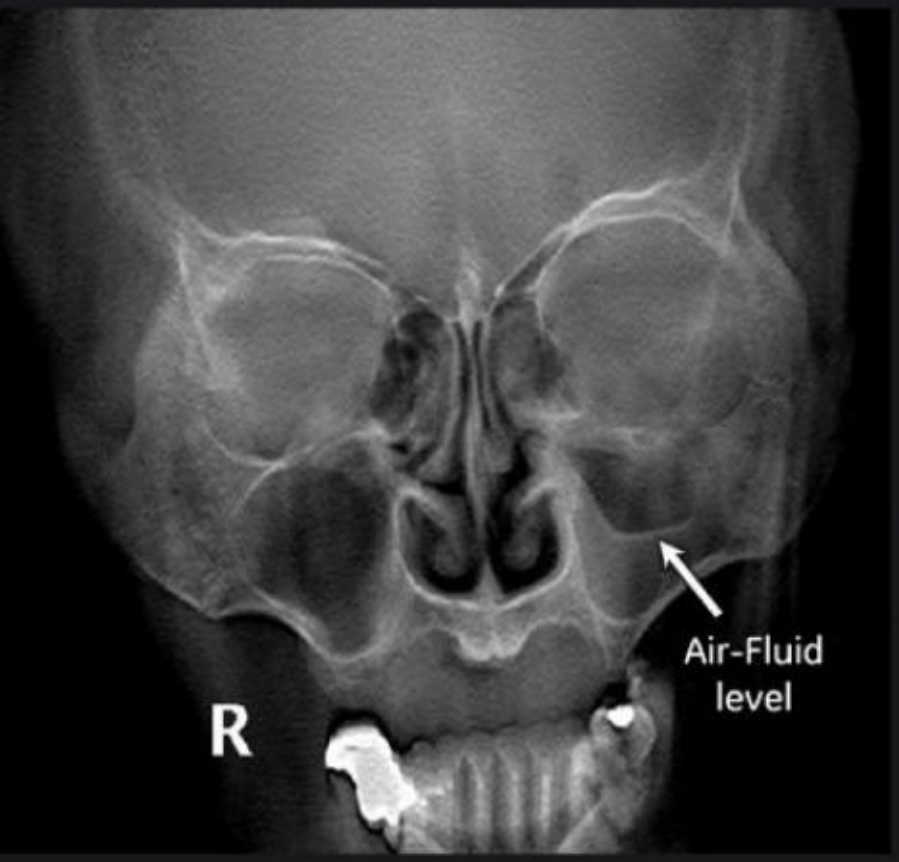

Tomosynthesis Image

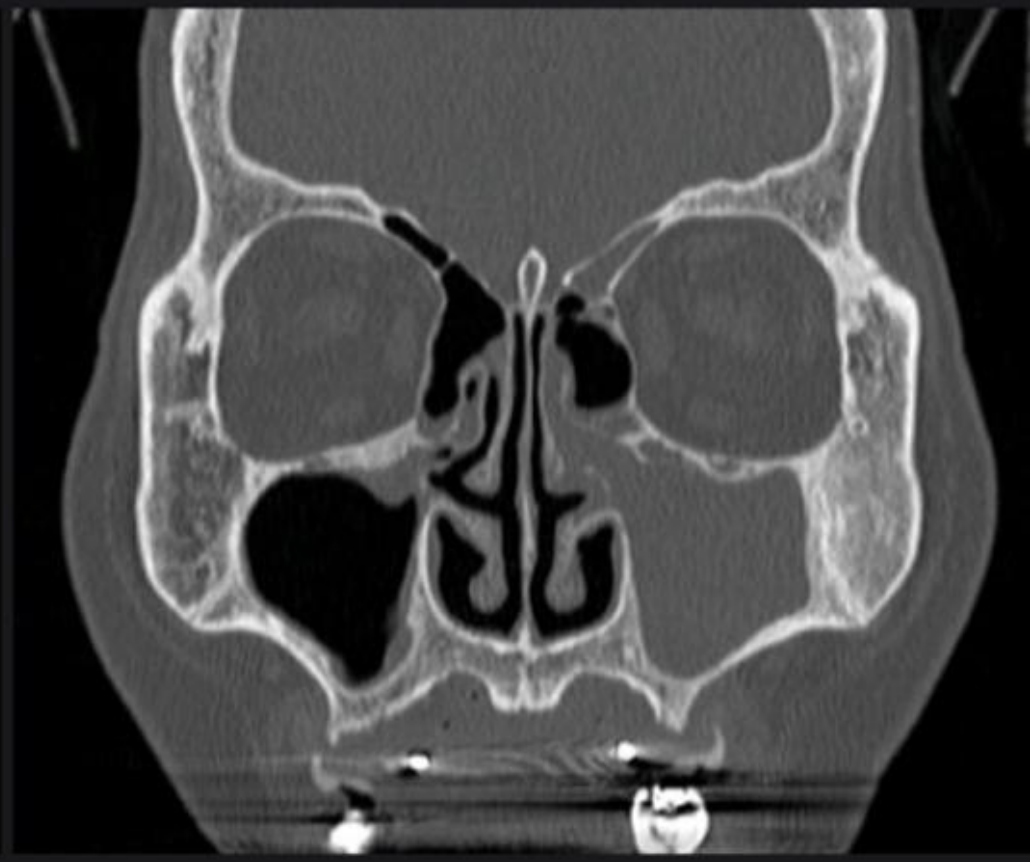

MDCT MPR Coronal Image

Tomosynthesis in upright position delineates air-fluid level in left maxillary sinus

	MDCT (μGy)	DT (μGy)	MDCT/DT dose ratio
Eye	32,500 ± 2500	112 ± 6	290
Skin	20,000 ± 9300	1160 ± 2100	17
Submandibular gland	17,000 ± 2300	1400 ± 80	12
Brain	14,300 ± 2200	1770 ± 560	8
Thyroid gland	1230 ± 160	230 ± 90	5

- Sinusitis prevalence
  - 14% in general public
  - 32% in children
- 31 million diagnosed each year

- CT is definitive
- CT lens dose is high (33 mGy)
- Cataractogenesis has a deterministic threshold of 0.5 Gy

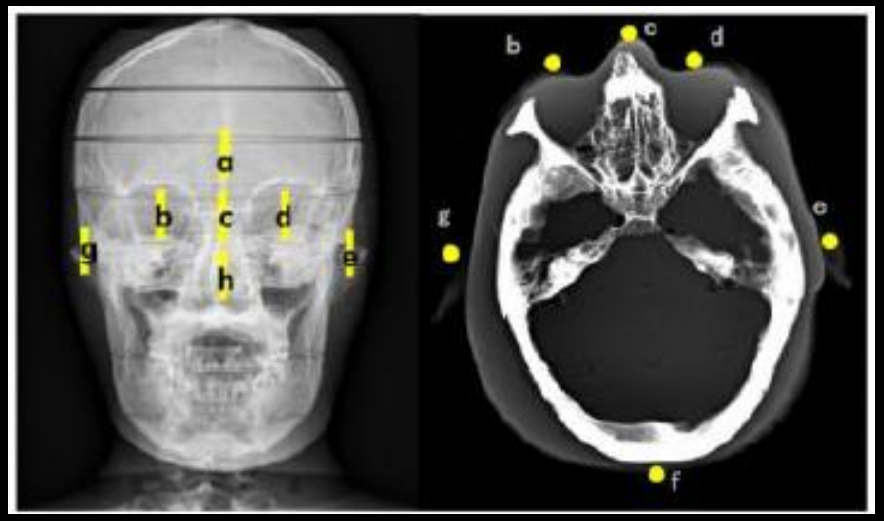

Comparison of Clinical Dose

- 43 Patients
- X-ray (Caldwell and Water's views)
- Single AP DTS acquisition
- MDCT standard clinical protocol

Average	X-Ray	Tomosynthesis
Sensitivity	50%	79 %
Specificity	86 %	94 %
Accuracy	76 %	89 %

Modality	Effective Dose
X-Ray	29 ± 6 μSv
Tomosynthesis	48 ± 10 μSv
MDCT	980 ± 250 μSv

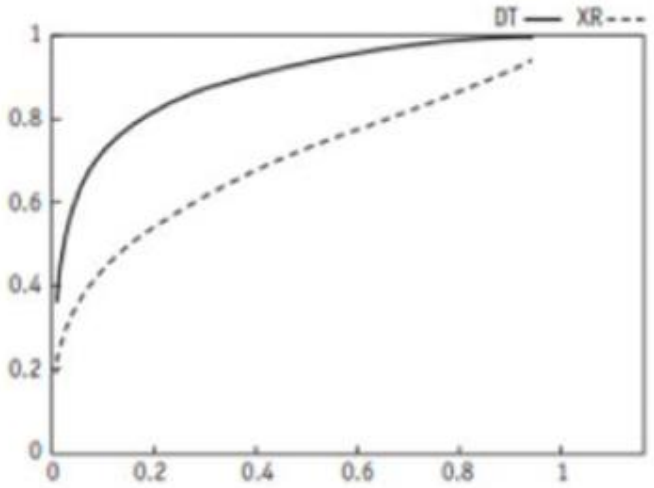

Yoo, *et al*, Korean J Radiol. 2012;**13**(2):136-143.

Future Directions

Super-Resolution

Acquiring multiple low resolution images at sub-pixel spacing generates a high resolution (i.e., super-resolution) image.

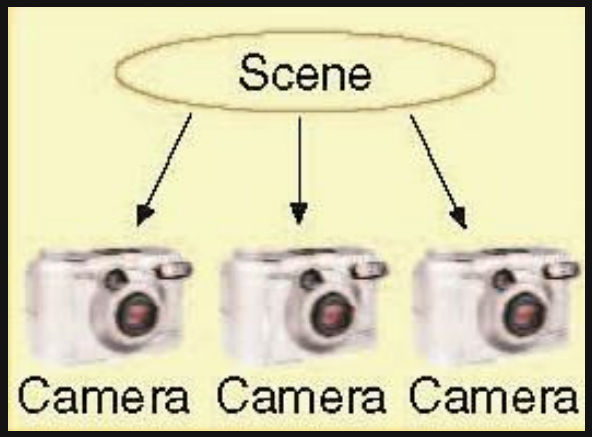

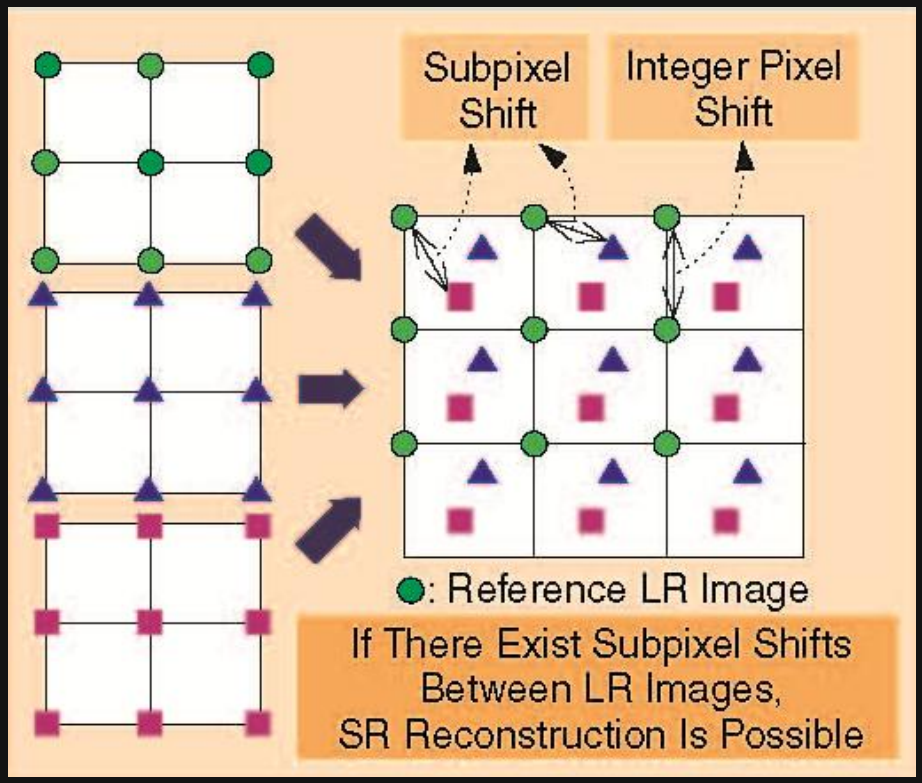

Bar Pattern Phantom

A) Central Projection

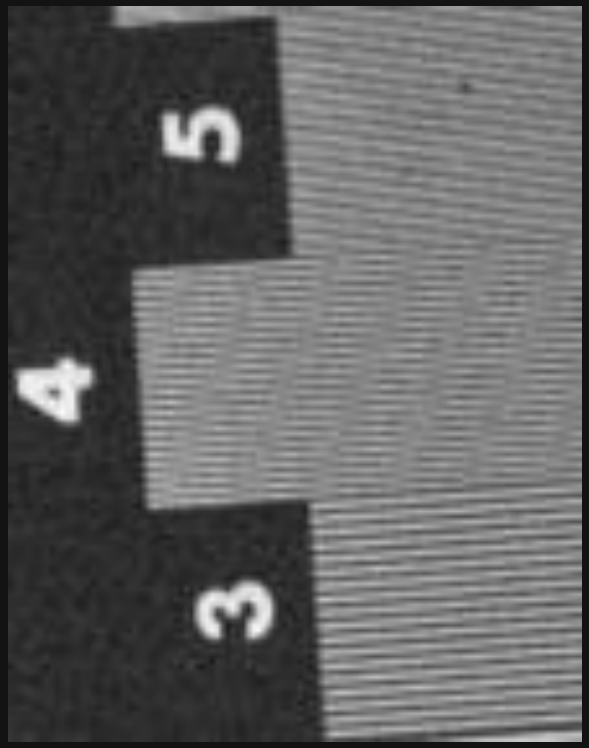

B) Reconstruction

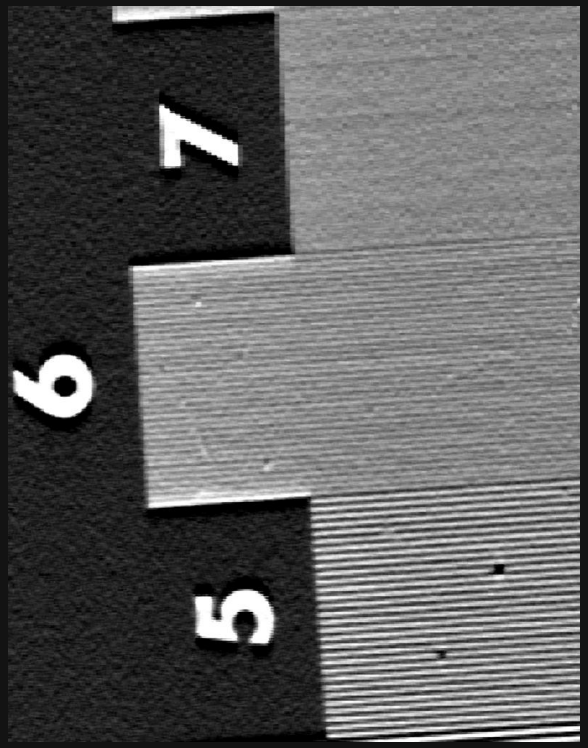

The reconstruction can clearly distinguish frequencies higher than the detector alias frequency $0.5a^{-1}$ (3.6 lp/mm). This ability is not present in acquiring the central projection alone.

Clinical Super-resolution

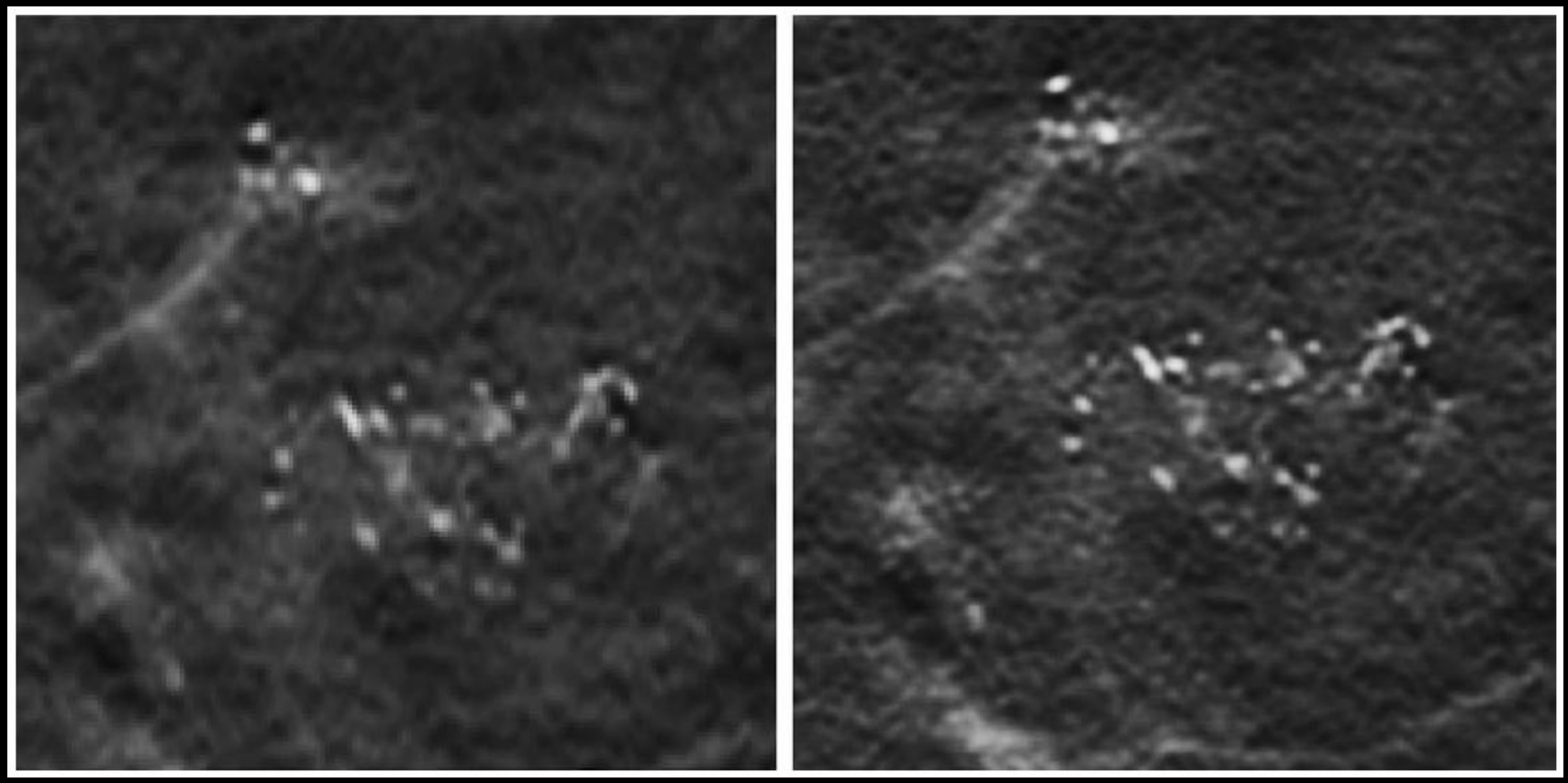

4x Mag

4x Super-resolution

Oblique Reconstructions

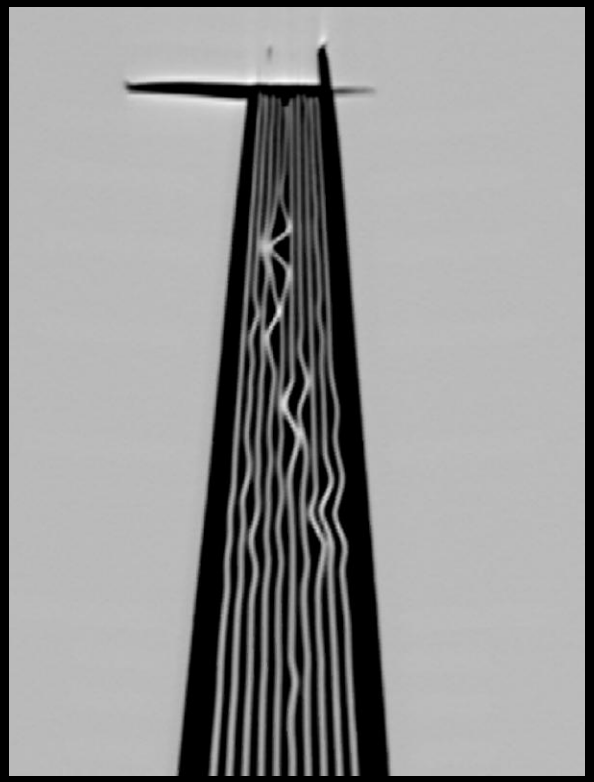

0º to the Detector Plane

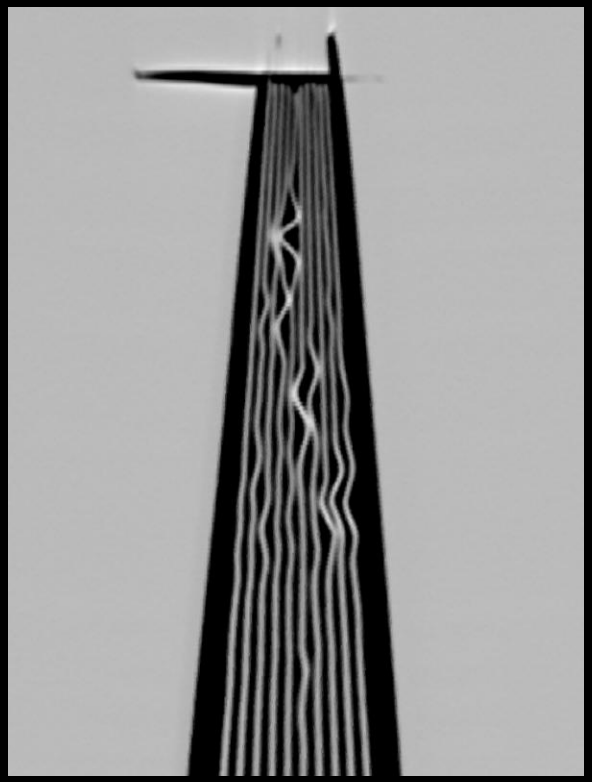

30º to the Detector Plane

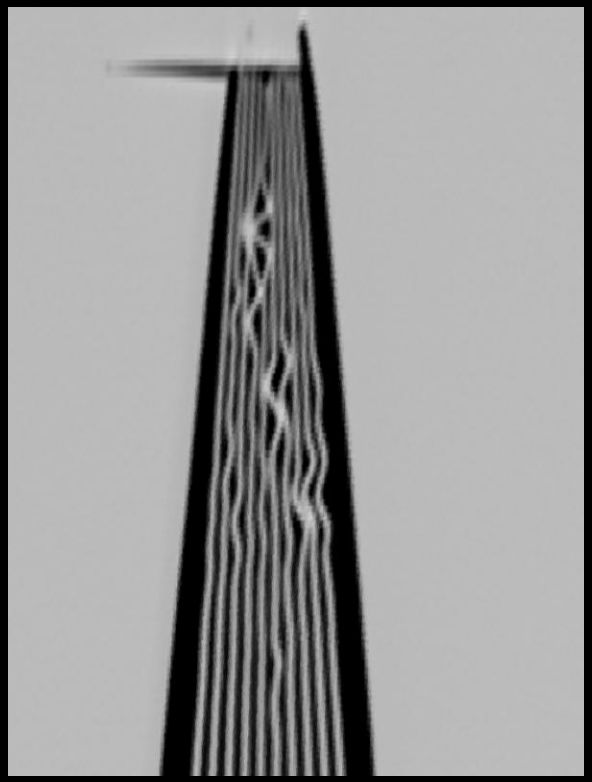

60º to the Detector Plane

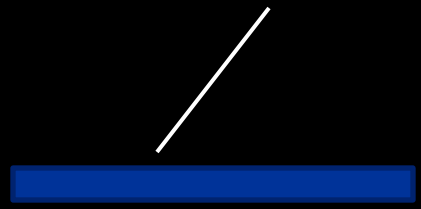

Oblique Reconstructions

Pitch 0°

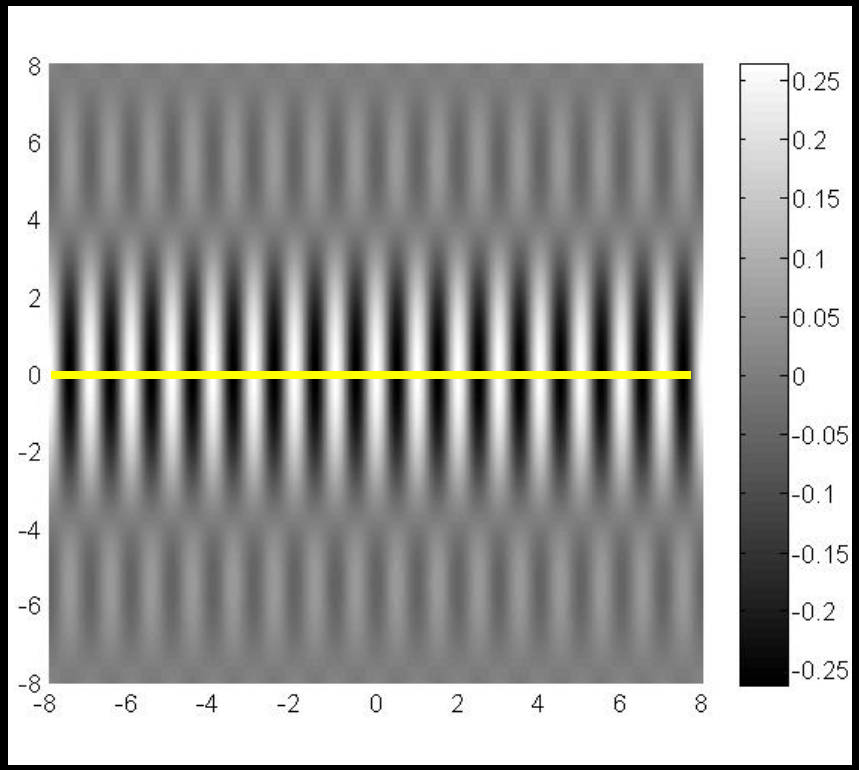

Pitch 45°

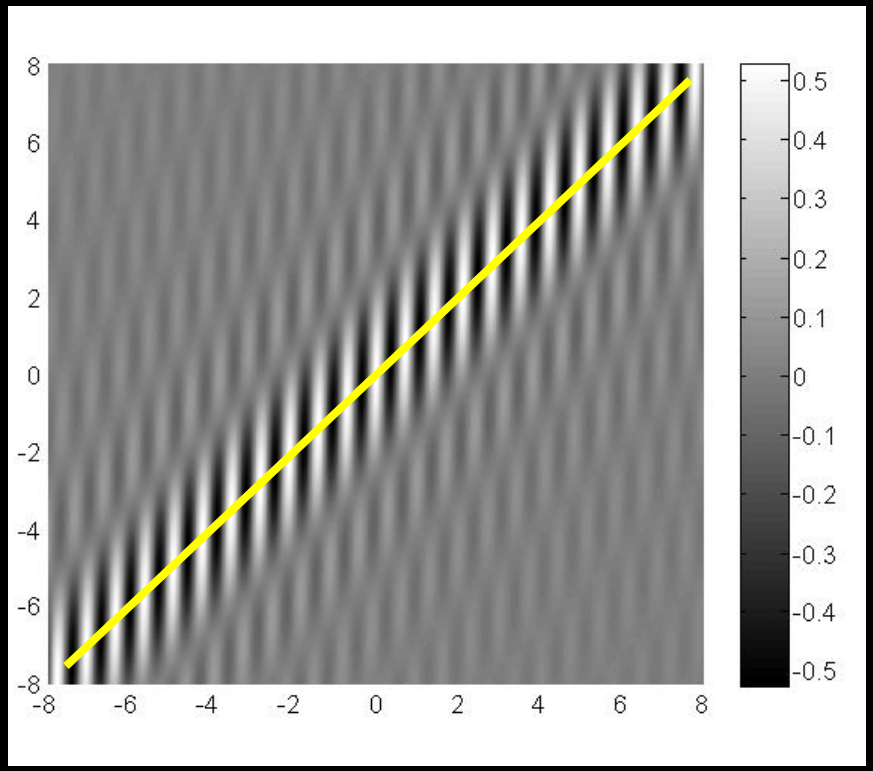

Despite the backprojection artifacts, the reconstruction can clearly resolve the input frequency within the mid-thickness of the sine plate at both pitches.

Clinical MPR

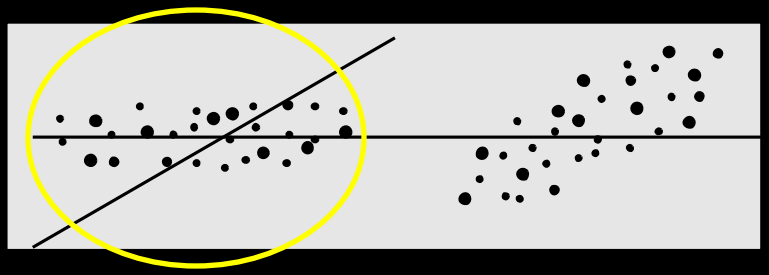

Recon. at
0° Pitch

Recon. at
30° Pitch

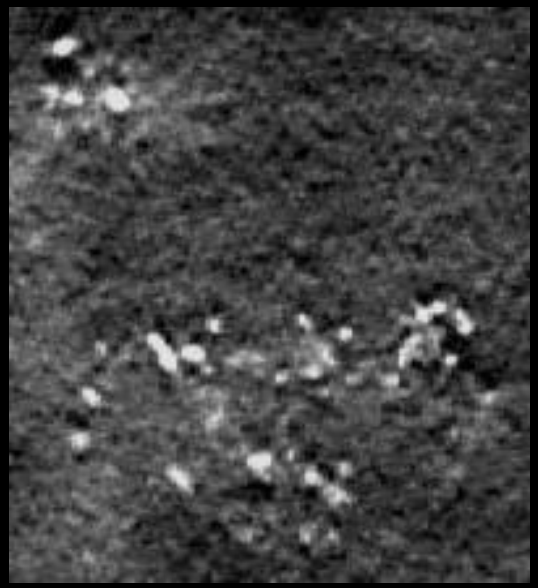

Recon. with
35 µm voxels
at 0° pitch

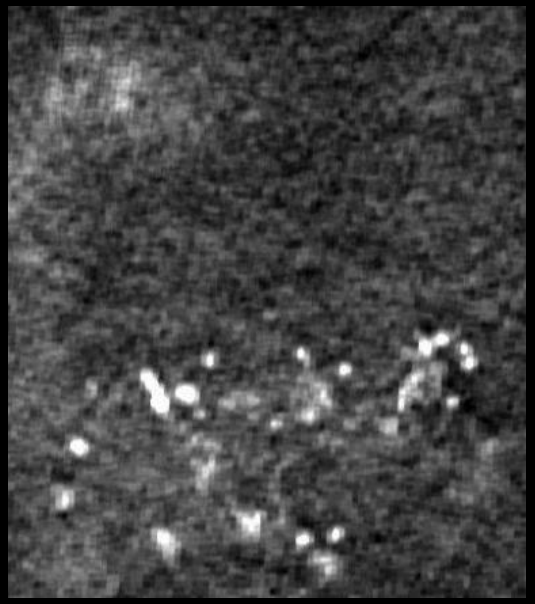

Recon. with
35 µm voxels
at 30° pitch

Clinical MPR

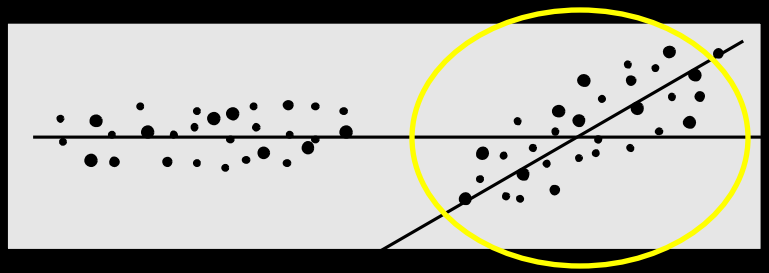

Recon. at
0° Pitch

Recon. at
30° Pitch

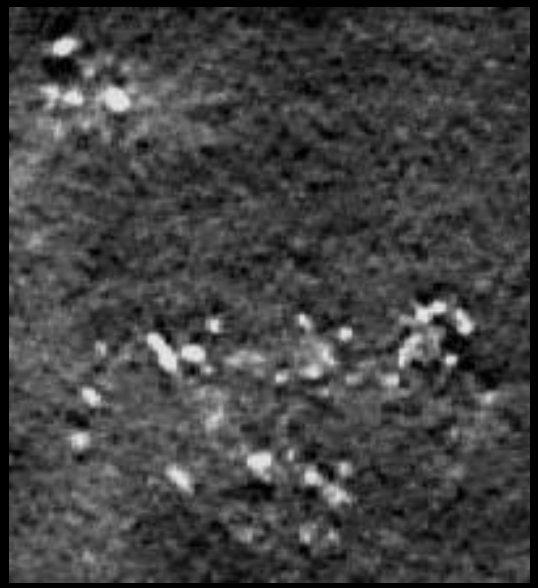

Recon. with
35 µm voxels
at 0° pitch

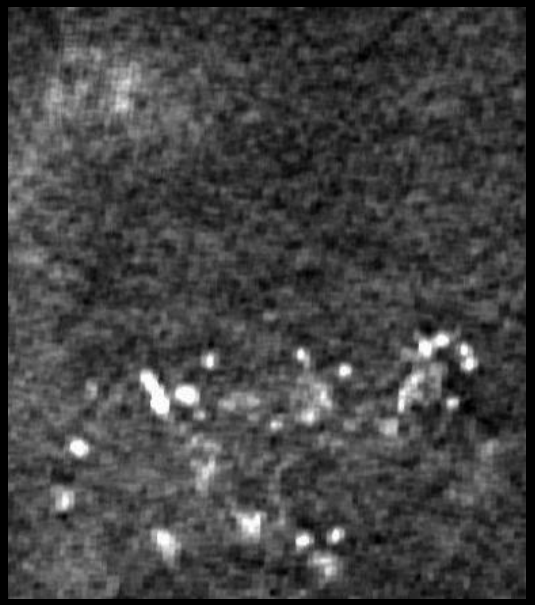

Recon. with
35 µm voxels
at 30° pitch

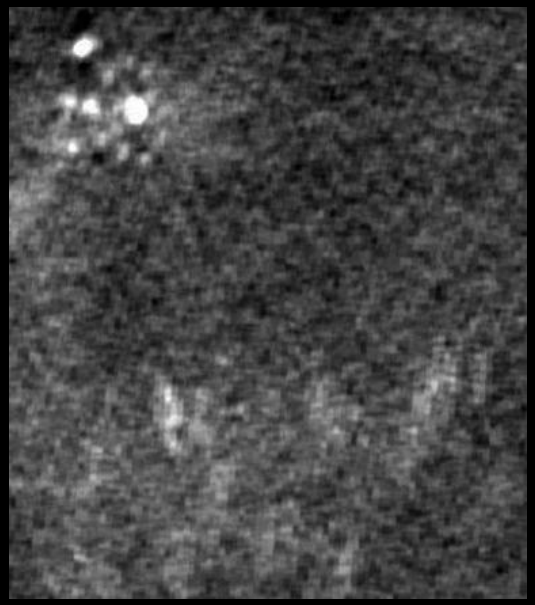

Translation of
Recon. Plane
at 30° pitch

Hologic Prototype CE-DBT System

Target	W
kVp	49 (HE) / 32 (LE)
Filter	Cu (HE) / Al (LE)
SID	70 cm
Detector	3 fps, 2x2 binning
Angular Range	15°
Scan Time	7.3 seconds

- Separate calibrations for LE and HE images
- Manual technique, no AEC
- DE subtraction factor k derived from CIRS Model 20 BR3D phantom

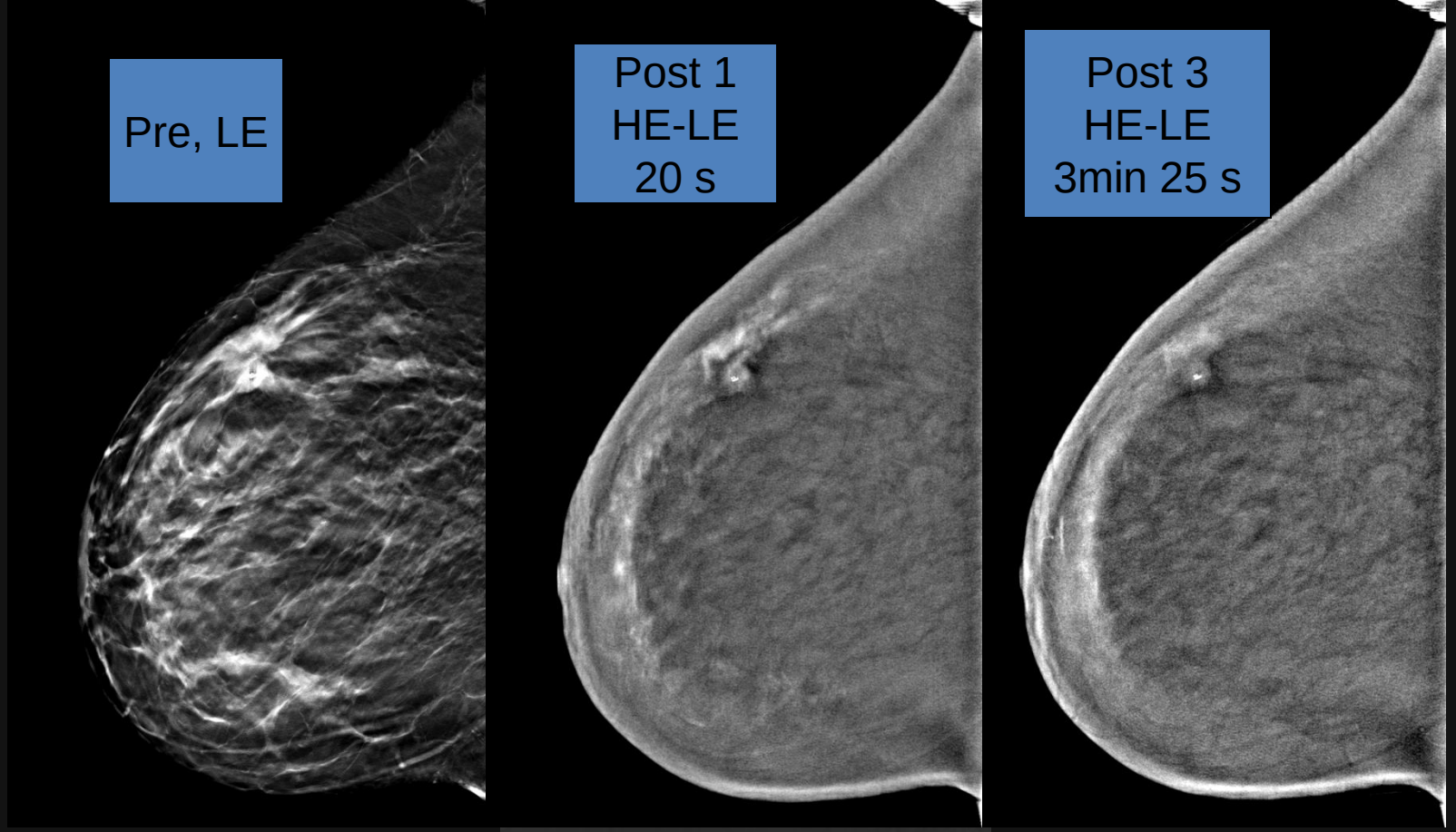
Pre, LE
Post 1
HE-LE
20 s
Post 3
HE-LE
3min 25 s

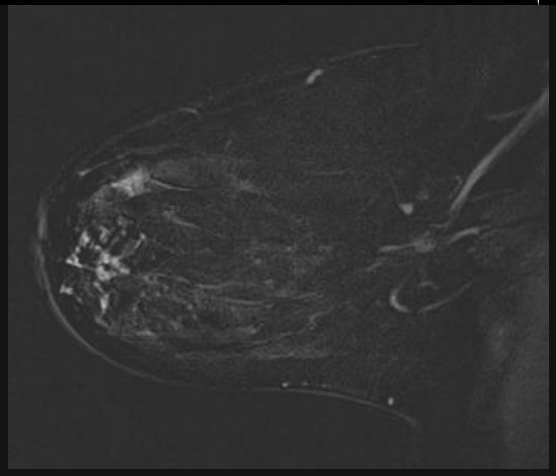

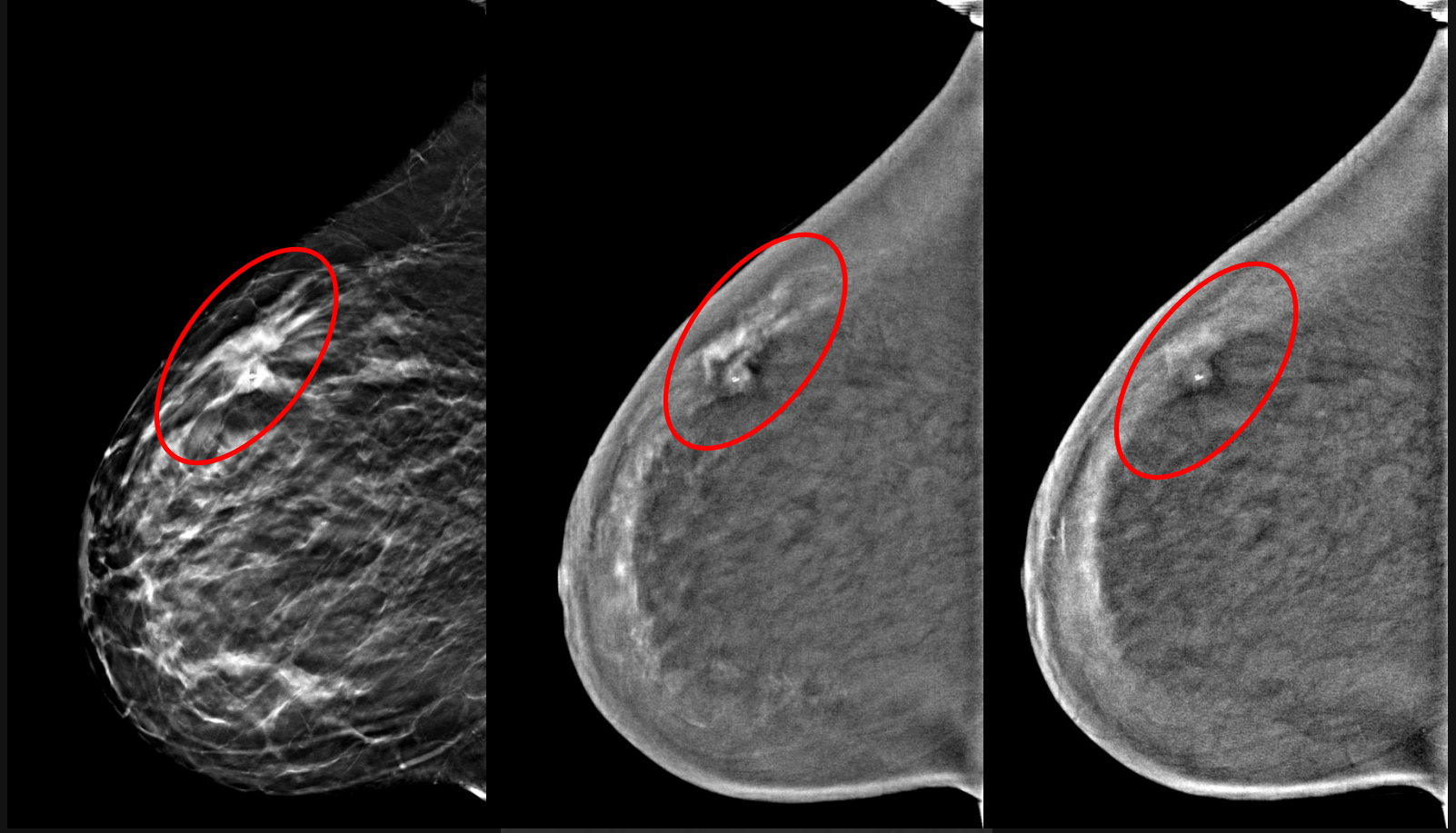

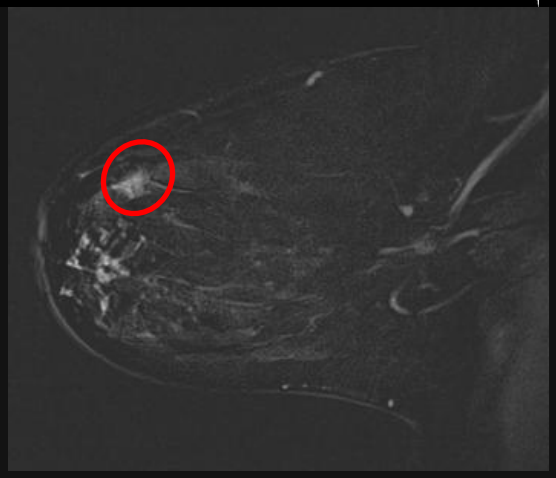

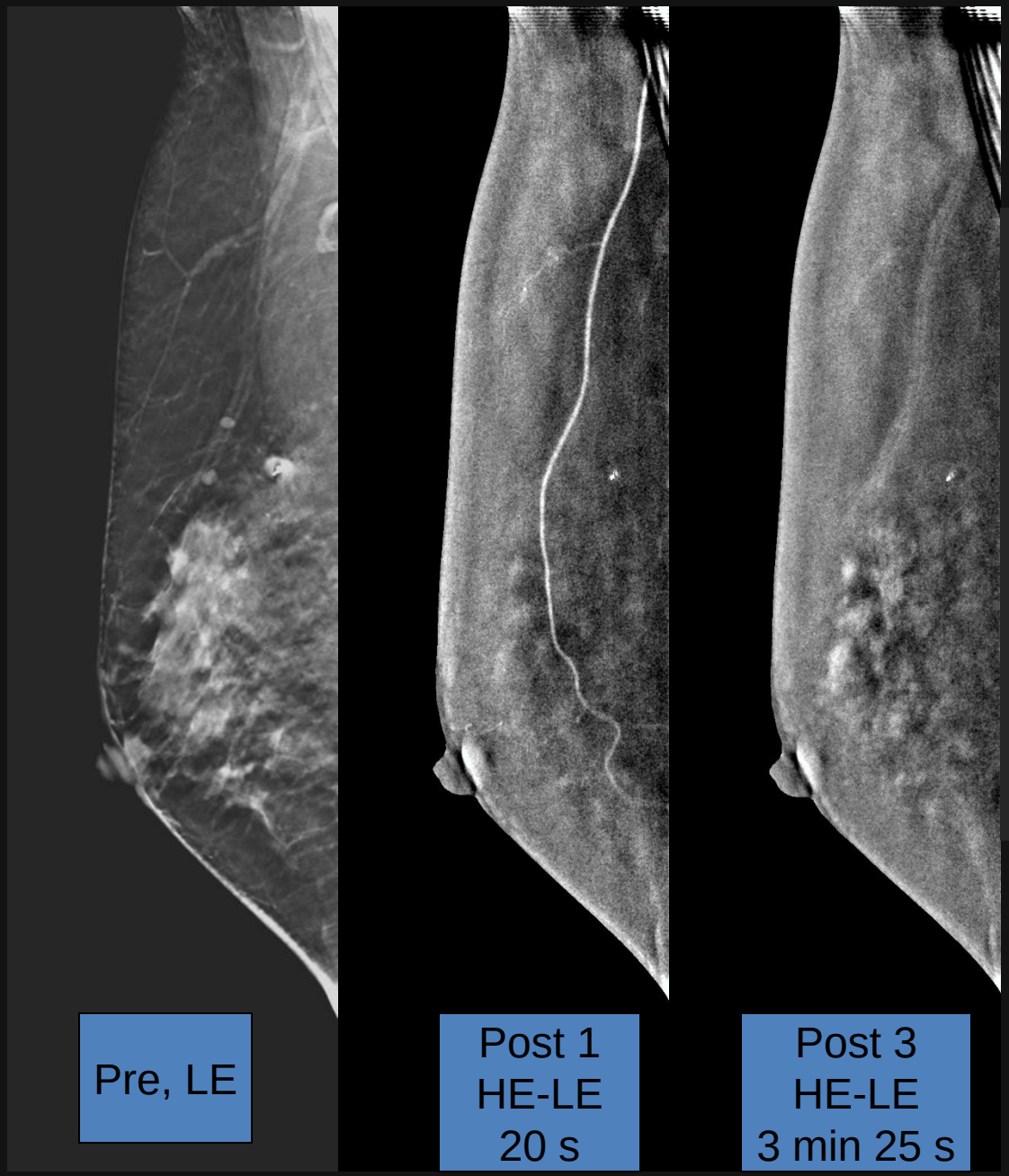
Pre, LE
Post 1
HE-LE
20 s
Post 3
HE-LE
3 min 25 s

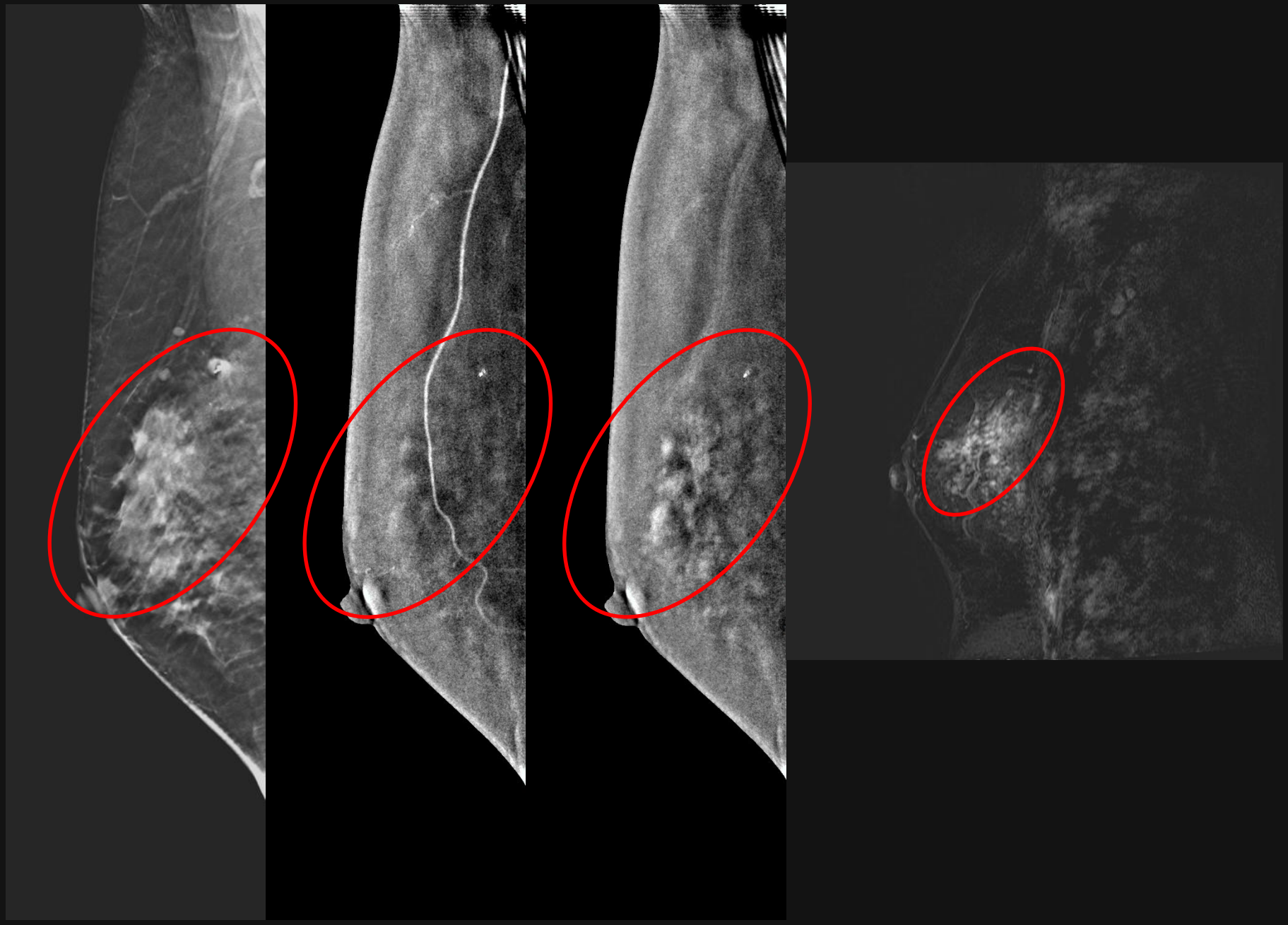

Advantages of tomosynthesis

- Improves conspicuity by removing overlying structures
- Permits section imaging with high resolution in coronal view
- Easily performed on the high volume of radiography patients
- Lower radiation dose compared with CT
- Lower cost compared with CT
- Excellent platform for quantitative imaging

Special thanks to

• J. Boone	UC Davis
• E.F. Conant	U of Pennsylvania
• J.T. Dobbins	Duke University
• L. Fajardo	U of Iowa
• M. Flynn	Henry Ford Hospital
• Z. Jing, T. Wu	Hologic
• D. Kopans	Mass. General Hospital
• T. Mertelmeyer	Siemens
• J. Sabol	GE

SAMs

1. Derive the central slice theorem from first principles
2. Prove that tomosynthesis demonstrates super-resolution using discrete and continuous integration
3. Given the dose at the orthogonal ray, formulate a closed form approximation for the dose at all other obliquities

Q1: How does the radiation dose of tomosynthesis compare to other imaging modalities?

4%	1. Slightly less than radiography
2%	2. Equal to radiography
93%	3. Slightly more than radiography
0%	4. Equal to computed tomography
1%	5. More than computed tomography

Answer:

3. Radiation dose of tomosynthesis imaging is slightly higher than the dose for a comparable radiograph. The small increase in dose is necessary to overcome the impact of detector readout noise arising from acquiring multiple projection images.

H. Machida, T Yuhara, et al. Radiation Dose of Digital Tomosynthesis for Sinonasal Examination: Comparison with Multi-Detector CT, Eur J Radiol 81, 1140-1145, 2012

Q2: CT and tomosynthesis images are acquired as a series of projections. How does a projection image sample the Fourier domain of an object?

20% 1. A line in the Fourier domain

55% 2. A plane in the Fourier domain

18% 3. A double-napped cone

7% 4. It fully samples the Fourier domain

Answer:

2. A projection image samples a single plane in the Fourier domain. The greater the number of projections made, the more completely the Fourier domain is sampled.

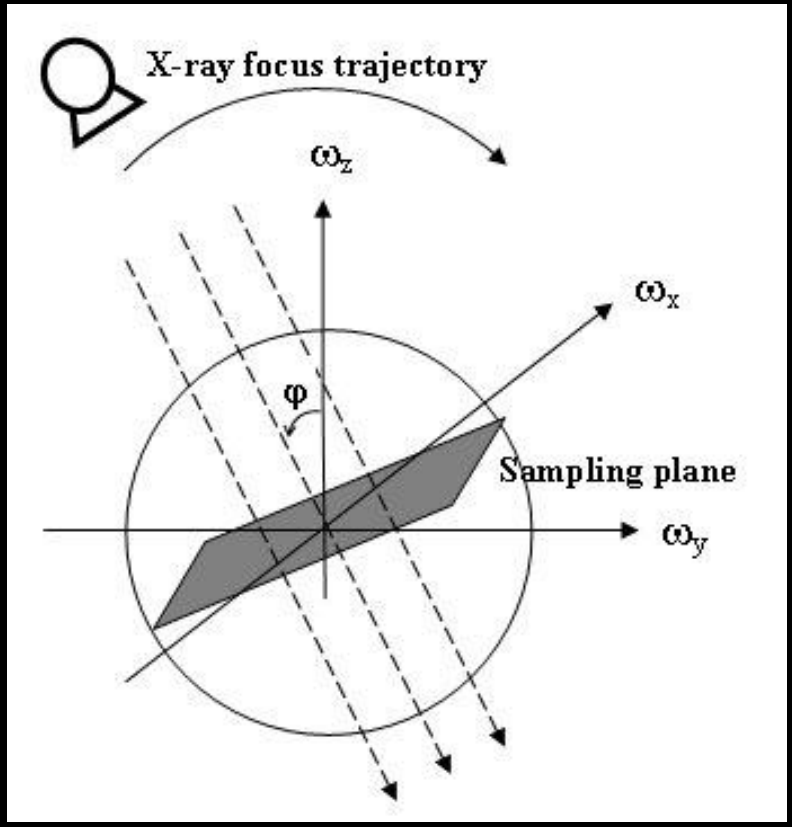

J. Zhang, C. Yu, A Novel Solid-Angle Tomosynthesis (SAT) Scanning Scheme, Medical Physics, 37(8), 2010

Q3: How does spatial resolution of tomosynthesis compare to CT?

3%	1. Poorer x, y, and z resolution
9%	2. Poorer x & y resolution; better z resolution
7%	3. Better x, y, and z resolution
81%	4. Better x & y resolution; poorer z resolution
0%	5. Same x, y, and z resolution

Answer:

4. Like linear tomography, the x and y resolution of tomosynthesis is comparable (or superior) to radiography, and substantially superior to CT. The penalty of tomosynthesis is poorer z resolution than CT.

Acciavatti RJ, Maidment ADA. Observation of Super-Resolution in Digital Breast Tomosynthesis. Med Phys. 2012;39(12):7518-39.

Q4: The radiation dose in tomosynthesis is determinedly primarily by which factor?

18%	1. Body part thickness
1%	2. Angular range
27%	3. Number of projections
0%	4. Number of reconstructed images
54%	5. Angular range AND number of projections

Answer:

1. Like radiography, tomosynthesis dose is primarily determined by body part thickness. Dose does NOT depend upon the number of images reconstructed. Dose depends only minimally upon the number of images acquired (detector noise) or angular range (obliquity).

T. Olgar, T Kahn, and D. Gosch, Average Glandular Dose in Digital Mammography and Breast Tomosynthesis, Rofo, 2012

Innovations and Applications of Tomosynthesis

Andrew D. A. Maidment, Ph.D.
University of Pennsylvania
Department of Radiology